

EVALUATING AND MERGING MODEL- AND SATELLITE-BASED
PRECIPITATION PRODUCTS OVER VARYING CLIMATE AND
TOPOGRAPHY

A THESIS SUBMITTED TO
THE GRADUATE SCHOOL OF NATURAL AND APPLIED SCIENCES
OF
MIDDLE EAST TECHNICAL UNIVERSITY

BY

MUHAMMAD AMJAD

IN PARTIAL FULFILLMENT OF THE REQUIREMENTS
FOR
THE DEGREE OF DOCTOR OF PHILOSOPHY
IN
CIVIL ENGINEERING

JANUARY 2020

Approval of the thesis:

**EVALUATING AND MERGING MODEL- AND SATELLITE-BASED
PRECIPITATION PRODUCTS OVER VARYING CLIMATE AND
TOPOGRAPHY**

submitted by **MUHAMMAD AMJAD** in partial fulfillment of the requirements for
the degree of **Doctor of Philosophy in Civil Engineering Department, Middle East
Technical University** by,

Prof. Dr. Halil Kalıpçılar
Dean, Graduate School of **Natural and Applied Sciences**

Prof. Dr. Ahmet TÜRER
Head of Department, **Civil Engineering**

Assoc. Prof. Dr. M. Tuğrul YILMAZ
Supervisor, **Civil Engineering, METU**

Examining Committee Members:

Prof. Dr. İsmail YÜCEL
Civil Engineering, METU

Assoc. Prof. Dr. M. Tuğrul YILMAZ
Civil Engineering, METU

Prof. Dr. M. Lütfi SÜZEN
Geological Engineering, METU

Assoc. Prof. Dr. Ahmet ÖZTOPAL
Meteorological Engineering, ITU

Assist. Prof. Dr. Ali Arda ŞORMAN
Civil Engineering, ESTU

Date: 31.01.2020

I hereby declare that all information in this document has been obtained and presented in accordance with academic rules and ethical conduct. I also declare that, as required by these rules and conduct, I have fully cited and referenced all material and results that are not original to this work.

Name, Surname: Muhammad Amjad

Signature:

ABSTRACT

EVALUATING AND MERGING MODEL- AND SATELLITE-BASED PRECIPITATION PRODUCTS OVER VARYING CLIMATE AND TOPOGRAPHY

Amjad, Muhammad
Doctor of Philosophy, Civil Engineering
Supervisor: Assoc. Prof. Dr. M. Tuğrul YILMAZ

January 2020, 113 pages

This study first evaluates and inter-compares a set of nine precipitation products (2 satellite estimation-based, 2 model reanalysis-based, and 5 model forecast-based products) over varying climate and topography by using the in-situ observed precipitation data as truth. The products are then merged, in the form of two groups, using two different merging techniques: 1. Taking ensemble mean (i.e., simple merging); 2. Taking ensemble mean after rescaling them by a linear regression method. The merged products are statistically evaluated and inter-compared with the individual products using the same in-situ precipitation data. The results show that the errors in the products increase, while their correlations with the observed data decrease with the increasing terrain complexity. Comparatively, wetness and terrain slope have a more prominent role than elevation in the error variability of the products. The performance of model-based products is more adversely affected by increasing terrain complexity than that of satellite-based products. Both the merging methods improve the errors and correlations of the products not only over the entire study area, but over all its sub-regions classified based on the wetness, elevation, and terrain slope. Simple merging improves the precipitation detection ability of the individual products the most. Merging the products after rescaling them in the space of ECMWF HRES and

IMERG adds the highest improvement in ErrSD (on average 28.5% and 34.8%, resp.) and CC (on average 17.6% and 23%, resp.) of the individual forecasts and individual research products, respectively.

Keywords: Precipitation, Satellite, Model, Evaluation, Precipitation Data Merging, Varying Topography.

ÖZ

MODEL VE UYDU TABANLI YAĞIŞ ÜRÜNLERİNİ DEĞİŞKEN İKLİM VE TOPOĞRAFYA ÜZERİNDE DEĞERLENDİRMEK VE BİRLEŞTİRMEK

Amjad, Muhammad
Doktora, İnşaat Mühendisliği
Tez Danışmanı: Doç. Dr. M. Tuğrul YILMAZ

Ocak 2020, 113 sayfa

Bu çalışma ilk olarak dokuz farklı yağış ürününü (2 uydu tahmin tabanlı, 2 model yeniden analiz tabanlı, 5 model tahmin tabanlı ürün) değişken iklim ve topografya üzerinde, yer gözlem istasyon verilerini referans kabul ederek değerlendirmekte ve karşılaştırmaktadır. Ürünler iki farklı birleştirme tekniği kullanılarak iki grup halinde birleştirilmiştir: 1. Çoklu ürün ortalaması almak (yani basit birleştirme); 2. Lineer regresyon yöntemiyle ölçeklendirildikten sonra çoklu ürün ortalamasının almak. Elde edilen birleştirilmiş ürünler hem istatistiksel hem de hidrolojik olarak değerlendirilmiş olup sırasıyla aynı yağış gözlem verilerini kullanan ürünler ve yüzeysel akış gözlem verileri ile karşılaştırılmıştır. Elde edilen sonuçlara göre, artan arazi karmaşıklığı ürünlerdeki hataların artmasına ve ürünler ile gözlem verileri arasındaki korelasyon değerlerinin azalmasına sebebiyet vermiştir. Sulaklık ve arazi eğimi ürünlerin hata değişkenliğinde yüksekliğe göre daha belirgin bir role sahiptir. Model tabanlı ürünlerin performansı, artan arazi karmaşıklığından uydu tabanlı ürünlere nazaran daha olumsuz etkilenmektedir. Her iki birleştirme yöntemi de, ürünlerin hata ve korelasyonlarını tüm çalışma alanı boyunca geliştirmekle kalmaz; sulaklık, yükseklik ve arazi eğimine göre sınıflandırılmış olan tüm alt bölgeler için de iyileştirir. Basit birleştirme ürünlerin en çok yağış tespit becerisini geliştirmektedir. Tahmin ve araştırma ürünlerinin ErrSD ve CC değerlerindeki en yüksek iyileştirmeler ürünler

ECMWF, HRES ve IMERG ürünlerini referans olarak yeniden ölçeklendirildikten sonra birleştirildiğinde elde edilmiştir (ErrSD'de tahmin ürünleri için ortalama %28.5, araştırma ürünleri için ortalama %34.8 ve CC'de tahmin ürünleri için ortalama % 17.6, araştırma ürünleri için ortalama %23).

Anahtar Kelimeler: Yağış, Uydu, Model, Değerlendirme, Yağış Verisi Birleştirme, Değişken Topoğrafya

This thesis is dedicated to my family for their sincere love, endless support, and encouragement.

ACKNOWLEDGEMENTS

This thesis owes its conception, development, and completion to people who have broadened my horizons, supported my endeavors, and will continue to inspire me throughout my life. To my parents, whose boundless love, patience, and sacrifice are blessings I have yet to realize fully.

To Assoc. Prof. Dr. M. Tuğrul Yılmaz, my thesis supervisor and mentor who has been a veritable fount of knowledge, wisdom, and motivation, and without whom this thesis would not have come to fruition. I am bound to express immense admiration to my teachers and thesis jury members Prof. Dr. İsmail Yücel, Assoc. Prof. Dr. Koray Yılmaz, Prof. Dr. M. Lütfi Süzen, Assoc. Prof. Dr. Ahmet Öztopal and Asst. Prof. Dr. Ali Arda Şorman, for their guidance in developing an understanding of the research in the field of statistical hydrology.

Special thanks to the Higher Education Commission of Pakistan for awarding me the scholarship with funding to support my Doctorate and my stay in Turkey.

To my brother Rashid Iqbal, who has always been a personality I have relied on the most through thick and thin of my life. To my friend Uzair Hashmi, I owe you for being a motivation to approach life with more in-depth perspectives.

I am obliged to thank Ammar Ashraf, Shajeea Shuja, Hassaan Altaf, Rabela Junejo, Nasir Javed, Mansoor Ahmed, Mohsin Ali, Ishfaq Bashir, and Jawad Zaidi, whose company has been a life-changing stimulus for me. I am grateful to Ibrahim Muradov, Rizwan Aziz, and Faisal Baig for their kind support. Finally, I would like to appreciate my friends and office mates Mehdi Afshar, Burak Bulut, Eren Düzenli, and Kaveh Yousefi, your company and support have been a blessing for me.

I wish to pay my gratitude to everyone related to me; I am obliged to all the well-wishers.

TABLE OF CONTENTS

ABSTRACT	v
ÖZ	vii
ACKNOWLEDGEMENTS	x
TABLE OF CONTENTS	xi
LIST OF TABLES	xvi
LIST OF FIGURES	xix
LIST OF ABBREVIATIONS	xxii
CHAPTERS	
1. INTRODUCTION	1
1.1. Precipitation: Measurement and Applications.....	1
1.2. Evaluation of Precipitation products	2
1.2.1. Inter- comparison of Satellite- and Model-based Products	2
1.2.2. Evaluation and Inter-comparison over Varying Topography	4
1.2.3. Evaluation Studies Over Turkey.....	4
1.3. Merging the Precipitation Products	5
1.4. Motivation for this Study	6
1.5. Goals of the Study	6
1.6. Innovation in this Study	7
2. METHODOLOGY	9
2.1. Study Area.....	9
2.1.1. Terrain Complexity and Variability of Climate.....	9
2.1.2. The Sparsity of Ground-based Gauges Network	10

2.2. Datasets	11
2.2.1. Gauge-based Precipitation Observations (Reference Data)	11
2.2.2. Satellite-based Precipitation Products	12
2.2.2.1. TMPA 3B42V7	12
2.2.2.2. GPM IMERG	13
2.2.3. Model-based Reanalysis Precipitation Products	13
2.2.3.1. ECMWF ERA-Interim	14
2.2.3.2. ECMWF ERA5	14
2.2.4. Model Forecast-based Precipitation Data	15
2.2.4.1. ECMWF HRES	15
2.2.4.2. ALARO	15
2.2.4.3. WRF	16
2.2.4.4. GFS	16
2.2.4.5. CFS	17
2.2.5. Selection of Common Study Period	17
2.3. Pre-processing of Data	18
2.3.1. Quality control of Reference Data	18
2.3.2. The Rationale and Preparation of Data for Point-to-Grid Evaluation	19
2.3.3. Classification of Stations for Wetness, Elevation, and Slope	19
2.4. Evaluation of Precipitation Products	22
2.4.1. Daily Time Scale	22
2.4.1.1. Daily Evaluation statistics	22
2.4.1.2. Intensity-Frequency Analysis	23
2.4.1.3. Categorical Performance Indices	24

2.4.2. Monthly Time Scale.....	25
2.4.2.1. Time Series Plots	25
2.4.2.2. Monthly Evaluation Statistics	26
2.4.3. Annual Time Scale.....	26
2.5. Merging Precipitation Products	27
2.5.1. Preparing Datasets for Merging.....	27
2.5.2. Merging Procedure	28
2.5.2.1. Simple Merging.....	28
2.5.2.2. Merging after Regression-based Rescaling.....	29
2.5.3. Evaluation of Merged Products	31
2.5.3.1. Categorical Performance Indices	31
2.5.3.2. Intensity-Frequency Analysis.....	31
2.5.3.3. Error Statistics of Individual and Merged Products.....	31
2.5.3.4. Investigating Improvement in Accuracy of Individual Products after Merging	31
3. RESULTS AND DISCUSSION	33
3.1. Evaluation of Precipitation Products	33
3.1.1. Daily Time Scale	33
3.1.1.1. Daily Evaluation Statistics	33
3.1.1.2. Intensity-Frequency Analysis.....	39
3.1.1.3. Categorical Performance Indices	40
3.1.2. Monthly Time Scale.....	45
3.1.2.1. Time Series Plots	45
3.1.2.2. Spatial Distribution of Statistics.....	50

3.1.2.3. Temporal Statistics – The Entire Study Area	52
3.1.2.4. Temporal Statistics – Wetness Classes	55
3.1.2.5. Temporal Statistics – Elevation Classes	55
3.1.2.6. Temporal Statistics – Slope Classes	60
3.1.2.7. Correlation Histograms.....	64
3.1.3. Annual Time Scale	66
3.2. Evaluation of Merged Forecasts	69
3.2.1. Daily Evaluation Statistics	69
3.2.2. Intensity-Frequency Analysis	75
3.2.3. Categorical Performance Indices.....	76
3.2.4. Improvement in ErrSD and CC Due to Merging	78
3.3. Evaluation of Merged Research-Grade Products.....	83
3.3.1. Daily and Monthly Evaluation Statistics.....	83
3.3.2. Intensity-Frequency analysis.....	88
3.3.3. Categorical Performance Indices.....	88
3.3.4. Improvement in ErrSD and CC Due to Merging	89
3.4. Discussion	91
4. SUMMARY AND CONCLUSIONS.....	95
4.1. Summary	95
4.2. Conclusions.....	96
4.2.1. Conclusions from the Initial Evaluation of Individual Products	96
4.2.2. Conclusions from Merging of the Real-Time Forecasts	97
4.2.3. Conclusions from Merging of the Research-Grade Products.....	97
4.3. Recommendations.....	98

4.4. Future Studies.....	98
REFERENCES.....	99
CURRICULUM VITAE.....	111

LIST OF TABLES

TABLES

Table 2.1. Information about the datasets used in the study (last checked on September 2019).....	17
Table 2.2. Classification of stations of entire area based on wetness, elevation, and slope.....	22
Table 2.3. Classification of precipitation intensities	23
Table 2.4. Algorithm for categorical performance indices.....	24
Table 3.1. Daily Mean and SD for the entire study area and wetness classes.....	34
Table 3.2. Daily Bias and ErrSD for the entire study area and wetness classes.....	34
Table 3.3. Daily CC for the entire study area and wetness classes	35
Table 3.4. Daily Mean and SD for the entire study area and elevation classes.....	35
Table 3.5. Daily Bias and ErrSD for the entire study area and elevation classes.....	36
Table 3.6. Daily CC for the entire study area and elevation classes	36
Table 3.7. Daily Mean and SD for the entire study area and slope classes	37
Table 3.8. Daily Bias and ErrSD for the entire study area and slope classes	38
Table 3.9. Daily CC for the entire study area and slope classes.....	38
Table 3.10. Monthly Mean and SD for the entire area and wetness classes.....	52
Table 3.11. Monthly Bias and ErrSD for the entire area and wetness classes	53
Table 3.12. Monthly CC for the entire area and wetness classes	54
Table 3.13. Monthly Mean and SD for the entire area and elevation classes.....	56
Table 3.14. Monthly Bias and ErrSD for the entire area and elevation classes	57
Table 3.15. Monthly CC for the entire area and elevation classes	58
Table 3.16. Monthly Mean and SD for the entire area and slope classes.....	60
Table 3.17. Monthly Bias and ErrSD for the entire area and slope classes.....	61
Table 3.18. Monthly CC for the entire area and slope classes	62
Table 3.19. Annual spatial mean precipitation and its SD	66

Table 3.20. Bias and ErrSD for 1-daily individual and merged forecasts over the entire study area and different wetness classes	72
Table 3.21. CC for 1-daily individual and merged forecasts over the entire study area and different wetness classes	72
Table 3.22. Bias and ErrSD for 1-daily individual and merged forecasts over the entire study area and different elevation classes	73
Table 3.23. CC for 1-daily individual and merged forecasts over the entire study area and different elevation classes	73
Table 3.24. Bias and ErrSD for 1-daily individual and merged forecasts over the entire study area and different slope classes	74
Table 3.25. CC for 1-daily individual and merged forecasts over the entire study area and different slope classes.....	74
Table 3.26. Percent improvement, due to merging, in ErrSD for Total Precipitation of the individual products.....	78
Table 3.27. Percent improvement, due to merging, in ErrSD for Convective Precipitation of the individual products	79
Table 3.28. Percent improvement, due to merging, in ErrSD for Large-scale Precipitation of the individual products	80
Table 3.29. Percent improvement, due to merging, in CC for Total Precipitation of the individual products.....	80
Table 3.30. Percent improvement, due to merging, in CC for Convective Precipitation of the individual products	81
Table 3.31. Percent improvement, due to merging, in CC for Large-scale Precipitation of the individual products	81
Table 3.32. Monthly Bias and ErrSD for individual and merged research-grade products over the entire study area and different wetness classes	85
Table 3.33. Monthly CC for individual and merged research-grade products over the entire study area and different wetness classes	85
Table 3.34. Monthly Bias and ErrSD for individual and merged research-grade products over the entire study area and different elevation classes.	86

Table 3.35. Monthly CC for individual and merged research-grade products over the entire study area and different elevation classes.....	86
Table 3.36. Monthly Bias and ErrSD for individual and merged research-grade products over the entire study area and different slope classes	87
Table 3.37. Monthly CC for individual and merged research-grade products over the entire study area and different slope classes	87
Table 3.38. Percent improvement, due to merging, in ErrSD of the individual research-grade products.....	90
Table 3.39. Percent improvement, due to merging, in CC of the individual research-grade products.....	90
Table 0.1. Bias and ErrSD for daily individual and merged research-grade products over wetness classes	107
Table 0.2. CC for daily individual and merged research-grade products over wetness classes	107
Table 0.3. Bias and ErrSD for daily individual and merged research-grade products over elevation classes	108
Table 0.4. CC for daily individual and merged research-grade products over elevation classes	108
Table 0.5. Bias and ErrSD for daily individual and merged research-grade products over slope classes.....	109
Table 0.6. CC for daily individual and merged research-grade products over slope classes	109

LIST OF FIGURES

FIGURES

Figure 2.1. Gauge density against varying a) Elevation above MSL (m), and b) Percent Terrain Slope.....	11
Figure 2.2. (a) Locations of stations ordered using four wetness classes plotted over observed annual average precipitation map of Turkey, (b) Locations of stations ordered using five elevation classes plotted over Digital Elevation Map (m), (c) Locations of stations ordered using five slope classes plotted over percent slope map	21
Figure 2.3. Merging Methodology. (a) Simple Merging, (b) – (f): Simple Merging after regression-based rescaling using ECM, ALR, WRF, GFS, and CFS as reference product (one at a time), respectively	29
Figure 3.1. Daily precipitation intensity vs. frequency bar plots for the entire study area	39
Figure 3.2. Categorical Performance Indices, a) POD, b) FAR, and c) CSI, against different intensity thresholds over the entire study area. The dashed lines show the optimum scores for the respective CPI	40
Figure 3.3. Categorical Performance Indices. POD (from (a) to (d)), FAR (from (e) to (h)), and CSI (from (i) to (l)) against different daily precipitation intensities over wetness classes; Dry (a,e,i), Mod-Dry (b,f,j)), Mod-Wet (c,g,k)), and Wet (d,h,l)), respectively. The dashed lines show the optimum scores for the respective CPI.....	41
Figure 3.4. Categorical Performance Indices. POD (from (a) to (e)), FAR (from (f) to (j)), and CSI (from (k) to (o)) against different daily precipitation intensities over elevation classes; Elev <500 (a,f,k), Elev 500-1000 (b,g,l)), Elev 1000-1500 (c,h,m)), Elev 1500-2000 (d,i,n)), Elev >2000 (e,j,o)), respectively. The dashed lines show the optimum scores for the respective CPI	43

Figure 3.5. Categorical Performance Indices. POD (from (a) to (e)), FAR (from (f) to (j)), and CSI (from (k) to (o)) against different daily precipitation intensities over slope classes; Slope <5% (a,f,k), Slope 5-10% (b,g,l), Slope 10-15% (c,h,m), Slope 15-20% (d,i,n), Slope >20% (e,j,o), respectively. The dashed lines show the optimum scores for the respective CPI 44

Figure 3.6. Monthly time series over the entire study area. a) complete time series, b) climatology, and c) anomaly. The color-coded horizontal lines in the climatology plot show the mean monthly precipitation for the respective datasets. The horizontal line in the anomaly plot shows zero anomaly level 45

Figure 3.7. Monthly climatology (from (a) to (d)) and monthly anomaly (from (e) to (h)) for wetness classes. The color-coded horizontal lines in the climatology plot show the mean monthly precipitation for the respective datasets. The horizontal line in the anomaly plot shows zero anomaly level 47

Figure 3.8. Monthly climatology (from (a) to (e)) and monthly anomaly (from (f) to (j)) for elevation classes. The color-coded horizontal lines in the climatology plot show the mean monthly precipitation for the respective datasets. The horizontal line in the anomaly plot shows zero anomaly level 48

Figure 3.9. Monthly climatology (from (a) to (e)) and monthly anomaly (from (f) to (j)) for slope classes. The color-coded horizontal lines in the climatology plot show the mean monthly precipitation for the respective datasets. The horizontal line in the anomaly plot shows zero anomaly level 49

Figure 3.10. Spatial distribution maps for monthly Bias (mm/month). Negative values denote dry Bias while positive ones denote wet Bias 50

Figure 3.11. Spatial distribution maps for monthly RMSE (mm/month) 51

Figure 3.12. Boxplots for monthly absolute Bias (from (a) to (e)) and monthly ErrSD (from (f) to (j)) for elevation classes 59

Figure 3.13. Boxplots for monthly absolute Bias (from (a) to (e)) and monthly ErrSD (from (f) to (j)) for slope classes 63

Figure 3.14. Histograms of monthly CC between the observed data and research-grade products; (a) Complete Time Series, (b) Climatology, and (c) Anomaly. The color-

coded vertical lines show mean monthly CC for the respective dataset with the observed data.....	64
Figure 3.15. Histograms of monthly CC between the observed data and research-grade products; (a) Complete Time Series, (b) Climatology, and (c) Anomaly. The color-coded vertical lines show mean monthly CC for the respective dataset with the observed data.....	65
Figure 3.16. Spatial distribution maps for annual average precipitation (mm/year) .	67
Figure 3.17. Annual average precipitation against varying (a) elevations, and (b) slopes.....	68
Figure 3.18. For individual and merged forecasts, boxplots for 1-daily CC (from (a) to (c)), Bias (from (d) to (f)), and ErrSD (from (g) to (i)) for TP, CP and LSP. The bold black dots show the mean of the particular statistics	70
Figure 3.19. Intensity-frequency analysis for 1-daily (a) TP, (b) CP, and (c) LSP. .	75
Figure 3.20. 1-daily Categorical Performance Indices. POD for TP, CP, and LSP ((a) to (c)); FAR for TP, CP, and LSP ((d) to (f)); CSI for TP, CP, and LSP ((g) to (i)). The bold black dots represent mean values for the particular CPI.....	77
Figure 3.21. Comparison of improvement, due to two merging methods, in ErrSD for TP (a), CP (b), and LSP (c) and CC for TP (d), CP (e), and LSP (f).....	82
Figure 3.22. For individual and merged research-grade products, boxplots for daily (a) and monthly (b) CC, daily (c) and monthly (d) Bias, and daily (e) and monthly (f) ErrSD. The bold black dots show the mean of the particular statistics.....	84
Figure 3.23. Daily intensity-frequency analysis of individual and merged research-grade products	88
Figure 3.24. Daily Categorical Performance Indices for individual and merged research-grade products. (a) POD, (b) FAR, and (c) CSI. The bold black dots represent mean values for the particular CPI.....	89
Figure 3.25. The improvement, added by SimpMRG, in the daily and monthly statistics of the individual research-grade products. (a) ErrSD and (b) CC.....	91

LIST OF ABBREVIATIONS

ABBREVIATIONS

WMO	World Meteorological Organization
NASA	National Aeronautics and Space Administration
MGM	Meteoroloji Genel Müdürlüğü (General Directorate of Meteorology)
ECMWF	European Centre of Medium-range Weather Forecast
NCEP	National Centers for Environmental Prediction
NCAR	National Center for Atmospheric Research
TRMM	Tropical Rainfall Measuring Mission
TMPA	TRMM Multi-satellite Precipitation Analysis
GPM	Global Precipitation Measurement
IMERG	Integrated Multi-satellite Retrievals for GPM
GCM	General Circulation Model
ERA-Interim	ECMWF Re-Analysis Interim
ERA5	5th generation of ECMWF Re-Analysis
HRES	High-Resolution
ALADIN	Aire Limitée Adaptation Dynamique Développement International
AROME	Application of Research to Operations at Mesoscale
ALARO	ALadin–AROME
WRF	Weather Research and Forecasting Model
GFS	Global Forecast System

CFS	Climate Forecast System
MW	Microwave
IR	Infrared
TMI	TRMM Microwave Imager
GMI	GPM Microwave Imager
DPR	Dual-frequency Precipitation Radar
IFS	Integrated Forecasting System
ARPEGE	Action de Recherche Petite Echelle Grande Echelle
MARS	Meteorological Archival and Retrieval System
3MT	Modular Multiscale Microphysics and Transport
RT	Real-Time
UTC	Coordinated Universal Time
SRTM	Shuttle Radar Topography Mission
DEM	Digital Elevation Map
NDVI	Normalized Difference Vegetation Index
MSL	Mean Sea Level
TP	Total Precipitation
CP	Convective Precipitation
LSP	Large-Scale Precipitation
SD	Standard Deviation
ErrSD	Error Standard Deviation
RMSE	Root Mean Square Error

CC	Correlation Coefficient
CPI	Categorical Performance Index
POD	Probability of Detection
FAR	False Alarm Ratio
CSI	Critical Success Index

CHAPTER 1

INTRODUCTION

1.1. Precipitation: Measurement and Applications

Precipitation is a vital element of the global hydrological and energy cycles and one of the most critical parameters for a range of natural and socioeconomic systems such as water resources management, agriculture, forestry, tourism, flood protection, and drought management. Being one of the most significant elements in the water and energy cycles (Kucera et al., 2013), a quantitative appraisal of precipitation amount and its spatiotemporal distribution is essential for many scientific and operational applications. However, the spatiotemporal heterogeneity of precipitation makes its correct estimation very difficult (Herold et al., 2016), especially with high spatial and temporal resolutions.

Precipitation is currently being determined by utilizing four major methodologies: ground-based gauges, ground-based remote sensing radars, remote sensing satellites, and atmospheric retrospective-analysis models (Michaelides et al., 2009). Ground-based gauge observations can be considered to be the most forthright and correct source of precipitation data (Ma et al., 2015). However, their installation and maintenance costs cause sparsely or unevenly distributed ground-based rain gauge networks in many areas of the world, which is the case, especially in several developing countries (Hughes, 2006). While the radars can monitor large areas with high spatial and temporal resolutions, their observations suffer from various error sources like mean-field systematic errors, systematic errors due to range, and random errors (Dinku et al., 2002). Model- and satellite-based estimates of precipitation may be considered as potential alternative sources of precipitation data as they offer spatially and temporally continuous and consistent estimates for a broad set of

variables including precipitation. However, despite their spatial and temporal advantages, both the satellite- and model-based products have been reported to have certain biases and errors (Chakraborty, 2010; Derin et al., 2016; Durai et al., 2010; Ghajarnia et al., 2015; Wang et al., 2010; Yuan et al., 2017). Hence, the accuracy and quality of these products should be carefully investigated before utilizing them in various applications requiring high-quality precipitation data.

1.2. Evaluation of Precipitation products

Several quasi-global satellite precipitation products with a variety of spatial and temporal resolutions have been established in recent years. Widely used satellite-based precipitation products include Tropical Rainfall Measuring Mission (TRMM) Multi-satellite Precipitation Analysis (TMPA) (Huffman et al., 2007) and IMERG (the Integrated Multi-satellitE Retrievals for Global Precipitation Measurement (GPM)) (Huffman et al., 2015). In addition to the satellite-based precipitation data sources, there are several centers releasing weather forecasts and reanalysis with various spatial and temporal resolutions by using global general circulation models (GCMs) (Chakraborty, 2010). Some of the model-based products from such centers include ERA-Interim (Dee et al., 2011) and ERA5 (Herbach and Dee, 2016) reanalysis products from European Centre of Medium-range Weather Forecast (ECMWF), High Resolution (HRES) deterministic forecasts from ECMWF, ALadin–AROME (ALARO, from AROME [Application of Research to Operations at Mesoscale] system of ALADIN model from Météo-France), Weather Research and Forecasting Model (WRF, maintained by Mesoscale and Microscale Meteorology Laboratory of National Center for Atmospheric Research (NCAR)), Global Forecast System (GFS, produced by National Centers for Environmental Prediction (NCEP)) and The Climate Forecast System (CFS, maintained by the National Centers for Environmental Prediction (NCEP)).

1.2.1. Inter- comparison of Satellite- and Model-based Products

The real added utility of the products estimated from different platforms via the observing sensors, retrieval algorithms, and/or dataset estimation methodologies is better understood when the products are validated using ground station-based observations and via inter-comparison studies validating multiple products simultaneously for the same location and time. Several studies in the literature focused on inter-comparison of satellite-based products only (e.g., Cai et al., 2016; Derin and Yilmaz, 2014; Guo et al., 2016; He et al., 2017; Murali Krishna et al., 2017; Prakash et al., 2018, 2016; Tan and Duan, 2017; Tang et al., 2016; Wang et al., 2017; Xu et al., 2017; Yuan et al., 2017; Zhang et al., 2018), or model-based products only (e.g., Davis et al., 2006; Done et al., 2004; Durai et al., 2010; Hamill et al., 2008; Manzato et al., 2016; Pappenberger and Buizza, 2009; Sooraj et al., 2012; Wang et al., 2010; Wolff et al., 2014; Ye et al., 2014), whereas the number of studies focusing on inter-comparison of both the satellite- and model-based products is relatively less (e.g., Chakraborty, 2010; Derin et al., 2016; Hénin et al., 2018; Li et al., 2018; Sahlu et al., 2017; Sharifi et al., 2016; Thiemig et al., 2012; Tong et al., 2014). Nevertheless, among the studies inter-comparing satellite- and model-based products, some of them (e.g., Chakraborty, 2010; Thiemig et al., 2012; Tong et al., 2014) have been completed before the release of some of the most promising recently-released products like IMERG (released in 2014) or ERA5 (released in 2018), some of them (e.g., Sahlu et al., 2017) did not include the recently-released products (e.g., ERA5 and IMERG), and some studies (e.g., Hénin et al., 2018; Sharifi et al., 2016) did not evaluate and inter-compare the products comprehensively (i.e., evaluating them over considerable span of time, area and number of gauges which could result in generalization of the error statistics of the products). There is a motivating gap in the literature regarding comprehensive studies that could consider evaluation and inter-comparison of the recently released satellite- and model-based products.

1.2.2. Evaluation and Inter-comparison over Varying Topography

Compared to non-complex (relatively flatter) topography, different factors may drive the accuracy of satellite- and model-based precipitation products over complex topography (i.e., having a high slope and/or elevation). Local and regional topographical complexity has the potential to exert a profound impact on atmospheric lapse rate and mesoscale circulations. In the regions having complex topography, extreme events show significant temporal and spatial variations and generate extensive amounts of precipitation in short durations, while the phenomenon associated with non-complex topography is expected to have less variability. Additionally, as compared to non-complex topography, complex topography is more prone to disasters like flash floods; highlighting different levels of significance of accurate estimation of precipitation over the regions with these two kinds of topography. Hence, for any given product, the performance results over complex and non-complex areas have their individual implications. Several studies (e.g., Beck et al., 2019; El Kenawy et al., 2015; Mayor et al., 2017; Sharifi et al., 2016) conducted the performance assessment of satellite- and model-based products over varying topography (considering both the complex and non-complex topography simultaneously). However, most of these studies, except Beck et al. (2019), have not included the recently released products like IMERG and ERA5. Similarly, some of these studies (Mayor et al., 2017; Sharifi et al., 2016) evaluated precipitation products for short/limited duration, so that estimated errors may not reflect long term error statistics. Accordingly, there is a pressing need for more studies comprehensively investigating the performances of recently released and their predecessor precipitation products with a varying topography focus.

1.2.3. Evaluation Studies Over Turkey

Characterized with varying climate and complexity, Turkey has terrain which varies in complexity owing to the high mountains stretching in east-west direction over both the northern and the southern parts while relatively flatter regions located in the central

parts of the country. There are some studies performed to characterize the accuracy of precipitation products over Turkey (Bıyık et al., 2009; Demir et al., 2018; Derin and Yilmaz, 2014; Toros et al., 2018; Yucel, 2015; Yucel et al., 2011; Yucel and Onen, 2014). However, these studies remain limited and narrow-focused (i.e., either used a low number of stations in validation efforts, implemented over limited regions, focused only on short precipitation events occurring within 1-2 days, or used only one or two products). Hence, more comprehensive studies are still needed by using more datasets acquired over more stations and representing more extended periods to characterize better the uncertainty of widely used recent precipitation products over this region, which is known for its varying climatic and topographical conditions.

1.3. Merging the Precipitation Products

Merging of precipitation datasets from different sources has been demonstrated to improve the overall quality of precipitation data. Several studies in the literature (e.g., Beck et al., 2019; Berg et al., 2016; Berndt et al., 2014; Boudevillain et al., 2016; Chiang et al., 2007; Goudenhoofd and Delobbe, 2009; Li and Shao, 2010; Rozante et al., 2010; Scheel et al., 2011; Yilmaz et al., 2010; Verdin et al., 2015; Woldemeskel et al., 2013; Xie and Xiong, 2011) have worked on improving various radar-, satellite- and model reanalysis-based precipitation products by merging them with data observed at ground-based gauges. Different merging techniques, including Bayesian kriging approach (Verdin et al., 2015), linearized weighting procedure (Woldemeskel et al., 2013), optimal interpolation technique (Xie and Xiong, 2011), ordinary cokriging algorithm (Scheel et al., 2011) and nonparametric kernel smoothing method (Li and Shao, 2010), have been adopted in the literature to merge different satellite-based and/or model-based reanalysis products with the gauge-based observed data on daily to monthly time scales. Moreover, Bayesian merging method (Luo et al., 2007) has been used to merge monthly precipitation forecasts with the observed climatology, while weighted average method (Xie and Arkin, 1996) was used to blend satellite-based estimates and model-based forecasts with the observed data on a monthly time scale. Systematic differences between variety of merged products exist; hence, in

order to improve the accuracy of the merged products reducing the systematic errors between them is necessary. Among merging methodologies, however, merging after rescaling the precipitation datasets using linear regression has never been conducted (although this technique has been used for merging different soil moisture datasets by Yilmaz and Crow, 2013). Another significant gap in the literature is that real-time (e.g., 1-3 daily) forecasts have never been merged to improve their statistical accuracy and applicability for operational purposes.

1.4. Motivation for this Study

Firstly, a comprehensive study, not only simultaneously considering evaluation and inter-comparison of several recently released precipitation products from various platforms like model-based forecast, model-based reanalysis and remote sensing-based estimates but also assessing their performance over varying climatic conditions and terrain complexity, is lacking. Secondly, although merging products from different sources has been reported to be improving their overall accuracy, there have been no effort (in our knowledge) to merge different real-time precipitation forecasts with the intention to get a better real-time input for operational fields, as improving the quality of precipitation forecasts might have definite implications in flood forecasting, natural hazard management and different water resources management processes. Thirdly, the impact of merging the precipitation products after rescaling them by linear regression has not been studied in the literature.

1.5. Goals of the Study

The goals of this study are:

1. A comprehensive evaluation of recently released precipitation products from model-based forecasts (ECMWF HRES, ALARO, WRF, GFS, and CFS), model-based reanalysis (ERA-Interim and ERA5), and satellite-based estimates (TMPA 3B42V7 and GPM IMERGv05) by using precipitation data from ground-based gauges as reference data over varying topographical and climatic conditions to assess the error variations associated with each product over daily, monthly and annual time scales.

2. Merging different real-time (1-3 daily) precipitation forecasts (ECMWF HRES, ALARO, WRF, GFS, and CFS) and assessing the impact of merging on their error variance.

3. Merging different post-real-time precipitation products (ERA-Interim, ERA5, TMPA 3B42V7, and GPM IMERGv05) and assessing the impact of merging on their error variance.

1.6. Innovation in this Study

Firstly, this study intends to comprehensively evaluate a set of nine precipitation products (including forecasts, reanalysis and satellite-based estimates) over varying topographical and climatic conditions of Turkey. Secondly, for the first time, this study merges up-to-date and state of the art satellite- and model- based products with special emphasis on varying climate and complexity of terrain. Thirdly, to author's knowledge, no study has ever merged different real-time (operational) forecasts; this study intends to merge them and to assess the impact of merging on their statistical performance. Lastly, this study is the first to apply the technique of merging different precipitation products after rescaling them, and to investigate the added utility of this technique of merging.

CHAPTER 2

METHODOLOGY

2.1. Study Area

2.1.1. Terrain Complexity and Variability of Climate

The study area is selected as Turkey, having an area of 783,500 km². The area is situated in the Mediterranean region with temperate climatic conditions, but in general, the diverse nature of its landscape and presence of the mountains contribute to significant differences in climatic conditions from one region to the other. The coastal areas enjoy milder climates while inland Anatolian plateau experiences extremes of hot summers and cold winters with limited precipitation (Sensoy, 2004). Depending on location, the annual precipitation in Aegean and Mediterranean coasts ranges between 580 mm and 1300 mm. The eastern coast of the Black Sea region receives 2200 mm annual precipitation and is the only region of the study area that receives precipitation throughout the year. The amount of total precipitation on the coastal and inland stations differs significantly due to mountain blockage. For example, Antalya station, which is located at the Mediterranean coast in the windward side of the Taurus Mountain, receives three times a higher amount of annual precipitation compared to Karaman and Burdur stations which are situated in the leeward side of that mountain. Similar mountain blockage makes the precipitation highly variable along the northern Black Sea Region (Derin and Yilmaz, 2014; Sensoy, 2004) where a coastal station (windward), named Hopa, receives 2182 mm annual rainfall while an inland station (leeward), named Bayburt, receives only 420 mm. Overall, the entire country consists of undulating regions, while most of the high mountainous ranges are situated in the eastern and northeastern parts of the country. Very long coastlines draw its borders with the Black Sea in the north, the

Mediterranean Sea in the south, and the Aegean Sea in the west. Most of the relatively flat and low-land areas are situated in western regions while most of the high-land areas and high mountainous areas are located in the eastern regions. Black Sea region (northeast of Turkey) and some of the southeastern regions have relatively higher mountainous areas there.

The term “complex topography” has been widely used in the literature to refer to the regions with high elevation (e.g., Hirpa et al., 2010) or standard deviation of elevation (e.g., Chiaravalloti et al., 2018). Even though more complex topographies are associated with a higher tendency to receive more orographic precipitation than less complex topographies, there seems a need to make a clear consensus over the definition of the term complex topography. Following earlier studies, this study associates the topographical complexity with slope and elevation, but it also classifies the regions into different classes of elevation and slope and specifies clearer thresholds for those classes.

2.1.2. The Sparsity of Ground-based Gauges Network

The ground-based gauge station density (area per gauge station) against the increasing elevation above mean sea level (MSL) is shown in Figure 2.1a and increasing terrain slope in Figure 2.1b. The proportion of the number of gauge stations is lower in the case of areas with higher elevations and slopes. World Meteorological Organization (WMO) standards suggest an average gauge density of 1 gauge per 575 km² area for hilly/undulating regions while 1 gauge per 250 km² area in case of mountainous regions (Awadallah, 2012). In the case of the study area under consideration, the rain gauges are sparser (especially at higher elevation and slope zones) than the average rain gauge density defined by WMO standards. Taking example of regions with slopes steeper than 15% (which could be associated with highly undulating or mountainous areas), gauge station density in the study area is one gauge station for an area of above 6000 km², which is way lower than the density (1 gauge per 250 km²) defined by WMO. This lower station density would impact the calculation of area-averaged

precipitation estimates over selected regions of interest. Therefore, here in this study, area-averaged estimates are not analyzed (rather station-based estimates, which are point data in nature, are utilized in the analyses). The detailed rationale for using station-based data (instead of area-averaged data) is discussed in section 2.3.2.

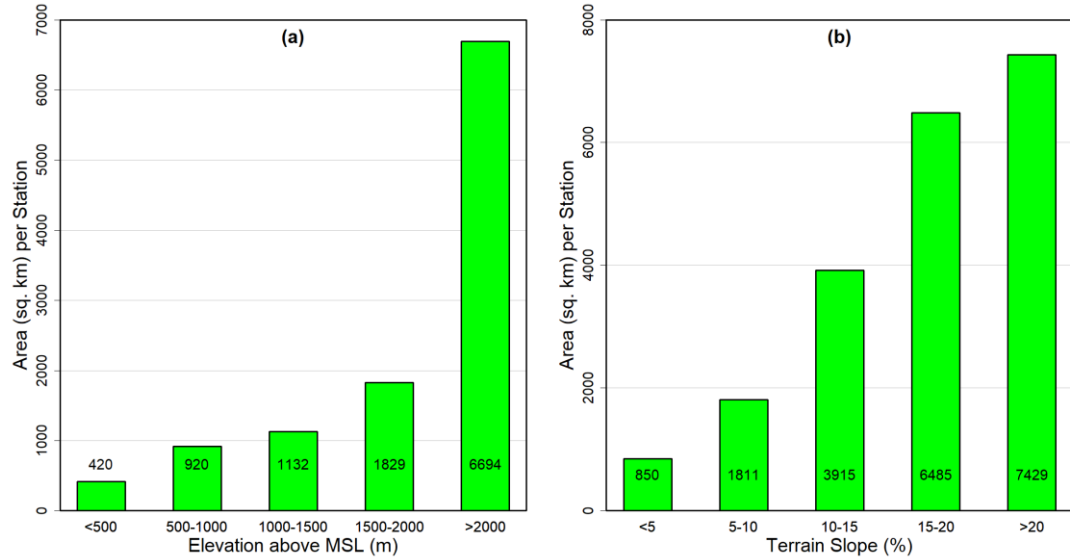


Figure 2.1. Gauge density against varying a) Elevation above MSL (m), and b) Percent Terrain Slope

2.2. Datasets

This study uses two satellite-based estimates, two model-based reanalysis products, five model-based forecasts, and their merged products for evaluation using ground-based observed precipitation data over gauge stations (755 in total). The detailed description of the input datasets is given below.

2.2.1. Gauge-based Precipitation Observations (Reference Data)

Subject to its availability, precipitation data observed through ground-based gauge stations can be considered as the most reliable data. Hence, evaluating the remotely sensed and model-based estimated precipitation datasets by using gauge stations data as a reference is the most common procedure in the literature adopted for accuracy assessment of those datasets.

Precipitation data from gauge stations (1936 in total) spread all over Turkey was obtained from the General Directorate of Meteorology (Turkish acronym: Meteoroloji Genel Müdürlüğü [MGM]) of Turkey. The obtained data contained certain discrepancies including outliers, discontinuities, and repetition of data entries. Therefore, it was undergone through certain quality control procedures to remove outliers or any apparent discrepancies in the raw data. The adopted quality control procedure is described in detail in Section 2.3.1. The daily precipitation data for a period of ~5.5 years (January 2014 to May 2019) from the stations passing the quality control filters were used for evaluation of individual products and further analyses.

2.2.2. Satellite-based Precipitation Products

Two satellite-based precipitation products were considered in this study for evaluation and further processes. A detailed description of each of these products is provided in the following paragraphs.

2.2.2.1. TMPA 3B42V7

The TMPA algorithm merges several ground-based observations (in the non-real-time products) with two types of satellite-based observations (i.e., microwave [MW] and infrared [IR]). The MW sensors include the Advanced Microwave Scanning Radiometer-Earth Observing System, Advanced Microwave Sounding Unit-B, TRMM Microwave Imager (TMI), and the Spectral Sensor Microwave Imager/Sounder, which combine to make the 3B40RT product. The IR observations combine the geostationary satellites. The MW and IR observations constitute the TMPA 3B40RT and 3B41RT products, respectively. Together these products are used to generate the 3B42RT product, which when combined with the Global Precipitation Climatology Center (GPCC), TMI, and TRMM Precipitation Radar produce the post-real-time 3B42 product (Huffman and Bolvin, 2018; Yong et al., 2014). Hence, the TMPA 3B42 retrievals consist of two products: near-real-time (3B42RT, spatial coverage: 60°N–60°S) and research-grade (3B42, spatial coverage: 50°N–50°S). The former is less accurate (Milewski et al., 2015) but provides estimates suitable for near-

real-time monitoring and modeling activities (Wu et al., 2012). The latter, available approximately two months after observation, is released after calibration with gauge data, different sensor calibration, and additional post-processing in the algorithm. The resulting product is more accurate and suitable for research (Huffman et al., 2007; Huffman and Bolvin, 2018). This study uses daily precipitation data from version 7 of research-grade daily product, TMPA 3B42V7, that has 0.25° spatial resolution.

2.2.2.2. GPM IMERG

The GPM Core Observatory carries a dual-frequency precipitation radar (DPR; the Ku-band at 13.6 GHz and Ka-band at 35.5 GHz) and a conical-scanning multi-channel GPM Microwave Imager (GMI; frequencies range between 10 and 183 GHz). GPM extends the sensor package compared to TRMM instruments, which had a single-frequency precipitation radar (PR) and a multichannel TRMM Microwave Imager (TMI). Therefore, the GPM sensors can detect light and solid precipitation more accurately than TRMM sensors (Hou et al., 2014). GPM IMERG algorithm provides three levels of products, including the near-real-time “Early” and “Late” run products, and the post-real-time “Final” run product, which is considered as a research-grade product. This study focuses on the Level-3 “Final” product, which is released after inter-calibration, merging, and interpolation of all microwave estimates of the GPM constellation, infrared estimates, gauge observations, and other data from potential sensors at $0.1^\circ \times 0.1^\circ$ (Huffman et al., 2015). The product used in this study is 3IMERGDFv05 (DFv05 denotes version 5 of Daily Final run product) with a spatial resolution of $0.1^\circ \times 0.1^\circ$.

For brevity, the short names IMERG and TMPA, are used from here on instead of complete names of satellite-based products, GPM 3IMERGDFv05 and TMPA 3B42V7, respectively.

2.2.3. Model-based Reanalysis Precipitation Products

Reanalysis datasets are generated by a data assimilation system combining observations with a numerical weather prediction model. For the entire reanalysis

period, the model physics remain unchanged in the forecast model for consistency of the output data. The reanalysis consequently provides a picture of the global climate over a period during which observational data are available. Reanalysis data can provide a multivariate, spatially complete, and coherent record of the global atmospheric circulation (Dee et al., 2011).

2.2.3.1. ECMWF ERA-Interim

The ECMWF ERA-Interim reanalysis (Dee et al., 2011) dataset is produced with a sequential data assimilation scheme, advancing forward in time using 12-hourly analysis cycles. In each cycle, available observations are combined with prior information from a forecast model to estimate the evolving state of the global atmosphere and its underlying surface. The analyses are then used to initialize a short-range model forecast, which provides the prior state estimates needed for the next analysis cycle. The spatial resolution of ERA-Interim data is 79 km (T255 spectral truncation) (Dee et al., 2011). For ERA-Interim data retrieval, the ECMWF web applications server (<http://apps.ecmwf.int>) offers a default spatial resolution grid of 0.75° as well as other spatial-resolution grids (ranging from 0.125° to 3°) based on a bilinear interpolation technique for continuous parameters. In this study, 0.75° spatial resolution for the ERA-Interim product is used.

2.2.3.2. ECMWF ERA5

In 2017, the ECMWF released a new reanalysis data ERA5 (Herbach and Dee, 2016). There are major improvements in ERA5 compared with ERA-Interim. For example, ERA5 provides datasets starting from 1950 (ERA-Interim from 1979) to present, has 0.25° spatial resolution (ERA-Interim has 0.75°) and hourly analysis fields (ERA-Interim has 6-hourly), improved variational bias scheme (in addition to satellite radiances now ozone, aircraft and surface pressure data are also used), includes more information on variation in quality over space and time, an improved representation of troposphere, better global balance of precipitation and evaporation, and more consistent sea surface temperature and sea ice coverage (Herbach and Dee, 2016). This

study uses ERA5 daily accumulated reanalysis data at the native spatial resolution of 0.25°.

For brevity, the short name ERAint is used from here on instead of the complete name of ERA-Interim.

2.2.4. Model Forecast-based Precipitation Data

This study uses five model-based precipitation forecast products including: (1) HRES deterministic forecasts from ECMWF, (2) ALARO forecasts, (3) WRF forecasts, (4) GFS forecasts, and (5) CFS forecasts.

2.2.4.1. ECMWF HRES

For the medium-range forecasts based on ECMWF Integrated Forecasting System (IFS), an ensemble of 52 individual ensemble members are created twice a day. One member is at a higher spatial resolution than the other members (called the HRES at ECMWF), its initial state is the most accurate estimate of the current conditions, and it uses the current best description of the model physics. It provides a highly detailed description of future weather and, averaged over many forecasts, it is considered as the most accurate forecast for a certain period, which is currently estimated as ten days for large scale properties of the atmosphere. This study used 1-daily accumulated total precipitation (TP) forecasts from these deterministic forecasts (with a spatial resolution of 0.1°) from ECMWF for initial evaluation, and 1-3 daily accumulated total precipitation (TP), convective precipitation (CP) and large-scale precipitation (LSP) forecasts for further merging analyses. These datasets can be retrieved from the Meteorological Archival and Retrieval System (MARS) of ECMWF.

2.2.4.2. ALARO

As the AROME software is computationally expansive, particularly for real-time weather forecasting, a framework for the transition, called ALARO, has been developed, based on the ALADIN model with a refined formulation of the physical parameterizations. ALARO uses an AROME-oriented mesoscale physics, and the aim

of this canonical configuration of the ALADIN System is to provide a setup that can also be used in intermediate resolutions between the mesoscale and the convection-permitting scales. For moist deep convection, the Modular Multiscale Microphysics and Transport scheme (3MT) has been developed to overcome problems when convection gets partly resolved at the so-called gray-zone model resolutions. The ALARO configuration is built upon this physics parameterization concept relying on the governing equations for the moist physics. Operational ALARO Turkey cycle 40t1 has 4.5 km horizontal resolution and 60 vertical layers. Boundary conditions are applied at 3-hour intervals from the global model ARPEGE (Action de Recherche Petite Echelle Grande Echelle). The model is run four times (00, 06, 12, and 18 UTC), and forecasts up to 72 hours are produced.

2.2.4.3. WRF

WRF, maintained by Mesoscale and Microscale Meteorology Laboratory of National Center for Atmospheric Research (NCAR), produces simulations based on actual atmospheric conditions (i.e., from observations and analyses) or idealized conditions. Running WRF model to get high-resolution precipitation data needs high-tech assembly of simulation running machines and currently, MGM has facilities to provide WRF data to the end-users. The data can be obtained at a spatial resolution of ~4.5 km.

2.2.4.4. GFS

GFS, produced by the National Centers for Environmental Prediction (NCEP), uses a coupled model to provide an accurate picture of weather conditions. Its forecasts starting from 2015 to today can be retrieved from the archive of the National Center for Atmospheric Research (NCAR) at a spatial resolution 0.25°. This study used 1-daily accumulated (derived from 6-hourly) total precipitation forecasts for initial evaluation analyses, while 1-3 daily accumulated (derived from 6-hourly) total precipitation, convective precipitation, and large-scale precipitation forecasts were utilized in further analyses related to merging of real-time forecasts.

2.2.4.5. CFS

CFS, maintained by the National Centers for Environmental Prediction (NCEP), is a model representing the global interaction between Earth's oceans, land, and atmosphere. CFS models are used in producing precipitation data reanalysis, reforecasting, and forecasting (based on reanalysis). This study used 1-daily (derived from 6-hourly) TP and CP data (with a spatial resolution of 0.5°) retrieved from NCAR archive. LSP data was further obtained by subtracting CP from TP.

For brevity, simple names (ECM, ALR, WRF, GFS, and CFS) will be used from here on instead of complete names of the real-time forecast products.

2.2.5. Selection of Common Study Period

Table 2.1 shows the maximum available period for each of the included datasets. Including the recently released precipitation products required a compromise on the length of the common study period. Hence, the longest possible common period of ~72 months (2014-2019) was selected as the study period for evaluation and merging of the precipitation products.

Table 2.1. *Information about the datasets used in the study (last checked on September 2019)*

Sr. No.	Dataset	Type	Spatial Resolution	Temporal Resolution	Availability Period	Source
1	Observed Data	Ground-based Gauges data	-	1-daily	2003-201905	MGM, Turkey
2	GPM 3IMERGDFv05	Satellite-based Estimates (Research-grade product)	0.1°	1-daily (Derived)	201404-201806	NASA Earth Data, Huffman et al. (2015)
3	TMPA 3B42V7	Satellite-based Estimates (Research-grade product)	0.25°	1-daily (Derived)	1998-201907	NASA Earth Data, Huffman et al. (2007)
4	ERA-Interim	Model-based Reanalysis	0.75°	1-daily	1979-201906	ECMWF, Dee et al. (2011)
5	ERA5	Model-based Reanalysis	0.25°	1-daily (Derived)	1979-201906	ECMWF, Herbach and Dee (2016)
6	ECMWF HRES	Model-based Forecasts	0.1°	1-3 daily	2007-201909	ECMWF MARS Archive
7	ALARO	Model-based Forecasts	0.045°	1-3 daily	2011-2018	MGM, Turkey
8	WRF	Model-based Forecasts	~0.045°	1-3 daily	2013-2018	MGM, Turkey
9	GFS	Model-based Forecasts	0.25°	1-3 daily (Derived)	2015-201909	NCEP, NCAR Archive
10	CFSv2	Model-based Forecasts	0.5°	1-3 daily (Derived)	2011-201909	NCEP, NCAR Archive

2.3. Pre-processing of Data

2.3.1. Quality control of Reference Data

Observed daily precipitation data over a total of 1936 gauge stations managed by Turkish State Meteorological Services (MGM) for a period of 16.5 years (January 2003 to May 2019) was initially obtained from MGM. The data was then subjected to a certain quality control procedure to remove any discontinuities or outliers. The adopted quality control procedure is described in the following paragraphs.

To remove outliers in the daily precipitation data, it was passed through a maximum precipitation threshold filter of 466 mm/day (which is, according to MGM, the most extreme daily precipitation observed in the recorded history of Turkey). After that, the remained daily data from those 1936 stations were trimmed to the required study period (~2014-2019). A further quality control procedure was applied to the daily data, which consisted of removing the stations with significant data gaps, removing the stations having many repeated data entries, and removing the stations with zero long term monthly means. Moreover, the stations whose average annual precipitation for the entire study period differed more than 200 mm/year from their long-term average annual precipitation were also removed. Finally, the stations whose data is being shared with the World Meteorological Organization (WMO) were excluded to ensure the independence of the reference dataset from the satellite- and the model-based datasets.

It is to note that most of the threshold filters during the quality control procedure were specified after getting information from MGM. Nevertheless, after application of all the quality control steps, the remaining daily data for 5.5 years (January 2014 to May 2019) from 755 gauge stations spread all over Turkey was utilized as the reference data for evaluation of individual precipitation products and further processes.

2.3.2. The Rationale and Preparation of Data for Point-to-Grid Evaluation

First, as the gauge-based observation data is point data in its kind, potential errors are resulted when interpolation techniques are applied to convert the point data into continuous spatial precipitation data (Kidd and Huffman, 2011). Moreover, the spatial representativeness of gauge-based observations (i.e., point) and satellite- and model-based datasets (i.e., grids) is different. In the studies performing comparisons of such datasets, in general, two different methodologies are commonly used to reconcile the spatial scale differences between the gauges data and the products: either the grids of satellite and the model data that are closest to the gauge stations are extracted (point-to-grid methodology following El Kenawy et al., 2015; Heidinger et al., 2012; Islam et al., 2012) or the station-based observations within the grids of satellite/model datasets are averaged so that a compatible and spatially distributed estimate can be obtained. Over many locations of the world, when a dense network of precipitation gauges is absent and/or in the case of precipitation products with coarse spatial resolution (like in our case: $\sim 0.10^\circ - 0.25^\circ$) are evaluated, only minority of the grids contain more than single station; hence, the second methodology is not viable in this study. Here in this study, the first methodology is adopted for all the analyses (i.e., data for satellite and model grids closest to the stations are extracted).

Following the above-discussed methodology, daily data from all nine precipitation products (gridded in nature), other than gauges data, were extracted over the locations of 755 gauge stations for compatible comparison between the observed and products data. Hence, a total of 10 datasets (including the observed data) over 755 stations were made ready for the further analyses.

2.3.3. Classification of Stations for Wetness, Elevation, and Slope

As mentioned in Section 2.1.1, the study area is quite diverse regarding the terrain complexity and varying climate. This diversity required a detailed evaluation of the precipitation products as the conclusions over the entire area would not be enough to make any generalization about the performance accuracy of the products. This

motivated the classification of the stations (755 in total) based on wetness, terrain elevation, and terrain slope so that the performance of the products could be investigated over varying climate and terrain complexity; where this study associates the climate variability with wetness and terrain complexity with elevation and slope.

For the classification based on wetness, the stations of the entire study area were grouped into four wetness classes: dry, moderately dry, moderately wet, and wet. Four arbitrary thresholds of average monthly precipitation amount of observed data (< 40, 40-60, 60-80, and > 80 mm/mon) were used to define wetness (dry, moderately dry, moderately wet, and wet, respectively) of individual stations (Table 2.2). Figure 2.2a shows locations of the stations of wetness classes plotted over the observed annual average precipitation map of Turkey. Under the elevation classification, the stations were grouped into five classes (i.e., <500 m, 500-1000 m, 1000-1500 m, 1500-2000 m, and >2000 m) depending on the elevation of individual stations above MSL (Table 2.2 and Figure 2.2b). Similarly, the stations were grouped into five classes (i.e., <5%, 5-10%, 10-15%, 15-20%, and >20%) based on percent terrain slope (Table 2.2 and Figure 2.2c). For elevation and slope classifications, 1 km mean elevation and percent slope data (source: NASA's Shuttle Radar Topography Mission, SRTM) obtained from <https://www.earthenv.org/topography> (Amatulli et al., 2018) were extracted over point locations of individual stations and the stations were then grouped into five classes each, respectively.

Considering the number of stations against each slope class, a major proportion (i.e., 499) of the total stations (i.e., 755) were situated in the regions with slope less than 5%. Whereas, only 30 stations were situated in much steeper slope classes (i.e., >15%). Here, the scope of meteorological application of terrain complexity is being forced by specifying some randomly selected threshold intervals. Otherwise, topographical complexity is a very complex term for which there exist no fixed and well-established thresholds in the literature, as well as only two parameters (i.e., elevation and slope) might not be enough to fully define the terrain complexity. As this study intended to investigate the variation in performance accuracy of the

precipitation products against varying terrain complexity, it was considered necessary to specify some thresholds for varying elevation and terrain slope.

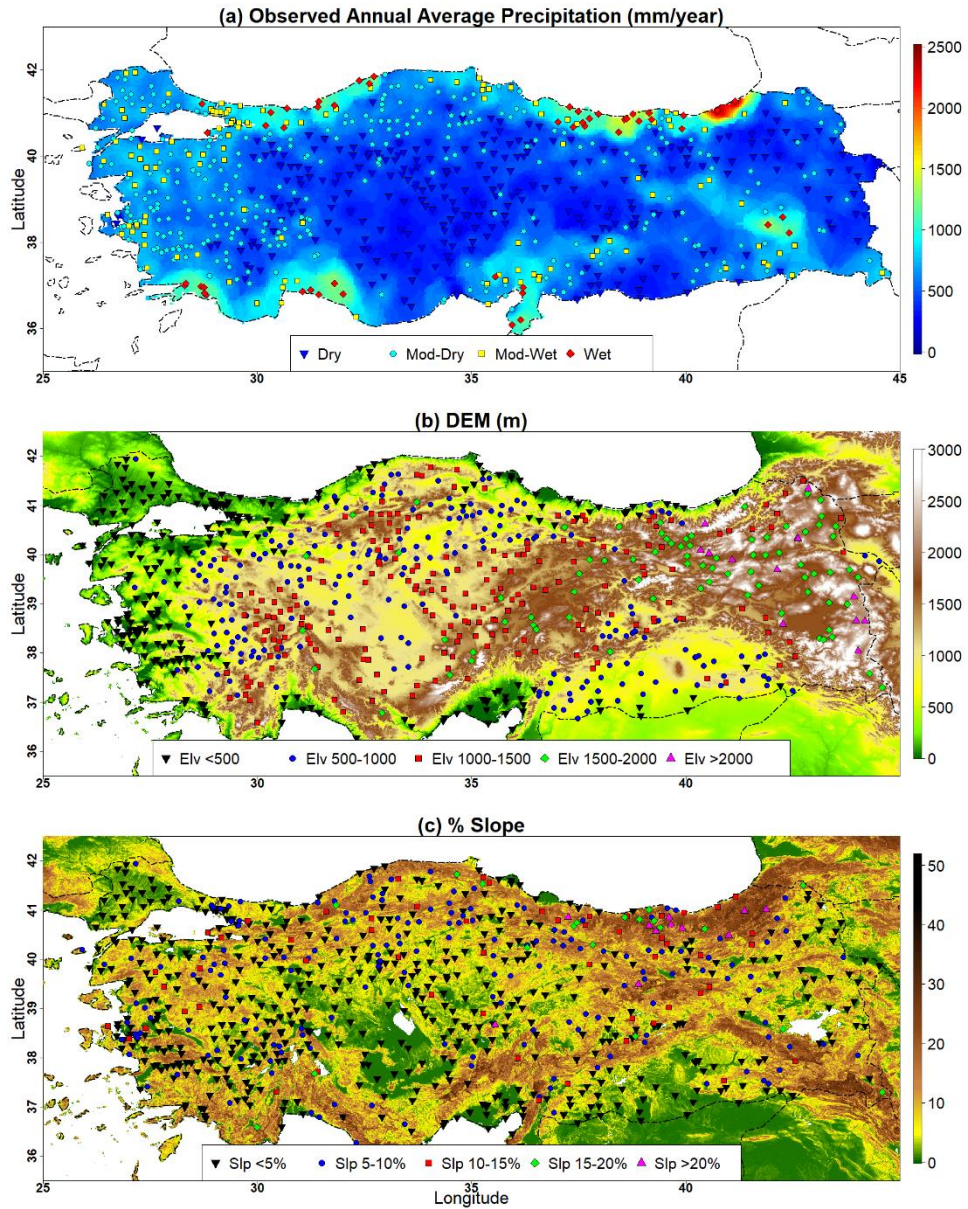


Figure 2.2. (a) Locations of stations ordered using four wetness classes plotted over observed annual average precipitation map of Turkey, (b) Locations of stations ordered using five elevation classes plotted over Digital Elevation Map (m), (c) Locations of stations ordered using five slope classes plotted over percent slope map

Table 2.2. Classification of stations of entire area based on wetness, elevation, and slope

Wetness (mm/mon)	No. of Stations	Elevation (m)	No. of Stations	Slope	No. of Stations
Entire	755	Entire	755	Entire	755
Dry (<40)	279	< 500	237	< 5%	499
Mod-dry (40-60)	303	500-1000	219	5-10%	170
Mod-wet (60-80)	123	1000-1500	209	10-15%	56
Wet (>80)	50	1500-2000	77	15-20%	19
-	-	> 2000	13	> 20%	11

Evaluation analyses were applied separately over stations of four wetness classes, five elevation classes, and five slope classes.

2.4. Evaluation of Precipitation Products

All nine products (Table 2.1) were initially evaluated using ground station-based observed precipitation data on daily, monthly, and annual time scales.

2.4.1. Daily Time Scale

2.4.1.1. Daily Evaluation statistics

Daily precipitation products were evaluated for their mean (\bar{P}) and standard deviation (SD):

$$\bar{P}_n = \frac{1}{t} \sum_{i=1}^t P_i \quad (1)$$

$$SD_n = \sqrt{\frac{1}{t} \sum_{i=1}^t (P_i - \bar{P}_n)^2} \quad (2)$$

as well as for their error statistics (Bias, Error Standard Deviation (ErrSD), and Root Mean Square Error (RMSE)) and Correlation Coefficient (CC):

$$Bias_n = \frac{1}{t} \sum_{i=1}^t P_{p,i} - \frac{1}{t} \sum_{i=1}^t P_{o,i} \quad (3)$$

$$ErrSD_n = SD[\sum_{i=1}^t (P_{p,i} - P_{o,i})] \quad (4)$$

$$RMSE_n = \sqrt{\frac{1}{t} \sum_{i=1}^t (P_i - O_i)^2} \quad (5)$$

$$CC_n = \frac{\sum_{i=1}^t (P_{p,i} - \bar{P}_p)(P_{o,i} - \bar{P}_o)}{\sqrt{\sum_{i=1}^t (P_{p,i} - \bar{P}_p)^2} \cdot \sqrt{\sum_{i=1}^t (P_{o,i} - \bar{P}_o)^2}} \quad (6)$$

where n is the station number (from 1 to 755, for the entire study area); t is the number of day; subscripts “ o ” and “ p ” denote observed data and products; $P_{p,i}$ is the product precipitation estimate (mm/day); $P_{o,i}$ is the observed precipitation (mm/day); \bar{P}_p is the product mean precipitation (mm/day); \bar{P}_o is the mean observed precipitation (mm/day).

All the statistics (\bar{P} , SD, Bias, ErrSD, RMSE, and CC) were determined for each product over stations of the entire study area as well as over stations of all the wetness, elevation, and slope classes.

2.4.1.2. Intensity-Frequency Analysis

To investigate the performance of the products in accurately matching the observed frequency of different precipitation intensities, their frequency of detection was plotted against 5 different thresholds/intervals of daily precipitation intensity. The intensity thresholds/intervals (Table 2.3) were defined following (Zambrano-Bigiarini et al., 2017).

Table 2.3. Classification of precipitation intensities

Name	Precipitation Intensity (mm/day)
No precipitation	0 – 1
Light precipitation	1 – 5
Moderate precipitation	5 – 20

Heavy precipitation	20 – 40
Extreme precipitation	> 40

2.4.1.3. Categorical Performance Indices

Over the entire area and individual wetness, elevation, and slope classes, three categorical performance indices (CPI) were investigated for different daily precipitation intensity thresholds (Table 2.4); namely probability of detection (POD), false alarm ratio (FAR) and critical success index (CSI). Here, POD and FAR measure the fraction of data points that are correctly and incorrectly (respectively) estimated to be above a threshold value, while CSI is also related with the depiction of the fraction of data points correctly estimated as having values above the threshold (Yucel et al., 2011). A perfect detection should have CSI and POD values equal to 1 and a FAR value of 0.

Table 2.4. Algorithm for categorical performance indices

		Observed Precipitation	
		Above Threshold	Below Threshold
Product Precipitation	Above Threshold	Hit (H)	False Alarm (F)
	Below Threshold	Miss (M)	Correct Negative (CN)

The categorical performance indices are calculated as:

$$POD = \frac{H}{(H+M)} \quad (7)$$

$$FAR = \frac{F}{(H+F)} \quad (8)$$

$$CSI = \frac{H}{(H+M+F)} \quad (9)$$

where H indicates a hit (i.e., a satellite/model estimate that correctly identifies an observed precipitation above a threshold), M is a miss (i.e., satellite/model showing daily precipitation less than a threshold while station-based observations show higher

precipitation than that threshold), F is a false alarm (i.e., satellite/model show precipitation greater than a threshold while station-based observations show lower precipitation rates than that threshold), and CN is when both the observed data and satellite/model data show daily precipitation less than a threshold.

Following Yucel et al. (2011), the statistics POD, FAR, and CSI were computed using six thresholds of precipitation intensity (1, 10, 20, 30, 40, and 50 mm/day). However, instead of using 0 mm/day threshold for “no precipitation” (Yucel et al., 2011), this study used the threshold of 1 mm/day to define “no precipitation” (Zambrano-Bigiarini et al., 2017).

2.4.2. Monthly Time Scale

To investigate the performance of the products over monthly time scale, the daily observed precipitation data as well as the daily precipitation data from the nine products were converted to monthly accumulated data.

2.4.2.1. Time Series Plots

For each dataset, monthly precipitation data for all the stations within each class were averaged for each month separately; thus, forming a monthly complete time series. Later, these complete time series were decomposed into climatology and anomaly components following the below equations:

$$P_{p,m}^{Climatology} = \sum_{y=1}^n P_{p,y,m} \quad (10)$$

$$P_{p,y,m}^{Anomaly} = P_{p,y,m} - P_{p,m}^{Climatology} \quad (11)$$

where, n is the total number of years (6 in our case); $P_{p,y,m}$ is the precipitation estimate in mm/mon for each product (p), year (y), and month (m); $P_{p,m}^{Climatology}$ is the seasonality component (mean of each product for a specific month of all the years); and $P_{p,y,m}^{Anomaly}$ is the remaining anomaly component. Here, the climatology of a specific month of the year is calculated by taking the average of precipitation for that month during all the study years (~6 years in our case).

Monthly complete time series, climatology, and anomaly were plotted for all the datasets over the entire study area to make a general view about their time-series performance. In addition to plots on the whole study area, monthly climatology and anomaly time series were plotted for all the datasets over different wetness, elevation, and slope classes to assess the time-series performance of all the datasets in detail over varying wetness, elevation, and slope.

2.4.2.2. Monthly Evaluation Statistics

2.4.2.2.1. Temporal Statistics

Like daily evaluation metrics, the evaluation metrics for monthly datasets included Mean, SD, Bias, ErrSD, RMSE, and CC. However, on the monthly time scale, all these statistics were computed not only for the complete time series but also for its climatology and anomaly components over the entire study area as well as over individual wetness, elevation, and slope classes.

2.4.2.2.2. Spatial Statistics

In addition to computation of the above-mentioned temporal statistics, the spatial distribution maps (of the entire study area) for Bias and RMSE were prepared to visually assess the performance of the products over different regions of the area. For this, the station-based point data for Bias and RMSE were converted from point to spatial maps using inverse distance weighting interpolation (using data from 3 closest neighboring stations).

Monthly evaluation analyses also included the investigation of how absolute Bias and ErrSD vary with the increasing terrain elevation and slope.

2.4.3. Annual Time Scale

The performance of the products over the annual time scale was assessed by converting the daily data to accumulated annual data for the individual datasets.

To visually assess the accuracy of the products in capturing the spatial variability of observed annual average precipitation, the spatial distribution maps were prepared by converting annual average precipitation for each dataset over stations to spatial maps by using inverse distance weighting interpolation (using data from 3 closest neighboring stations).

Moreover, the variability of the annual average precipitation for each dataset was plotted against different elevations and slopes.

2.5. Merging Precipitation Products

This study does not merge the ground-based observed data with the precipitation products, rather it keeps the observed data independent so that, later, the individual and merged products could be evaluated using this independent data.

2.5.1. Preparing Datasets for Merging

The satellite estimation-based and model reanalysis-based products are released after a lag of 2-3 months as these products undergo certain calibration processes (in case of satellite-based products) or data assimilation processes (in case of reanalysis products); this study terms four of the products (i.e., IMERG, TMPA, ERAint, and ERA5) as “Research-grade products” or “Research products”. Similarly, the remaining five real-time forecast products (i.e., ECM, ALR, WRF, GFS, and CFS) are termed as “Real-time Forecasts” in this study. Thus, the set of nine precipitation products (i.e., IMERG, TMPA, ERAint, ERA5, ECM, ALR, WRF, GFS, and CFS) was divided into two groups based on the accessibility and type of the individual products. The two groups of the individual products were separately merged and evaluated afterwards.

1-daily total precipitation data from IMERG, TMPA, ERAint and ERA5 were merged and evaluated using the ground-based observed data as the reference over daily as well as over monthly time scales (as these products are research-grade products, merging

and evaluating them over monthly time scale finds its implication in the fields like drought management).

Total precipitation, as well as its convective and large-scale components for 1-3 daily real-time forecast data from ECM, ALR, WRF, GFS, and CFS were merged and evaluated. Here, CFS forecasts do not include large-scale precipitation variable, because of this, LSP amounts were determined by subtracting CP from TP.

Now, as the observed 1-daily TP data obtained from MGM did not contain any information about the proportions of CP and LSP within TP for a specific day, this study had to rely on the skills of the ECMWF forecast model in segregating CP and LSP proportions. Thus, the observed 1-daily TP data was split to CP and LSP using proportions provided by ECM data each day, and then this 1-daily observed TP, CP, and LSP data was converted to 2-daily and 3-daily accumulated data for later evaluation of individual and merged datasets.

2.5.2. Merging Procedure

2.5.2.1. Simple Merging

Simple merging of data on a specific day is calculated by taking the mean of data from all the merged products on that day (in other words, it is the same as the ensemble mean, where all the individual products combine to form the ensemble). Say if five products a, b, c, d, and e are being merged, their simple merge (SimpMRG) will be produced as:

$$SimpMRG = \frac{a_i + b_i + c_i + d_i + e_i}{5} \quad (12)$$

where i denotes the specific day on which the SimpMRG is being produced.

SimpMRG was produced for each of the 755 stations on each day of the study period separately for research-grade products (IMERG, TMPA, ERAint, and ERA5) and real-time forecasts (ECM, ALR, WRF, GFS, and CFS).

As an example, Figure 2.3a visually depicts simple merging method for the five forecast products to obtain SimpMRG by applying the Eq. 12.

2.5.2.2. Merging after Regression-based Rescaling

This method includes two steps: (1) Rescaling the individual products in the space of a reference product (here, reference product does not indicate the observed data, but it is one of the products which is taken at a time as a reference for rescaling the other products), and (2) Merging the rescaled products with simple merging method (Eq. 12).

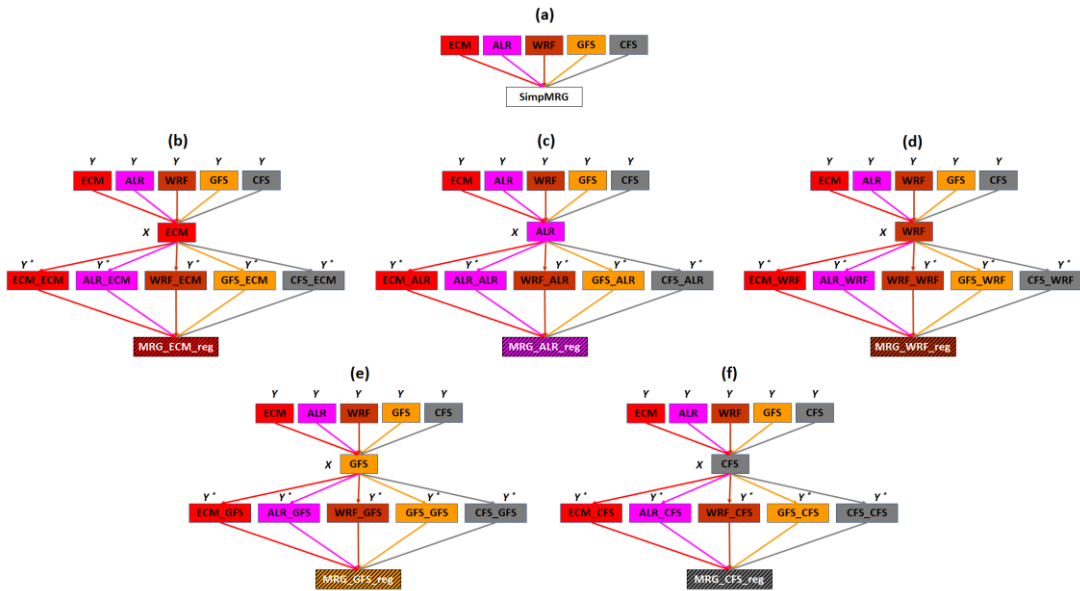


Figure 2.3. Merging Methodology. (a) Simple Merging, (b) – (f): Simple Merging after regression-based rescaling using ECM, ALR, WRF, GFS, and CFS as reference product (one at a time), respectively

Rescaling the products with linear regression is done by considering one of the products at a time as the reference product and rescaling the other products on the space of this reference products. Hence, if we are rescaling five products by linear regression, we consider five different scenarios, where one of the five products are considered as the reference product in each scenario. Now, rescaling by linear

regression is implemented by using a simple linear relation between unscaled product (Y) and the reference product (X) as:

$$Y^* = \mu_X + (Y - \mu_Y)C_Y \quad (13)$$

where Y^* is the rescaled form of Y; μ_X and μ_Y are time averages of X and Y, respectively; and C_Y is the rescaling factor which can be found through linear regression method (Yilmaz and Crow, 2013):

$$C_Y = \rho_{XY} \sigma_X / \sigma_Y \quad (14)$$

where C_Y is the rescaling factor, σ_X and σ_Y are the standard deviations of X and Y products; and ρ_{XY} is the correlation coefficient between X and Y. After rescaling the individual products, they were simply merged by using Eq. 12.

The process of “selecting one of the products as a reference, applying regression-based rescaling on all the products based on that reference product, and merging rescaled products using Eq. 12” was repeated five times (Figures 2.3b to 2.3f) for the five forecast products. Similarly, it was repeated four times for the four research products.

The resulting merged real-time forecasts were denoted as SimpMRG (ensemble mean of all the forecasts), MRG_ECM_REG, MRG_ALR_REG, MRG_WRF_REG, MRG_GFS_REG, and MRG_CFS_REG (simply merged products obtained after rescaling all the forecasts in the space of ECM, ALR, WRF, GFS, and CFS, respectively). The merged products were produced for 1-3 daily TP, CP and LSP.

Similarly, the satellite-based estimates and model-based reanalysis were merged by using the two methods of merging, and the resulting merged products were denoted as SimpMRG, MRG_IMERG_REG, MRG_TMPA_REG, MRG_ERAIint_REG, and MRG_ERA5_REG.

2.5.3. Evaluation of Merged Products

2.5.3.1. Categorical Performance Indices

Over 1-daily time scale, individual real-time forecasts and their merged products for TP, CP, and LSP were analyzed for their performance in the detection of daily precipitation events and boxplots for POD, FAR, and CSI averaged over the entire area were prepared for discussion on this analysis. A similar study was conducted in the case of 1-daily individual research-grade (satellite and reanalysis) products and their merged products but only for TP data.

2.5.3.2. Intensity-Frequency Analysis

To investigate and compare the performance of individual and merged products in accurately matching the observed frequency of different precipitation intensities, their frequency of detection was plotted against 5 different thresholds/intervals (Table 2.3) of daily precipitation intensity. This analysis was conducted for TP, CP, and LSP for real-time forecasts, while only TP was considered in the case of satellite and reanalysis products.

2.5.3.3. Error Statistics of Individual and Merged Products

Evaluation metrics including Bias, ErrSD, and CC were determined for 1-3 daily individual and merged forecasts considering TP as well as its Cp and LSP components. These metrics were determined for individual and merged research-grade products over 1-daily and monthly time scales.

2.5.3.4. Investigating Improvement in Accuracy of Individual Products after Merging

To investigate the added utility of merging methods, an overall percent improvement in the accuracy of individual products due to merging was analyzed where ErrSD and CC were considered as accuracy indicators.

CHAPTER 3

RESULTS AND DISCUSSION

3.1. Evaluation of Precipitation Products

The initial assessment of precipitation data from four research-grade products (i.e., IMERG, TMPA, ERAint, and ERA5) and five real-time forecast products (i.e., ECM, ALR, WRF, GFS, and CFS) was conducted using observation gauges data on daily, monthly and annual time scales. The results are presented and discussed below.

3.1.1. Daily Time Scale

3.1.1.1. Daily Evaluation Statistics

Daily data from ALR shows the best accuracy in reproducing the mean observed precipitation (Table 3.1) by showing almost no Bias (Table 3.2) over the entire study area, where CFS data shows the most substantial wet Bias (0.6 mm/day). Contrary to the Bias related results, overall, ERA5 and ECM both show the least ErrSD (3.9 mm/day) and the highest daily CC (0.66) with the observed data (Table 3.3) while TMPA performed the worst regarding ErrSD (5.7 mm/day) and CC (0.47).

All the datasets, except ALR, overestimate the observed daily precipitation not only over the entire study area but over dry to moderately dry regions as well. IMERG, TMPA, ERAint, GFS, and CFS datasets tend to underestimate the observed precipitation over wetter regions while ERA5, ECM, and WRF consistently overestimated it over all the wetness classes (Table 3.2); with ERA5 and WRF showing more pronounced overestimation. ErrSD for a given product increases with increasing wetness of the region, which is obvious that increased amounts of precipitation tend to increase the errors; CC, on the other hand, does not follow such trend (Table 3.3).

Table 3.1. Daily Mean and SD for the entire study area and wetness classes

Region		Entire	Dry	Mod-dry	Mod-wet	Wet
No. of Stations		755	279	303	123	50
Mean (mm/day)	Obs	1.6	1.1	1.6	2.2	3.2
	IMERG	1.9	1.5	1.9	2.3	2.8
	TMPA	1.8	1.5	1.9	2.0	2.4
	ERAint	1.9	1.7	1.9	2.0	2.2
	ERA5	2.0	1.6	2.0	2.5	3.4
	ECM	1.8	1.4	1.8	2.4	3.3
	ALR	1.6	1.0	1.5	2.2	3.2
	WRF	1.9	1.4	1.9	2.5	3.7
	GFS	1.9	1.5	2.0	2.4	2.4
CFS	2.2	1.8	2.4	2.6	2.6	
SD (mm/day)	Obs	5.0	3.5	5.0	6.5	9.0
	IMERG	5.4	4.2	5.6	6.6	7.6
	TMPA	5.8	4.8	6.0	6.7	7.9
	ERAint	4.0	3.6	4.0	4.4	4.4
	ERA5	4.3	3.4	4.3	5.5	6.8
	ECM	4.3	3.2	4.2	5.6	7.2
	ALR	4.6	3.2	4.6	6.2	8.3
	WRF	5.1	3.7	5.1	6.6	9.5
	GFS	4.6	3.6	4.8	6.0	6.1
CFS	5.1	4.0	5.5	6.3	6.4	

Table 3.2. Daily Bias and ErrSD for the entire study area and wetness classes

Region		Entire	Dry	Mod-dry	Mod-wet	Wet
No. of Stations		755	279	303	123	50
Bias (mm/day)	IMERG	0.3	0.4	0.3	0.1	-0.4
	TMPA	0.2	0.4	0.3	-0.2	-0.8
	ERAint	0.3	0.6	0.3	-0.1	-0.9
	ERA5	0.4	0.5	0.4	0.3	0.3
	ECM	0.2	0.3	0.2	0.2	0.2
	ALR	0.0	-0.1	-0.1	0.0	0.0
	WRF	0.3	0.3	0.3	0.3	0.5
	GFS	0.3	0.4	0.4	0.3	-0.8
	CFS	0.6	0.7	0.8	0.4	-0.6
ErrSD (mm/day)	IMERG	4.6	3.7	4.6	5.4	7.7
	TMPA	5.7	4.7	5.7	6.7	9.2
	ERAint	4.2	3.4	4.1	4.9	7.1
	ERA5	3.9	3.1	3.9	4.7	6.8
	ECM	3.9	3.0	3.9	4.7	6.5
	ALR	4.4	3.3	4.4	5.5	7.8
	WRF	4.5	3.4	4.5	5.5	7.8
	GFS	4.5	3.6	4.5	5.5	7.2
	CFS	4.8	3.9	4.9	5.5	7.3

Table 3.3. Daily CC for the entire study area and wetness classes

Region		Entire	Dry	Mod-dry	Mod-wet	Wet
No. of Stations		755	279	303	123	50
CC with the Observed Data	IMERG	0.62	0.59	0.64	0.66	0.57
	TMPA	0.47	0.44	0.49	0.49	0.40
	ERAint	0.62	0.58	0.62	0.66	0.64
	ERA5	0.66	0.63	0.67	0.72	0.68
	ECM	0.66	0.63	0.67	0.71	0.70
	ALR	0.58	0.55	0.59	0.63	0.59
	WRF	0.62	0.59	0.62	0.66	0.66
	GFS	0.60	0.55	0.61	0.66	0.62
CFS	0.59	0.54	0.60	0.66	0.62	

Table 3.4. Daily Mean and SD for the entire study area and elevation classes

Elevation (m)		Entire	< 500	500-1000	1000-1500	1500-2000	> 2000
No. of Stations		755	237	219	209	77	13
Mean (mm/day)	Obs	1.6	2.0	1.4	1.4	1.4	1.5
	IMERG	1.9	2.3	1.8	1.7	1.7	1.9
	TMPA	1.8	2.1	1.7	1.6	1.7	1.8
	ERAint	1.9	1.9	1.8	1.8	2.3	2.4
	ERA5	2.0	2.3	1.8	1.8	2.1	2.2
	ECM	1.8	2.2	1.6	1.6	1.8	1.9
	ALR	1.6	2.1	1.4	1.2	1.1	1
	WRF	1.9	2.3	1.7	1.7	1.9	2.2
	GFS	1.9	1.8	1.8	1.9	2.3	2.5
	CFS	2.2	2.5	2.1	2.0	2.3	2.7
SD (mm/day)	Obs	5.0	6.8	4.2	4.1	4.1	4.1
	IMERG	5.4	7.1	5.0	4.5	4.2	4.4
	TMPA	5.8	7.2	5.3	5.0	5.0	5.2
	ERAint	4.0	4.2	3.9	3.7	4.2	4.2
	ERA5	4.3	5.4	4.0	3.7	3.9	3.7
	ECM	4.3	5.4	3.8	3.6	3.8	3.6
	ALR	4.6	6.4	4.2	3.6	3.3	3
	WRF	5.1	6.6	4.4	4.3	4.7	4.9
	GFS	4.6	5.1	4.3	4.3	4.7	4.7
	CFS	5.1	6.4	4.9	4.3	4.4	4.5

Usually, the highest precipitation amounts are associated with the regions with higher elevations. However, this is not strictly the case with the study area under consideration. The observed data, TMPA, and ALR show the highest average daily precipitation amounts to be received by the regions with the lowest elevations (Table 3.4), whereas all the other datasets show the regions with the highest elevations being

the wettest ones. With a few exceptions (e.g., Bias in ALR over the regions with elevation > 1000 m), all the precipitation products overestimate the observed precipitation over all the elevation classes (Table 3.5).

Table 3.5. Daily Bias and ErrSD for the entire study area and elevation classes

Elevation (m)		Entire	< 500	500-1000	1000-1500	1500-2000	> 2000
No. of Stations		755	237	219	209	77	13
Bias (mm/day)	IMERG	0.3	0.3	0.3	0.3	0.3	0.5
	TMPA	0.2	0.1	0.2	0.2	0.3	0.3
	ERAint	0.3	-0.1	0.4	0.4	0.8	0.9
	ERA5	0.4	0.3	0.4	0.4	0.7	0.7
	ECM	0.2	0.1	0.2	0.2	0.4	0.4
	ALR	0.0	0.1	0.0	-0.2	-0.4	-0.5
	WRF	0.3	0.3	0.2	0.3	0.5	0.8
	GFS	0.3	-0.2	0.4	0.5	0.9	1.1
CFS	0.6	0.5	0.7	0.6	0.9	1.3	
ErrSD (mm/day)	IMERG	4.6	5.9	4.0	3.9	4.2	4.7
	TMPA	5.7	7.1	5.0	4.9	5.3	5.6
	ERAint	4.2	5.4	3.6	3.5	4.0	4.3
	ERA5	3.9	5.2	3.4	3.3	3.6	3.8
	ECM	3.9	5.2	3.3	3.2	3.5	3.8
	ALR	4.4	5.9	3.8	3.7	3.8	4.1
	WRF	4.5	6.0	3.7	3.7	4.1	4.6
	GFS	4.5	5.4	4.0	4.0	4.5	4.9
CFS	4.8	6.0	4.3	4.0	4.5	4.8	

Table 3.6. Daily CC for the entire study area and elevation classes

Elevation (m)		Entire	< 500	500-1000	1000-1500	1500-2000	> 2000
No. of Stations		755	237	219	209	77	13
CC with the Observed Data	IMERG	0.62	0.66	0.64	0.59	0.52	0.45
	TMPA	0.47	0.51	0.49	0.43	0.38	0.34
	ERAint	0.62	0.63	0.63	0.61	0.57	0.49
	ERA5	0.66	0.68	0.68	0.65	0.61	0.55
	ECM	0.66	0.68	0.68	0.66	0.62	0.56
	ALR	0.58	0.62	0.60	0.55	0.50	0.45
	WRF	0.62	0.62	0.63	0.62	0.59	0.54
	GFS	0.60	0.62	0.60	0.58	0.56	0.49
	CFS	0.59	0.63	0.59	0.57	0.52	0.46

The combined average ErrSD (5.8 mm/day) for all the products over regions with the lowest elevation is higher than that (4.3 mm/day) over regions with elevations above 1500 m (Table 3.5). This implies (keeping in mind that most of the products associate

the regions with the lowest elevations receiving more average precipitation) that wetness has a prominent role in the error statistics of the products over the study area. However, for all the products, the daily CC with the observed data decreases with the increasing regional elevation (Table 3.6). The combined average daily CC of all the products decreases from 0.63 over regions with the lowest elevations to 0.48 over those with the highest elevations.

Table 3.7. Daily Mean and SD for the entire study area and slope classes

Slope		Entire	< 5%	5-10%	10-15%	15-20%	> 20%
No. of Stations		755	499	170	56	19	11
Mean (mm/day)	Obs	1.6	1.5	1.7	2.0	2.3	1.9
	IMERG	1.9	1.8	2.0	2.1	2.4	2.6
	TMPA	1.8	1.7	1.9	1.9	2.1	2.1
	ERAint	1.9	1.8	2.0	2.2	2.6	3
	ERA5	2.0	1.8	2.1	2.6	3.3	4.1
	ECM	1.8	1.7	1.9	2.3	2.9	3
	ALR	1.6	1.5	1.5	2.0	2.2	1.8
	WRF	1.9	1.8	2.0	2.4	3.1	2.4
	GFS	1.9	1.7	2.0	2.5	3.3	4.5
	CFS	2.2	2.1	2.3	2.6	2.3	3.4
SD (mm/day)	Obs	5.0	4.9	4.8	5.7	5.9	4.4
	IMERG	5.4	5.4	5.4	5.6	5.8	5.3
	TMPA	5.8	5.7	5.8	6.0	6.2	5.6
	ERAint	4.0	3.9	4.1	4.3	4.7	4.7
	ERA5	4.3	4.2	4.4	5.0	5.6	6.1
	ECM	4.3	4.1	4.3	4.8	5.4	4.9
	ALR	4.6	4.5	4.5	5.3	5.8	4.5
	WRF	5.1	4.9	5.1	5.8	6.9	5.6
	GFS	4.6	4.4	4.7	5.4	6.4	7.1
	CFS	5.1	5.1	5.2	5.4	4.8	6.4

Contrary to the variability of daily precipitation averages related to the varying elevations, the observed data, as well as all the products, indicate that the higher the terrain slope is, the wetter is the region (Table 3.7). Except for ALR and WRF, all the products have the highest Bias occurring over regions with the highest slopes (Table 3.8), while the relationship between ErrSD and terrain slope is not as linear. However, on average, the products show lower ErrSD (4.4 mm/day) over regions with the lowest terrain slopes (i.e., < 5%) as compared to that (4.9 mm/day) over regions with the highest terrain slopes (i.e., > 20%); which depicts the impact of terrain complexity on

error variation. Increasing terrain slopes have an inverse effect on the daily CC of a given product (Table 3.9), which results in the combined average daily CC of all the products to drop from 0.60 over regions with the lowest terrain slopes to 0.55 over those with the highest slopes.

Table 3.8. *Daily Bias and ErrSD for the entire study area and slope classes*

Slope		Entire	< 5%	5-10%	10-15%	15-20%	> 20%
No. of Stations		755	499	170	56	19	11
Bias (mm/day)	IMERG	0.3	0.3	0.3	0.1	0.1	0.7
	TMPA	0.2	0.2	0.2	-0.1	-0.3	0.2
	ERAint	0.3	0.3	0.3	0.1	0.3	1.1
	ERA5	0.4	0.3	0.4	0.5	1.0	2.2
	ECM	0.2	0.2	0.2	0.3	0.5	1.1
	ALR	0.0	0.0	-0.1	0.0	-0.1	-0.1
	WRF	0.3	0.3	0.3	0.3	0.8	0.5
	GFS	0.3	0.2	0.3	0.4	0.9	2.6
	CFS	0.6	0.6	0.7	0.5	0.0	1.5
ErrSD (mm/day)	IMERG	4.6	4.5	4.5	5.2	5.7	4.9
	TMPA	5.7	5.6	5.6	6.4	7.1	6.1
	ERAint	4.2	4.1	4.0	4.7	4.8	4
	ERA5	3.9	3.9	3.8	4.5	4.7	4.6
	ECM	3.9	3.9	3.7	4.4	4.4	3.9
	ALR	4.4	4.3	4.3	5.1	5.5	4.6
	WRF	4.5	4.4	4.3	5.1	5.4	4.6
	GFS	4.5	4.4	4.4	5.5	5.9	6
	CFS	4.8	4.7	4.6	5.4	5.3	5.4

Table 3.9. *Daily CC for the entire study area and slope classes*

Slope		Entire	< 5%	5-10%	10-15%	15-20%	> 20%
No. of Stations		755	499	170	56	19	11
CC with the Observed Data	IMERG	0.62	0.63	0.62	0.59	0.52	0.49
	TMPA	0.47	0.48	0.46	0.43	0.36	0.3
	ERAint	0.62	0.61	0.63	0.62	0.64	0.62
	ERA5	0.66	0.66	0.68	0.67	0.69	0.63
	ECM	0.66	0.65	0.68	0.68	0.71	0.67
	ALR	0.58	0.58	0.58	0.58	0.56	0.47
	WRF	0.62	0.61	0.63	0.63	0.67	0.63
	GFS	0.60	0.59	0.61	0.59	0.61	0.58
	CFS	0.59	0.58	0.59	0.59	0.59	0.58

3.1.1.2. Intensity-Frequency Analysis

The model-based products, except ALR, show a smaller number of dry days (i.e., with “no precipitation”) compared to observed data (Figure 3.1), which is a common thing related to this kind of products (e.g., Gampe and Ludwig, 2017; Hénin et al., 2018). ALR shows the highest accuracy in matching the observed frequency of days against all the intensity intervals while ERAInt and CFS show converse of this. The poor performance of ERA-Interim and CFS in estimating the precipitation events can be related to their coarser spatial resolutions (0.75° and 0.5° , respectively) at which cloud-precipitation systems are weakly resolved, and lower number of observations assimilated into the models.

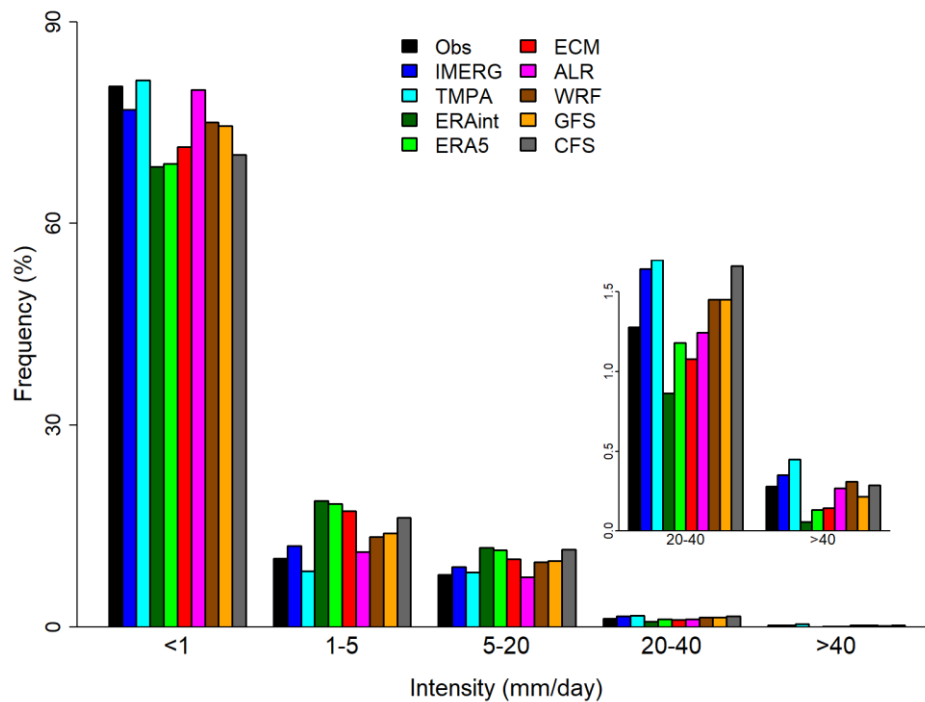


Figure 3.1. Daily precipitation intensity vs. frequency bar plots for the entire study area

Although, both the model-based reanalysis products (ERAInt and ERA5) underestimate the frequency of observed days with “heavy precipitation” and “extreme precipitation” (Figure 3.1), ERA5 shows some improvement over ERA-

Interim in recording the frequency of these specific days. Among the satellite-based products, TMPA performs slightly better than IMERG in intensity-frequency analysis against almost all the daily precipitation intensity intervals.

3.1.1.3. Categorical Performance Indices

As in this study, CPI were computed against different precipitation intensity thresholds (not the intervals) (please refer to Section 2.4.1.3); the results related to CPI must be considered differently than intensity-frequency analysis.

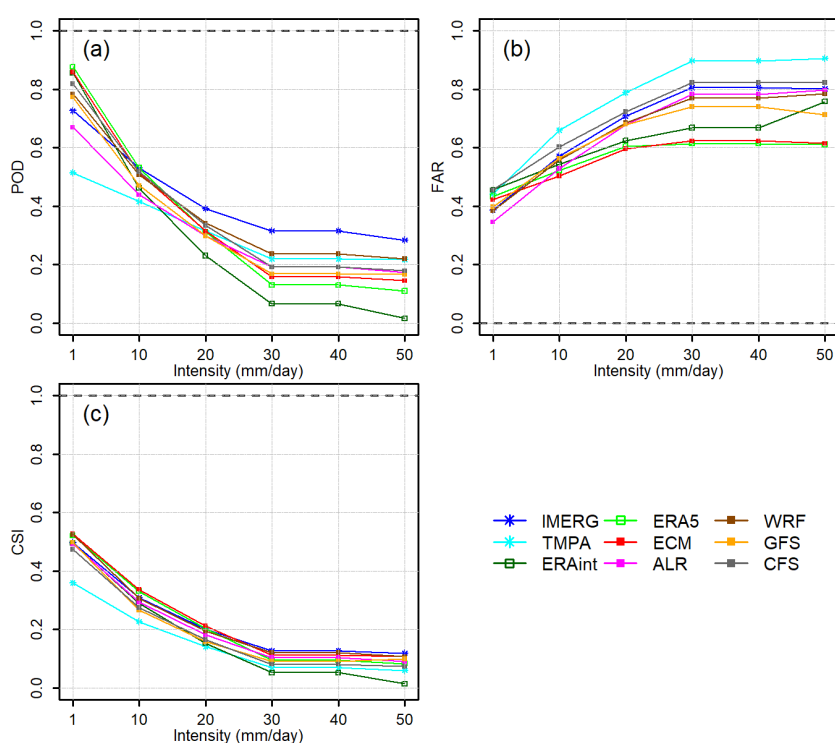


Figure 3.2. Categorical Performance Indices, a) POD, b) FAR, and c) CSI, against different intensity thresholds over the entire study area. The dashed lines show the optimum scores for the respective CPI

Over the entire study area, better POD, FAR and CSI (Figure 3.2a, 3.2b, and 3.2c, respectively) of IMERG as compared to TMPA indicate its improved precipitation detection ability against almost all the intensity thresholds. Similarly, ERA5 performs better than ERAInt in all the CPI against all the intensity thresholds. The CPI of the real-time forecast, ECM, are well in line with those of ERA5, thus depicting its utility

in operational fields. Increasing the magnitude of precipitation intensity threshold causes lower POD, higher FAR, and lower CSI.

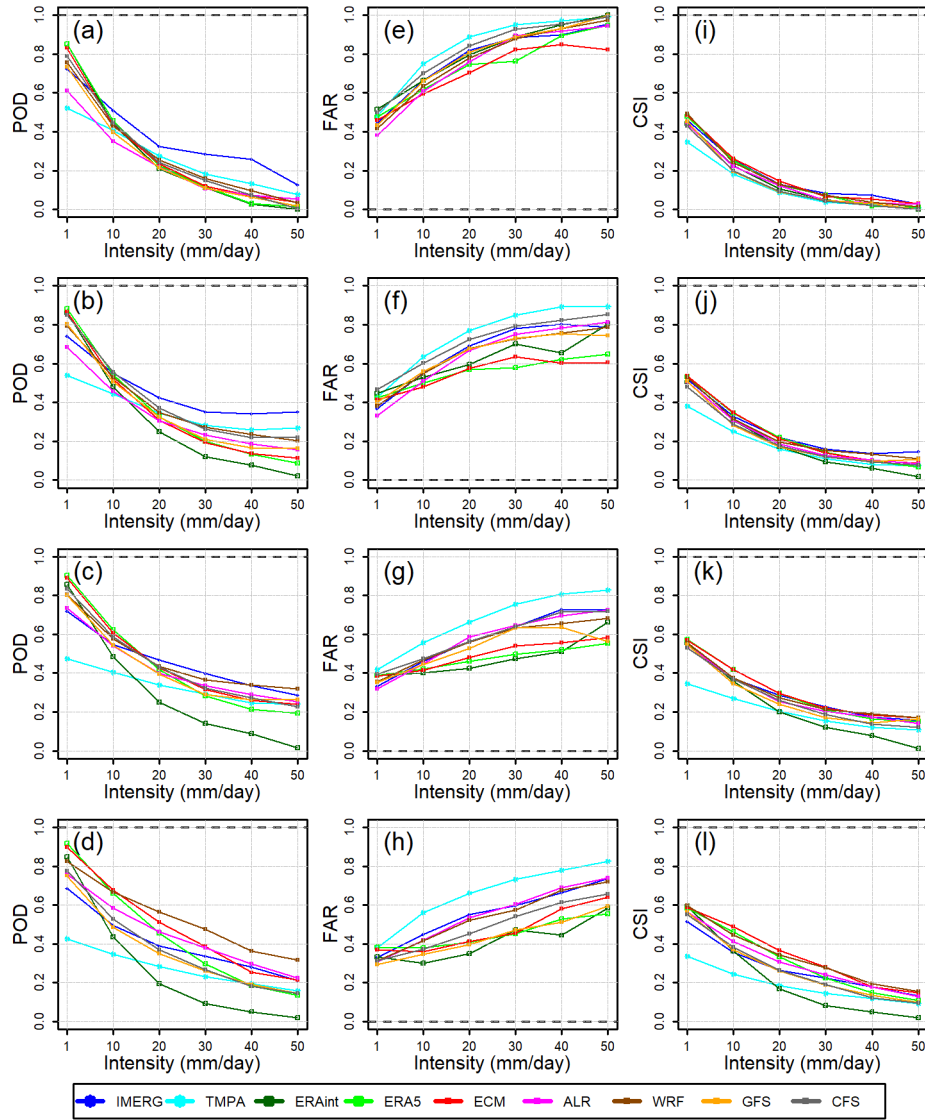


Figure 3.3. Categorical Performance Indices. POD (from (a) to (d)), FAR (from (e) to (h)), and CSI (from (i) to (l)) against different daily precipitation intensities over wetness classes; Dry (a,e,i), Mod-Dry (b,f,j), Mod-Wet (c,g,k), and Wet (d,h,l), respectively. The dashed lines show the optimum scores for the respective CPI

With the increasing wetness of the region, the differences between the CPI of different products increase (Figure 3.3). Moreover, the increasing wetness causes a decrease in POD for both the satellite-based products while it results in raised POD for model-

based products (Figures 3.3a to 3.3d). Low FAR for model-based products (Figures 3.3e to 3.3h) is an indication of them underestimating the frequency of dry days. Among all the products, TMPA consistently shows higher FAR over all the wetness classes; IMERG shows much improved FAR. TMPA and ERAint show the worst CSI (Figures 3.3i to 3.3l) among the products over all the wetness classes, while CFS and GFS have moderate ability regarding CPI. Among all the model-based products, ECM shows the best CSI, especially against light to moderate precipitation intensities.

The POD of satellite-based products is inversely affected by an increase in the elevation of the regions (Figures 3.4a to 3.4e); the POD of ALR also has the same trend. Overall, ERA5 shows better POD than ERAint over all the elevation classes. Like its performance over wetness classes, TMPA shows the highest FAR over all the elevation classes (Figures 3.4f to 3.4j). ECM, again, counts it among the top performers regarding CSI over varying elevation regions (Figures 3.4k to 3.4o). With some exceptions, the CPI results for the products over elevation classes are like those over wetness classes.

The difference between performances of ERA5 and ERAint regarding CPI over varying terrain slopes (Figure 3.5) is even more substantial as compared to that over varying elevations. IMERG shows the highest POD score over regions with the lowest slopes (Figure 3.5a); however, its POD score is inversely affected by increasing terrain slopes. ECM consistently shows the highest CSI scores (Figures 3.5k to 3.5o), especially over steeper terrain slopes.

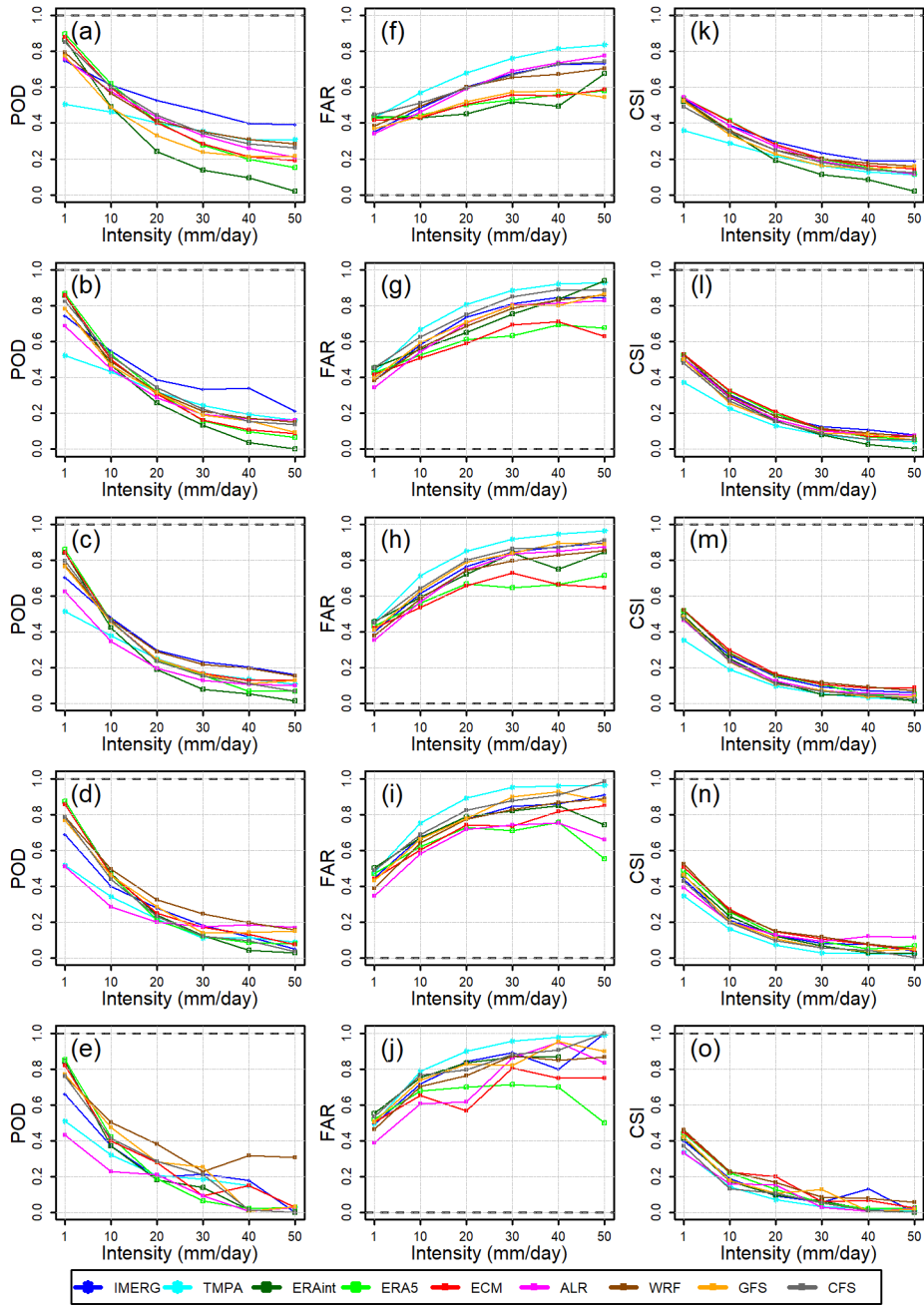


Figure 3.4. Categorical Performance Indices. POD (from (a) to (e)), FAR (from (f) to (j)), and CSI (from (k) to (o)) against different daily precipitation intensities over elevation classes; Elev <500 (a,f,k), Elev 500-1000 (b,g,l), Elev 1000-1500 (c,h,m), Elev 1500-2000 (d,i,n), Elev >2000 (e,j,o), respectively. The dashed lines show the optimum scores for the respective CPI

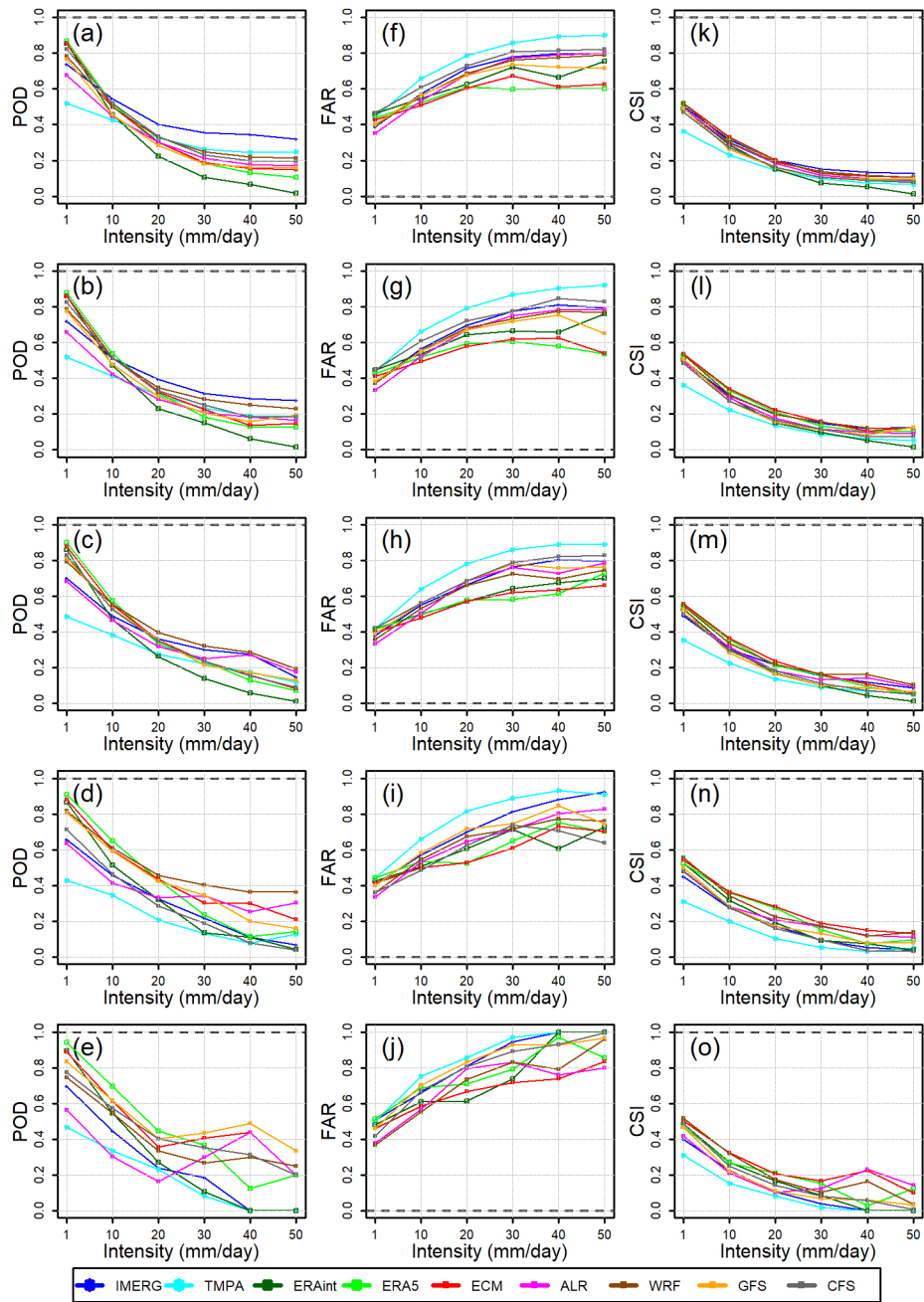


Figure 3.5. Categorical Performance Indices. POD (from (a) to (e)), FAR (from (f) to (j)), and CSI (from (k) to (o)) against different daily precipitation intensities over slope classes; Slope $< 5\%$ (a,f,k), Slope 5-10% (b,g,l), Slope 10-15% (c,h,m), Slope 15-20% (d,i,n), Slope $> 20\%$ (e,j,o), respectively. The dashed lines show the optimum scores for the respective CPI

3.1.2. Monthly Time Scale

3.1.2.1. Time Series Plots

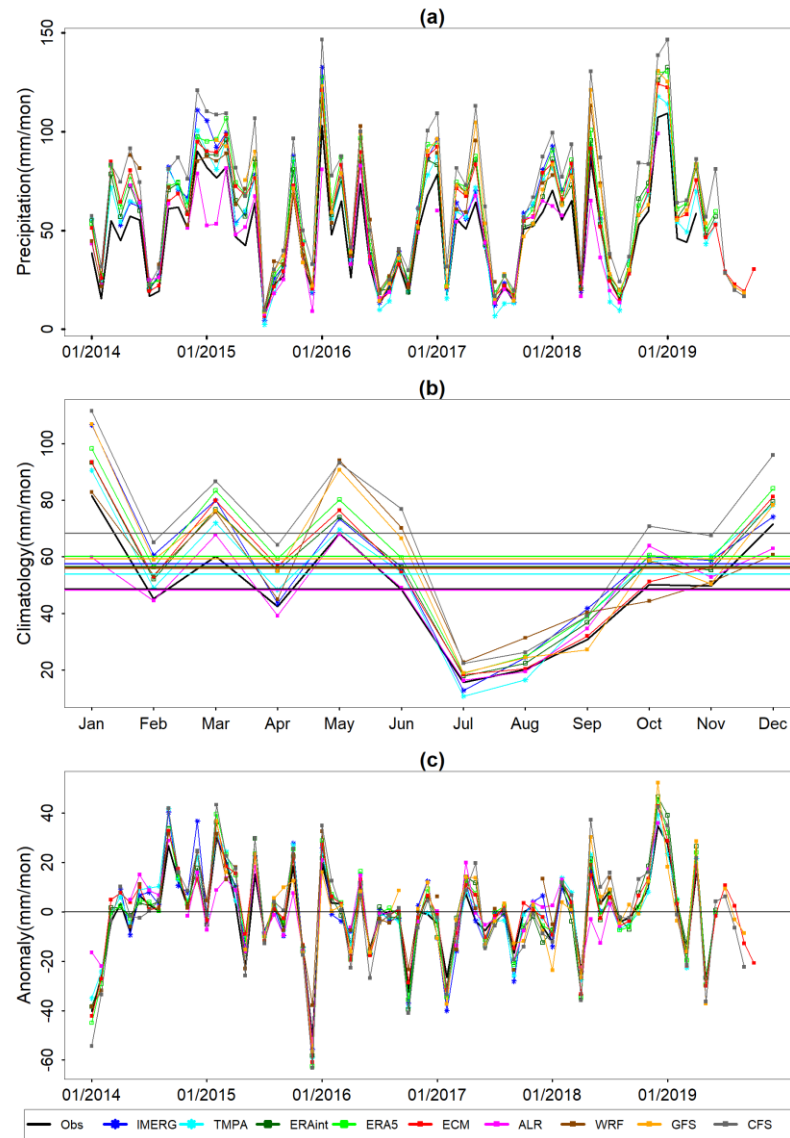


Figure 3.6. Monthly time series over the entire study area. a) complete time series, b) climatology, and c) anomaly. The color-coded horizontal lines in the climatology plot show the mean monthly precipitation for the respective datasets. The horizontal line in the anomaly plot shows zero anomaly level

Investigating the country-scale monthly precipitation time series variability (Figure 3.6a) suggests that the products follow the trends of observed data time series very well. There are a few patches of time (e.g., March 2016 to November 2016) where

monthly complete time series of all the products perfectly match the observed data time series. However, during most of the study period, product time series show differences with the observed data. Discrepancies at the peaks have implications in water resources management, where the product data may cause more optimistic management decisions. Overall, the climatology of the products (Figure 3.6b) shows that July to September are the driest months, while December to May are the wettest months over the study area. The products' overestimation of the observed precipitation is more pronounced in winter as compared to the summer season. Overall, the products, except ALR, overestimate the monthly observed data; CFS does it the most. Monthly anomaly time series of all the products, on the other hand, very closely follow the anomaly time series of the observed data throughout the study period (Figure 3.6c).

Monthly precipitation data from ALR, ECM, and ERAint could better be recommended for hydrological applications during the summer months (June-August) as they follow the climatology of the observed data better than all the other products (Figure 3.6b). ECM follows the monthly observed precipitation during autumn (September-November) better than the other products, while ALR also shows consistency with the observed data especially during the months of September and October. During the winter season (December-February), none of the products has a consistent matching for the trends in climatology of observed data. Nevertheless, WRF, ALR, and TMPA could be considered as better recommendable products during winter season. The trends and magnitudes of monthly observed precipitation during the spring season (March-May) are better followed by ALR compared with all the other products.

The country-scale monthly precipitation time series variability is assessed in more detail by plotting its climatology and anomaly components for the individual wetness (Figure 3.7), elevation (Figure 3.8), and slope classes (Figure 3.9). IMERG, TMPA, ERAint, GFS, and CFS overestimate the observed monthly precipitation over dry to moderately wet regions (Figures 3.7a to 3.7c) while they do the inverse over wet regions (Figure 3.7d). However, all the other products, except ALR, consistently

overestimate the observed precipitation over all the wetness classes. The discrepancies in following the observed monthly anomaly time series increase with the increasing wetness (Figures 3.7e to 3.7h).

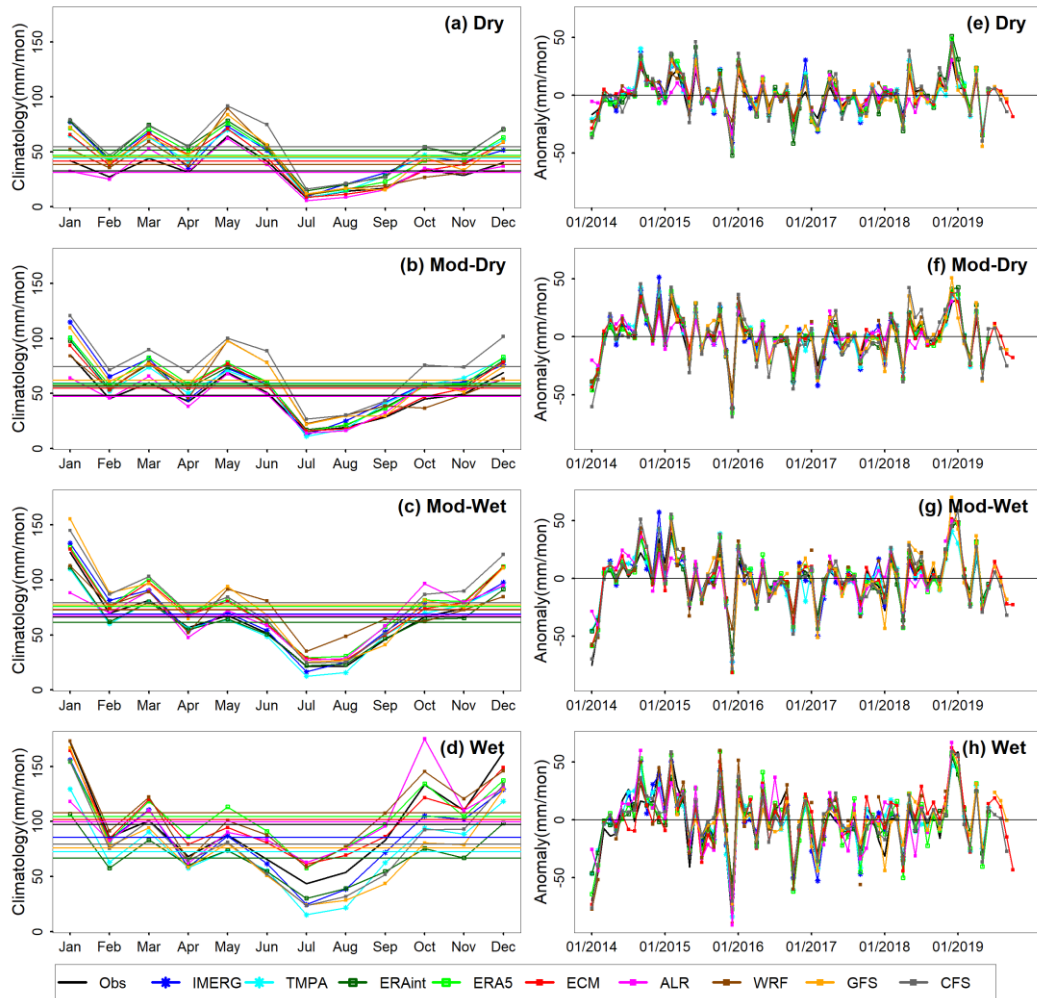


Figure 3.7. Monthly climatology (from (a) to (d)) and monthly anomaly (from (e) to (h)) for wetness classes. The color-coded horizontal lines in the climatology plot show the mean monthly precipitation for the respective datasets. The horizontal line in the anomaly plot shows zero anomaly level

As an only exception, ALR overestimates the monthly observed data over regions with the lowest elevations (i.e., <500 m) and does the inverse over regions with elevations above 1000 m (Figures 3.8a to 3.8e). Climatology plots for all the other products show a consistent overestimation over each elevation class. The differences in climatology time series between the observed data and the products are more pronounced over the

regions with elevations above 1500m, which is evidence of the impact of elevation increase on the accuracy of the products. A similar conclusion is valid for monthly anomaly time series over regions with elevations above 1500m (Figures 3.8i and 3.8j).

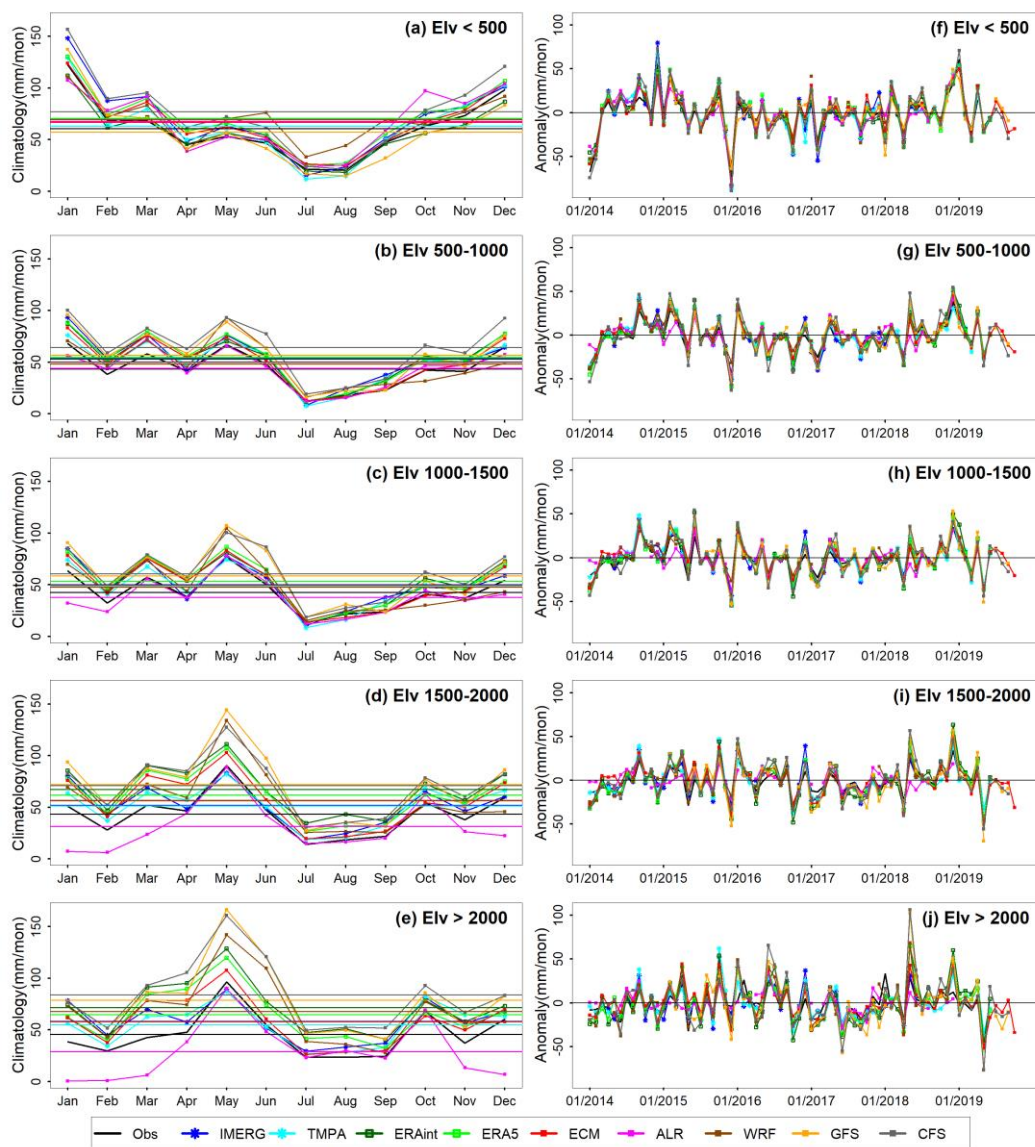


Figure 3.8. Monthly climatology (from (a) to (e)) and monthly anomaly (from (f) to (j)) for elevation classes. The color-coded horizontal lines in the climatology plot show the mean monthly precipitation for the respective datasets. The horizontal line in the anomaly plot shows zero anomaly level

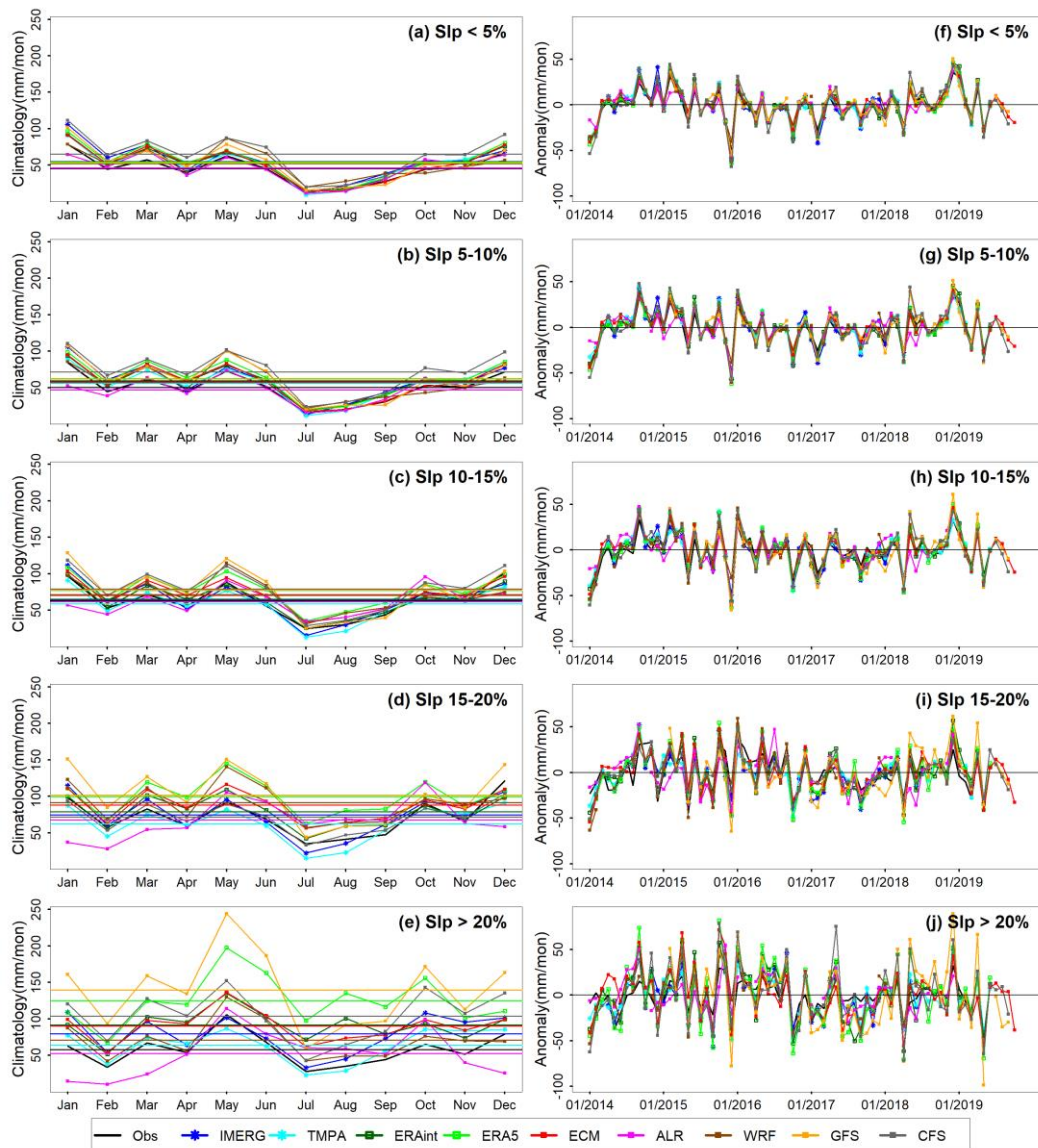


Figure 3.9. Monthly climatology (from (a) to (e)) and monthly anomaly (from (f) to (j)) for slope classes. The color-coded horizontal lines in the climatology plot show the mean monthly precipitation for the respective datasets. The horizontal line in the anomaly plot shows zero anomaly level

Differences between climatology plots of the observed data and the products increase with the increasing terrain slopes (Figures 3.9a to 3.9e), where the climatology time series of ERA5, GFS, and CFS show the most differences (overestimation) with the observed ones. Climatology plots for ALR show a slight underestimation of the observed data, especially over the higher terrain slopes. It is to note that the effect of increasing terrain slopes is more pronounced on the climatology plots of model-based

products. Contrary to their variation with wetness and elevation, the monthly anomaly time series of the products show larger discrepancies with increasing terrain slopes (Figures 3.9f to 3.9j), thus indicating the impact of increasing terrain complexity on the accuracy of the products.

Summarizing, investigating the time-series variability shows that the variabilities of monthly and seasonal precipitation and, in turn, the accuracy of the products are profoundly affected by all three factors (i.e., wetness, elevation, and slope).

3.1.2.2. Spatial Distribution of Statistics

The spatially distributed maps for monthly Bias show sharp transitions of Bias values frequently occurring in cases of GFS (Figure 3.10h), and CFS (Figure 3.10i) forecasts depicting their very wet and very dry biases over different parts of the area.

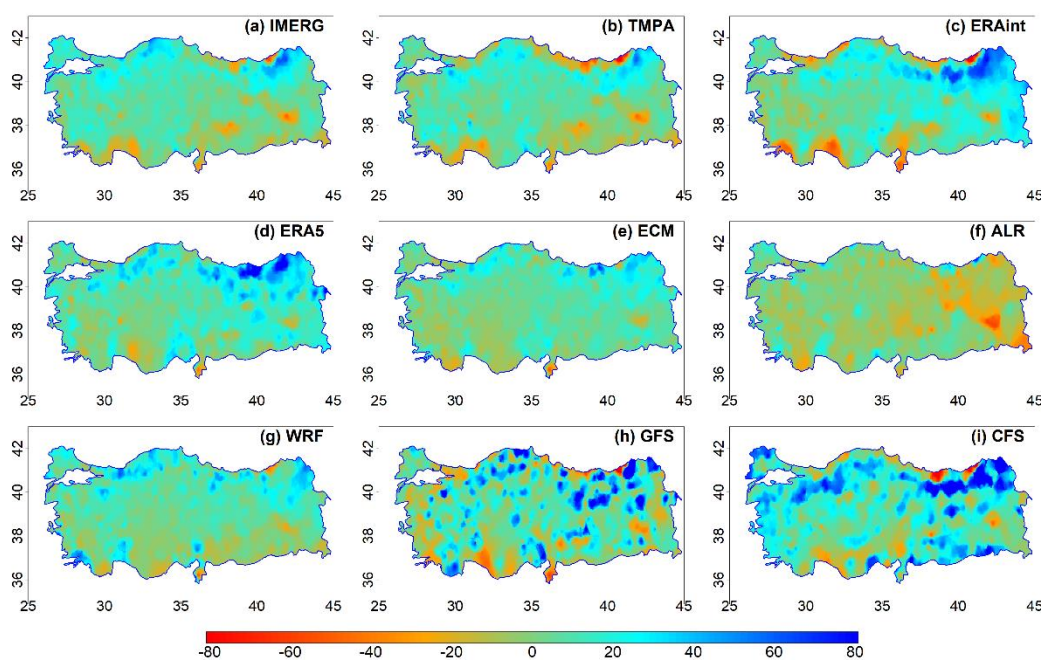


Figure 3.10. Spatial distribution maps for monthly Bias (mm/month). Negative values denote dry Bias while positive ones denote wet Bias

Along most of the Black Sea coastline (the entire northern side of the study area), the products tend to underestimate the observed precipitation, which is the case with IMERG (Figure 3.10a), TMPA (Figure 3.10b), ERAInt (Figure 3.10c), and ALR

(Figure 3.10f). Almost all the products have less Bias display over the central parts of the region where most of the dry to moderately dry areas exist. Regarding terrain complexity, all the products, except ERA5 (Figure 3.10d), tend to show dry Bias over a mountainous patch of northeastern Black Sea region, while they show wet bias over the regions situated right below that patch; this pattern is prominent in cases of IMERG, TMPA, ERAInt, GFS, and CFS. The apparent reason behind this behavior is the orographic character of precipitation falling over that region.

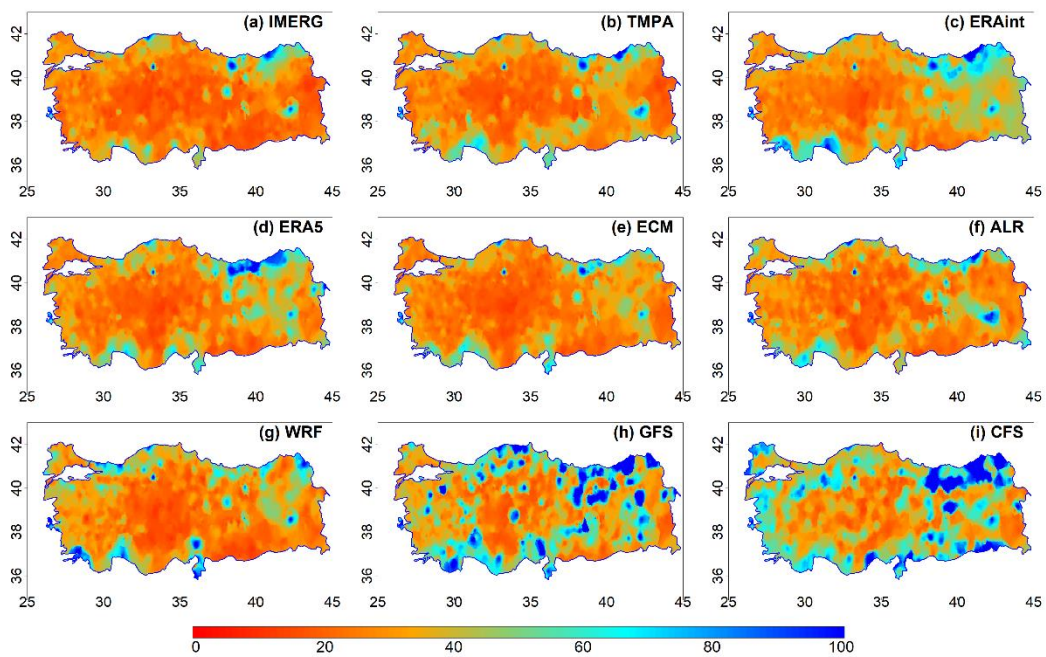


Figure 3.11. Spatial distribution maps for monthly RMSE (mm/month)

The spatially distributed maps for monthly RMSE (which is a combination of Bias and ErrSD) provide an overall picture of the errors associated with the products (Figure 3.11). GFS and CFS are, again, the two worst performers showing large monthly RMSE over several regions of the study area, especially over the eastern parts of it, which are known for their complex topography. Although ECM shows larger monthly Bias compared to ALR, it shows overall slightly less RMSE than ALR (Figures 3.11e and 3.11f), especially over eastern and northeastern regions with complex topography. Similar patterns exist in research-grade products, where IMERG (Figure 3.11a) shows slightly less RMSE than TMPA (Figure 3.11b) over western

regions, and ERA5 (Figure 3.11d) performs better than ERAint (Figure 3.11c) over some eastern regions of the study area.

3.1.2.3. Temporal Statistics – The Entire Study Area

Table 3.10. Monthly Mean and SD for the entire area and wetness classes

Region		Entire	Dry	Mod-dry	Mod-wet	Wet	
No. of Stations		755	279	303	123	50	
Mean (mm/month)	Complete Time Series	Obs	49.2	32.9	48.8	67.5	97.7
		IMERG	57.6	46.0	59.3	68.6	84.7
		TMPA	54.8	45.5	57.4	62.3	73.0
		ERAint	57.5	52.8	58.4	62.3	67.3
		ERA5	61.4	48.0	60.4	76.8	104.8
		ECM	55.8	41.5	54.5	72.7	101.0
		ALR	46.6	30.6	46.0	64.6	95.3
		WRF	57.8	40.7	58.6	74.2	107.9
		GFS	58.3	44.7	61.2	75.6	73.9
		CFS	67.9	54.7	73.9	78.6	78.4
SD (mm/month)	Complete Time Series	Obs	41.6	28.9	42.1	55.6	75.4
		IMERG	40.3	32.4	42.0	47.9	55.6
		TMPA	41.2	33.5	43.3	47.6	55.4
		ERAint	39.4	36.5	40.2	43.3	41.0
		ERA5	42.1	34.4	42.1	51.6	61.6
		ECM	40.6	32.1	40.5	51.1	62.6
		ALR	40.7	29.0	40.9	54.0	72.7
		WRF	45.2	34.6	45.7	54.4	79.2
		GFS	47.0	37.6	48.7	59.6	57.9
		CFS	50.5	41.3	54.1	59.5	58.1
	Climatology	Obs	29.0	20.3	29.1	38.8	53.3
		IMERG	29.1	23.1	30.4	34.5	40.9
		TMPA	28.7	23.3	30.2	32.9	39.5
		ERAint	27.7	25.7	28.3	30.4	28.2
		ERA5	30.2	24.9	30.2	36.3	44.0
		ECM	29.0	23.8	28.9	35.4	43.1
		ALR	30.0	21.6	29.5	39.5	56.2
		WRF	32.0	25.9	32.3	35.8	55.2
		GFS	34.4	27.0	35.7	43.8	45.5
		CFS	35.5	29.3	37.5	41.7	42.4
	Anomaly	Obs	29.4	20.6	29.8	38.9	53.1
		IMERG	27.9	22.5	29.1	33.5	37.7
		TMPA	29.4	24.0	30.8	34.3	38.5
		ERAint	27.8	25.9	28.2	30.5	29.3
		ERA5	29.2	23.6	29.2	36.4	42.2
		ECM	27.9	21.3	27.9	36.1	44.4
		ALR	26.7	18.7	27.0	36.1	47.3
		WRF	29.8	20.7	30.2	39.0	55.0
		GFS	31.2	25.2	32.4	39.8	35.9
		CFS	35.2	28.5	38.0	41.7	39.0

Over the entire study area, ALR shows the closest average monthly precipitation to the observed data (Table 3.10) with a dry Bias of 2.6 mm/month (Table 3.11). All the other products overestimate (i.e., wet Bias) the observed monthly data, with CFS data showing the most substantial wet Bias (18.7 mm/month).

Table 3.11. *Monthly Bias and ErrSD for the entire area and wetness classes*

Region		Entire	Dry	Mod-dry	Mod-wet	Wet	
No. of Stations		755	279	303	123	50	
Bias (mm/month)	Complete Time Series	IMERG	8.4	13.1	10.5	1.1	-13.0
		TMPA	5.6	12.6	8.6	-5.2	-24.6
		ERAint	8.3	19.9	9.6	-5.2	-30.4
		ERA5	12.2	15.1	11.6	9.3	7.1
		ECM	6.6	8.6	5.7	5.2	3.3
		ALR	-2.6	-2.4	-2.8	-2.9	-2.4
		WRF	8.6	7.8	9.8	6.7	10.2
		GFS	9.0	11.7	12.4	8.1	-23.8
		CFS	18.7	21.8	25.1	11.1	-19.3
ErrSD (mm/month)	Complete Time Series	IMERG	24.3	19.5	24.1	27.9	42.9
		TMPA	27.7	21.8	27.4	33.4	48.4
		ERAint	29.5	25.5	27.7	33.4	54.0
		ERA5	27.6	22.7	26.6	32.3	49.8
		ECM	26.6	21.2	25.9	32.7	45.9
		ALR	30.4	22.0	30.6	38.7	54.8
		WRF	30.6	22.6	31.5	38.1	52.0
		GFS	35.8	28.8	36.1	43.4	54.2
		CFS	35.9	29.8	36.8	40.5	53.2
	Climatology	IMERG	17.9	14.1	18.0	21.3	30.5
		TMPA	17.7	14.2	18.1	20.3	28.9
		ERAint	18.4	16.5	16.8	19.5	35.5
		ERA5	17.8	15.3	16.9	19.9	32.0
		ECM	16.5	14.2	15.8	18.8	27.6
		ALR	21.4	14.2	20.9	30.0	44.6
		WRF	22.8	16.2	23.1	30.5	39.5
		GFS	23.4	19.5	23.6	27.3	34.0
		CFS	22.8	19.8	23.3	24.5	32.9
	Anomaly	IMERG	21.6	16.9	21.5	26.4	37.1
		TMPA	23.2	18.2	22.9	28.8	40.1
		ERAint	24.6	20.4	23.9	29.0	41.9
		ERA5	23.0	18.0	22.7	28.1	40.6
		ECM	22.8	17.2	22.6	29.3	39.9
		ALR	26.1	19.1	26.4	33.1	45.6
		WRF	26.2	19.0	26.6	33.7	46.1
		GFS	29.1	22.3	29.9	36.7	43.6
		CFS	29.0	23.5	30.1	33.5	42.3

Compared to the anomaly SD of the observed data (29.4 mm/month), a larger anomaly SD of CFS data (35.2 mm/month) (Table 3.10) along with its substantial wet Bias of 18.7 mm/month (Table 3.11) suggest it to be, probably, less beneficent in operational fields like flood forecasting. Whereas, both the anomaly SD (26.7 mm/month), as well as the Bias (2.6 mm/month) of ALR are the lowest among all the products. IMERG shows the lowest ErrSD (24.3 mm/month) among all the products when the complete time series, as well as the anomaly components, are considered (Table 3.11) over the entire area.

Table 3.12. Monthly CC for the entire area and wetness classes

Region		Entire	Dry	Mod-dry	Mod-wet	Wet	
No. of Stations		755	279	303	123	50	
CC with the Observed Data	Complete Time Series	IMERG	0.82	0.81	0.84	0.84	0.78
		TMPA	0.79	0.79	0.79	0.78	0.72
		ERAint	0.76	0.74	0.77	0.79	0.71
		ERA5	0.79	0.77	0.80	0.82	0.73
		ECM	0.79	0.77	0.81	0.82	0.77
		ALR	0.72	0.74	0.72	0.72	0.66
		WRF	0.78	0.79	0.77	0.76	0.76
		GFS	0.74	0.73	0.75	0.76	0.69
		CFS	0.75	0.73	0.76	0.76	0.70
	Climatology	IMERG	0.81	0.81	0.82	0.82	0.80
		TMPA	0.82	0.81	0.82	0.83	0.79
		ERAint	0.81	0.79	0.82	0.84	0.75
		ERA5	0.82	0.81	0.84	0.84	0.74
		ECM	0.83	0.82	0.85	0.85	0.78
		ALR	0.74	0.80	0.75	0.68	0.59
		WRF	0.75	0.81	0.75	0.65	0.66
		CFS	0.79	0.77	0.80	0.80	0.75
	Anomaly	IMERG	0.71	0.69	0.72	0.72	0.68
		TMPA	0.69	0.69	0.71	0.68	0.63
		ERAint	0.65	0.64	0.66	0.67	0.63
		ERA5	0.69	0.67	0.70	0.72	0.68
		ECM	0.68	0.66	0.70	0.71	0.68
		ALR	0.56	0.54	0.56	0.59	0.57
		WRF	0.61	0.57	0.62	0.63	0.65
		CFS	0.58	0.59	0.57	0.62	0.58
		CFS	0.63	0.61	0.64	0.66	0.61

ERA5 shows improved ErrSD (27.6 mm/month) compared to that of ERAint (29.5 mm/month), while GFS and CFS are among the products with the highest ErrSD.

Besides having the lowest ErrSD, IMERG data shows the highest monthly CC (with the observed data) as well (Table 3.12), while ALR data comes out to have the least CC. The climatology components of the products have lower ErrSD (on average, 19.9 mm/month) and higher CC (on average, 0.80) as compared to their anomaly components (ErrSD: 25.1 mm/month, CC: 0.64).

3.1.2.4. Temporal Statistics – Wetness Classes

As it is mentioned already while discussing the daily statistics, higher precipitation amounts tend to cause higher ErrSD. Hence, monthly ErrSD for a given product increases with the increasing wetness of the region (Table 3.11); this is valid for monthly complete time series, as well as for climatology and anomaly components of all nine products. As the larger values of ErrSD result into lower correlation, the combined average monthly CC of the products over wet regions (0.72) is lower than that over dry regions (0.76) (Table 3.12). Over the wet regions (i.e., receiving higher amounts of precipitation), IMERG, ERA5, and ECM show the highest monthly anomaly CC (0.68) while ALR and GFS are among the products showing lower anomaly CC there.

3.1.2.5. Temporal Statistics – Elevation Classes

Means and SD are higher for the observed precipitation as well as for the products over the regions having the lowest elevations (Table 3.13) as these regions receive the highest total amount of precipitation. Hence the conclusion “wetness has a prominent role in the error statistics of the products over the study area” over the daily time scale is also valid over the monthly time scale. Over the highest elevations (i.e., > 2000m), ALR shows very less anomaly SD (16.3 mm/month) compared to that (27.7 mm/month) of the observed data while, among all the products, GFS shows the highest SD for complete time series and both of its components over these regions.

Table 3.13. Monthly Mean and SD for the entire area and elevation classes

Region		Entire	Elv < 500	Elv 500-1000	Elv 1000-1500	Elv 1500-2000	Elv > 2000	
No. of Stations		755	237	219	209	77	13	
Mean (mm/month)	Complete Time Series	Obs	49.2	61.8	44.1	42.7	43.6	44.3
		IMERG	57.6	69.4	53.4	50.5	52.5	58.6
		TMPA	54.8	63.9	50.8	49.7	52.1	55.2
		ERAint	57.5	58.2	54.7	54.7	68.6	72.8
		ERA5	61.4	71.3	56.0	55.0	63.1	66.1
		ECM	55.8	66.2	50.1	49.6	56.3	57.8
		ALR	46.6	64.2	42.7	37.3	31.3	29.7
		WRF	57.8	70.2	50.4	50.2	59.5	69.6
		GFS	58.3	55.9	55.7	57.7	70.9	78.2
CFS	67.9	76.1	63.9	60.5	71.0	84.0		
SD (mm/month)	Complete Time Series	Obs	41.6	55.1	35.6	34.4	37.1	40.9
		IMERG	40.3	51.9	36.8	34.0	32.7	32.3
		TMPA	41.2	53.3	37.2	35.1	33.2	32.3
		ERAint	39.4	41.6	38.2	36.8	42.5	43.4
		ERA5	42.1	50.4	39.1	37.0	39.6	38.0
		ECM	40.6	48.2	37.2	36.1	39.8	36.2
		ALR	40.7	53.7	36.4	33.4	33.9	34.8
		WRF	45.2	53.9	39.5	39.8	48.7	51.7
		GFS	47.0	48.6	43.7	46.0	52.8	55.4
	CFS	50.5	60.7	48.0	43.5	45.2	52.3	
	Climatology	Obs	29.0	37.5	24.9	24.2	28.0	29.8
		IMERG	29.1	37.8	26.5	24.4	23.2	22.5
		TMPA	28.7	36.8	26.0	24.6	23.5	22.1
		ERAint	27.7	29.0	26.8	25.8	30.4	31.5
		ERA5	30.2	35.2	28.1	26.8	29.7	28.4
		ECM	29.0	33.0	26.9	26.5	29.9	26.7
		ALR	30.0	38.9	26.4	24.5	27.5	30.5
		WRF	32.0	35.4	28.2	29.6	37.6	38.9
		GFS	34.4	36.5	31.3	33.1	39.6	40.9
	CFS	35.5	42.0	33.6	30.6	33.4	39.3	
	Anomaly	Obs	29.4	39.5	25.4	24.3	24.1	27.7
		IMERG	27.9	36.0	25.5	23.5	22.8	22.9
		TMPA	29.4	38.2	26.6	25.0	23.4	23.4
		ERAint	27.8	29.4	27.1	26.1	29.3	29.2
		ERA5	29.2	35.9	27.1	25.2	25.8	24.6
		ECM	27.9	34.8	25.3	24.0	25.7	23.9
		ALR	26.7	36.4	24.6	21.6	18.7	16.3
		WRF	29.8	39.3	25.9	24.0	26.7	31.5
		GFS	31.2	32.0	29.7	30.9	33.0	35.2
	CFS	35.2	42.8	33.7	30.1	29.6	33.7	

Although the lowest elevation regions receive the most substantial amounts of average precipitation, monthly ErrSD for a given product is not the highest over these regions (Table 3.14). Instead, the elevation effect dominates in the regions with the highest elevations where all the products show the highest ErrSD. Generally, the elevation effect is more prominent on the monthly CC of the products over the regions with elevations higher than 1000 m (Table 3.15).

Table 3.14. Monthly Bias and ErrSD for the entire area and elevation classes

Region		Entire	Elv < 500	Elv 500-1000	Elv 1000-1500	Elv 1500-2000	Elv > 2000	
No. of Stations		755	237	219	209	77	13	
Bias (mm/month)	Complete Time Series	IMERG	8.4	7.6	9.3	7.8	8.9	14.3
		TMPA	5.6	2.1	6.8	7.0	8.5	10.9
		ERAint	8.3	-3.6	10.7	12.0	25.0	28.5
		ERA5	12.2	9.5	12.0	12.3	19.5	21.8
		ECM	6.6	4.3	6.1	6.9	12.6	13.4
		ALR	-2.6	2.4	-1.3	-5.4	-12.3	-14.6
		WRF	8.6	8.3	6.3	7.5	15.8	25.2
		GFS	9.0	-5.9	11.6	15.1	27.3	33.9
		CFS	18.7	14.3	19.9	17.8	27.3	39.6
ErrSD (mm/month)	Complete Time Series	IMERG	24.3	29.8	19.8	21.3	26.0	35.5
		TMPA	27.7	34.0	24.3	24.2	26.9	32.2
		ERAint	29.5	34.9	25.1	26.4	32.4	39.7
		ERA5	27.6	33.6	23.6	24.1	28.9	33.6
		ECM	26.6	33.0	22.0	23.3	27.7	32.2
		ALR	30.4	36.6	25.8	27.6	30.4	37.7
		WRF	30.6	39.6	24.7	25.4	31.6	43.3
		GFS	35.8	39.3	31.2	33.6	41.6	50.9
		CFS	35.9	42.2	31.9	31.3	38.4	47.2
	Climatology	IMERG	17.9	21.7	15.4	15.3	19.6	24.3
		TMPA	17.7	20.7	15.8	15.7	18.7	22.4
		ERAint	18.4	20.8	15.7	16.6	21.8	26.5
		ERA5	17.8	20.4	15.8	15.7	20.4	23.3
		ECM	16.5	19.0	14.3	14.7	19.4	22.5
		ALR	21.4	26.8	17.4	18.4	23.6	27.2
		WRF	22.8	29.5	18.9	18.0	25.2	30.9
		GFS	23.4	24.3	20.8	22.6	28.7	31.8
		CFS	22.8	25.7	20.5	20.5	25.2	32.3
	Anomaly	IMERG	21.6	26.7	18.5	19.0	21.4	26.1
		TMPA	23.2	29.0	20.2	20.2	22.0	25.4
		ERAint	24.6	29.3	21.3	22.0	25.9	30.8
		ERA5	23.0	28.9	19.6	19.8	22.6	27.2
		ECM	22.8	29.1	18.9	19.6	22.4	26.6
		ALR	26.1	32.8	22.7	22.6	24.0	27.4
		WRF	26.2	34.2	21.9	21.6	25.3	32.8
		GFS	29.1	33.6	25.4	26.7	30.7	39.6
		CFS	29.0	35.2	25.7	25.1	29.2	35.5

Summarizing, the combined average monthly CC of all the products decreases from 0.78 for the lowest elevation regions to 0.66 for the highest elevation regions, whereas ErrSD increases from 35.9 mm/month for the lowest elevation regions to 39.1 mm/month for the highest elevation regions.

Table 3.15. Monthly CC for the entire area and elevation classes

Region		Entire	Elv < 500	Elv 500-1000	Elv 1000-1500	Elv 1500-2000	Elv > 2000	
No. of Stations		755	237	219	209	77	13	
CC with the Observed Data	Complete Time Series	IMERG	0.82	0.84	0.85	0.82	0.75	0.68
		TMPA	0.79	0.79	0.80	0.79	0.75	0.7
		ERAint	0.76	0.77	0.78	0.76	0.71	0.61
		ERA5	0.79	0.80	0.81	0.79	0.75	0.68
		ECM	0.79	0.80	0.81	0.79	0.76	0.69
		ALR	0.72	0.75	0.74	0.70	0.66	0.6
		WRF	0.78	0.74	0.79	0.81	0.79	0.69
		GFS	0.74	0.74	0.75	0.74	0.72	0.65
		CFS	0.75	0.76	0.77	0.74	0.69	0.63
	Climatology	IMERG	0.81	0.83	0.83	0.81	0.74	0.68
		TMPA	0.82	0.83	0.83	0.80	0.78	0.73
		ERAint	0.81	0.83	0.83	0.80	0.76	0.68
		ERA5	0.82	0.83	0.83	0.82	0.78	0.75
		ECM	0.83	0.84	0.85	0.83	0.80	0.75
		ALR	0.74	0.73	0.78	0.73	0.70	0.69
		WRF	0.75	0.66	0.78	0.82	0.79	0.74
		GFS	0.79	0.79	0.78	0.79	0.79	0.76
		CFS	0.79	0.81	0.82	0.77	0.74	0.72
	Anomaly	IMERG	0.71	0.74	0.73	0.70	0.58	0.61
		TMPA	0.69	0.71	0.71	0.69	0.59	0.58
		ERAint	0.65	0.69	0.67	0.65	0.55	0.46
		ERA5	0.69	0.72	0.71	0.69	0.59	0.53
		ECM	0.68	0.71	0.71	0.67	0.59	0.52
		ALR	0.56	0.62	0.58	0.54	0.39	0.4
		WRF	0.61	0.64	0.62	0.60	0.51	0.55
		GFS	0.58	0.59	0.63	0.58	0.50	0.42
		CFS	0.63	0.67	0.65	0.62	0.52	0.47

The factor of increasing elevations most pronouncedly affects the monthly absolute Bias and monthly ErrSD of GFS and CFS (Figure 3.12), while boxplots for WRF also show the inverse effect of increasing elevations. Overall, the products tend to have the most substantial absolute Bias and ErrSD over elevations higher than 1500 m. Very few stations lying under the highest elevation bins might also be contributing towards the larger errors by the products.

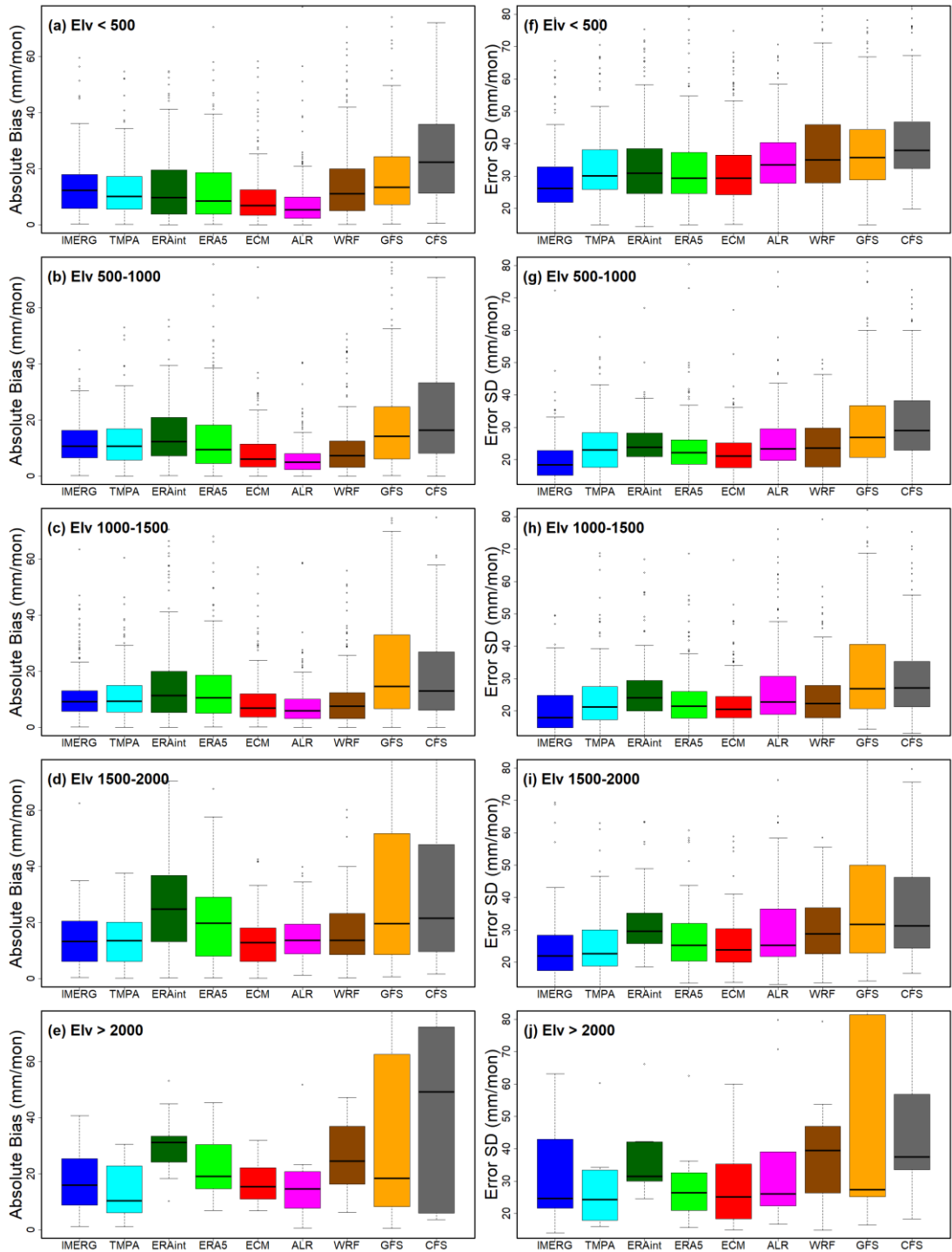


Figure 3.12. Boxplots for monthly absolute Bias (from (a) to (e)) and monthly ErrSD (from (f) to (j)) for elevation classes

3.1.2.6. Temporal Statistics – Slope Classes

Table 3.16. Monthly Mean and SD for the entire area and slope classes.

Region		Entire	Slp < 5%	Slp 5-10%	Slp 10-15%	Slp 15-20%	Slp > 20%	
No. of Stations		755	237	219	209	77	13	
Mean (mm/month)	Complete Time Series	Obs	49.2	46.0	51.0	63.4	71.1	56.7
		IMERG	57.6	55.0	59.4	64.9	74.5	79.7
		TMPA	54.8	52.9	57.4	59.6	63.2	64.4
		ERAInt	57.5	54.0	60.6	65.7	80.0	92.0
		ERA5	61.4	55.9	63.6	78.1	100.6	125.4
		ECM	55.8	51.5	57.4	71.1	87.7	90.1
		ALR	46.6	44.4	45.7	60.4	67.4	53.7
		WRF	57.8	54.0	59.4	72.1	93.1	72.6
		GFS	58.3	52.1	60.8	76.0	99.9	137.2
		CFS	67.9	64.6	71.2	78.7	70.8	103.0
SD (mm/month)	Complete Time Series	Obs	41.6	40.8	41.1	49.3	48.7	36.1
		IMERG	40.3	40.1	40.0	42.0	43.3	41.2
		TMPA	41.2	41.5	40.5	41.7	40.1	37.2
		ERAInt	39.4	38.9	39.7	40.9	43.2	41.4
		ERA5	42.1	41.0	41.8	47.2	50.6	57.0
		ECM	40.6	39.7	40.7	45.5	46.0	44.2
		ALR	40.7	39.8	39.4	48.4	52.4	46.2
		WRF	45.2	43.8	45.8	50.9	59.0	49.7
		GFS	47.0	44.4	47.6	56.6	63.4	76.9
		CFS	50.5	50.6	50.2	52.4	41.0	55.9
	Climatology	Obs	29.0	28.0	28.8	36.1	37.9	27.3
		IMERG	29.1	29.0	28.7	30.3	31.6	28.5
		TMPA	28.7	28.8	28.6	28.9	27.8	25.0
		ERAInt	27.7	27.5	28.1	28.4	28.9	24.7
		ERA5	30.2	29.3	30.3	33.3	35.9	38.7
		ECM	29.0	28.4	29.5	32.2	31.4	27.4
		ALR	30.0	29.1	28.6	36.7	39.3	36.1
		WRF	32.0	31.0	32.6	35.9	40.5	34.4
		GFS	34.4	32.4	35.0	42.0	46.1	56.7
		CFS	35.5	35.5	35.5	37.2	29.2	39.4
	Anomaly	Obs	29.4	29.2	28.9	33.4	30.4	23.7
		IMERG	27.9	27.7	27.8	29.3	29.8	29.8
		TMPA	29.4	29.6	28.7	30.1	29.1	27.7
		ERAInt	27.8	27.4	27.9	29.1	31.6	32.7
		ERA5	29.2	28.4	28.5	33.1	34.9	40.8
		ECM	27.9	27.4	27.6	31.5	32.6	34.1
		ALR	26.7	26.1	26.0	31.5	34.8	28.4
		WRF	29.8	28.9	29.5	34.3	40.5	33.7
		GFS	31.2	29.7	31.2	37.1	41.9	49.6
		CFS	35.2	35.3	34.8	36.1	28.6	39.4

All the datasets (including the observed and product data) associate the lowest amounts of average precipitation with the regions having the lowest terrain slopes (Table 3.16), while the average precipitation generally increases by going towards higher slopes. ALR and WRF follow the observed data in showing the highest monthly average precipitation amounts over the regions having slopes between 15-20%, while

all the other products show it over the highest slope regions (i.e., with > 20% slopes). Monthly ErrSD does not necessarily follow the trend mentioned above.

Table 3.17. *Monthly Bias and ErrSD for the entire area and slope classes*

Region		Entire	Slp < 5%	Slp 5-10%	Slp 10-15%	Slp 15-20%	Slp > 20%	
No. of Stations		755	237	219	209	77	13	
Bias (mm/month)	Complete Time Series	IMERG	8.4	9.0	8.4	1.5	3.4	23.0
		TMPA	5.6	6.9	6.4	-3.7	-7.9	7.8
		ERAint	8.3	7.9	9.6	2.4	8.8	35.4
		ERA5	12.2	9.9	12.6	14.8	29.5	68.8
		ECM	6.6	5.5	6.4	7.7	16.6	33.5
		ALR	-2.6	-1.7	-5.3	-3.0	-3.8	-2.9
		WRF	8.6	7.9	8.4	8.7	22.0	16.0
		GFS	9.0	6.0	9.8	12.6	28.7	80.6
		CFS	18.7	18.6	20.2	15.4	-0.3	46.3
ErrSD (mm/month)	Complete Time Series	IMERG	24.3	23.4	23.9	29.1	33.4	27.5
		TMPA	27.7	27.2	26.9	31.8	36.7	28
		ERAint	29.5	28.8	28.8	35.7	38.3	29.4
		ERA5	27.6	26.6	26.6	33.2	39.4	40.4
		ECM	26.6	25.9	25.7	31.7	35.1	29.6
		ALR	30.4	28.4	30.9	37.9	48.3	39.7
		WRF	30.6	30.0	30.1	35.1	40.0	27.9
		GFS	35.8	33.5	35.1	47.1	52.9	62.6
		CFS	35.9	35.0	34.9	42.3	41.8	48.6
	Climatology	IMERG	17.9	17.1	17.4	21.9	29.7	24.2
		TMPA	17.7	17.0	17.1	21.7	28.6	21.8
		ERAint	18.4	17.6	17.4	24.4	27.5	20.8
		ERA5	17.8	16.8	16.8	23.3	31.2	29.5
		ECM	16.5	15.7	15.8	21.3	27.8	18.7
		ALR	21.4	19.4	21.3	29.7	43.5	35.4
		WRF	22.8	22.1	22.0	28.6	33.4	23.3
		GFS	23.4	21.6	23.0	32.1	35.9	43.6
		CFS	22.8	21.8	22.4	27.8	33.1	32.1
	Anomaly	IMERG	21.6	20.9	21.6	26.2	28.0	21.7
		TMPA	23.2	22.8	22.7	26.6	29.8	23.5
		ERAint	24.6	23.9	24.3	29.0	31.8	25.9
		ERA5	23.0	22.2	22.3	27.7	31.4	31.6
		ECM	22.8	22.2	22.1	27.4	29.7	26.5
		ALR	26.1	24.9	26.3	31.6	36.6	27
		WRF	26.2	25.5	25.8	31.7	33.2	25.6
		GFS	29.1	27.5	28.6	37.1	42.7	45.3
		CFS	29.0	28.6	27.9	34.1	32.0	35.7

Wet bias (Table 3.17) in the precipitation products, except ALR, over very complex topography (i.e., slopes > 20%), may result in an increased number of false alarms for floods. Among all the products, GFS shows the largest ErrSD over the regions with terrain slopes greater than 5% (Table 3.17); the same is valid for complete time series, climatology, and anomaly. IMERG consistently performs the best regarding ErrSD over varying slopes, while ECM shows the second-best ErrSD values after IMERG; this is true for both the complete time series and anomaly.

ECM and IMERG both show the equal amount of monthly CC (0.75) over the steepest slope regions (Table 3.18), which depicts the utility of this real-time product against a gauge-adjusted research-grade product over complex topography. Here, the inverse effect of increasing terrain complexity over the accuracy of the products is noticeable, as the combined average anomaly CC drops from 0.66 over the lowest slope regions to 0.56 over the highest slope regions, whereas ErrSD increases from 28.8 mm/month to 37 mm/month on the same criteria.

Table 3.18. *Monthly CC for the entire area and slope classes*

Region		Entire	Slp < 5%	Slp 5-10%	Slp 10-15%	Slp 15-20%	Slp > 20%	
No. of Stations		755	237	219	209	77	13	
CC with the Observed Data	Complete Time Series	IMERG	0.82	0.83	0.82	0.82	0.76	0.75
		TMPA	0.79	0.79	0.79	0.77	0.70	0.7
		ERAint	0.76	0.76	0.77	0.74	0.70	0.72
		ERA5	0.79	0.79	0.80	0.79	0.73	0.68
		ECM	0.79	0.79	0.80	0.80	0.76	0.75
		ALR	0.72	0.74	0.70	0.71	0.56	0.58
		WRF	0.78	0.77	0.78	0.79	0.78	0.8
		GFS	0.74	0.75	0.74	0.72	0.66	0.64
	CFS	0.75	0.75	0.75	0.73	0.64	0.61	
	Climatology	IMERG	0.81	0.83	0.81	0.79	0.65	0.62
		TMPA	0.82	0.82	0.83	0.80	0.65	0.65
		ERAint	0.81	0.82	0.83	0.75	0.67	0.64
		ERA5	0.82	0.83	0.84	0.80	0.65	0.64
		ECM	0.83	0.84	0.84	0.82	0.68	0.74
		ALR	0.74	0.77	0.74	0.67	0.40	0.45
		WRF	0.75	0.75	0.78	0.69	0.66	0.73
		GFS	0.79	0.79	0.79	0.74	0.70	0.71
	CFS	0.79	0.81	0.79	0.76	0.58	0.59	
	Anomaly	IMERG	0.71	0.72	0.71	0.66	0.63	0.66
		TMPA	0.69	0.70	0.70	0.65	0.57	0.6
		ERAint	0.65	0.66	0.65	0.62	0.54	0.61
		ERA5	0.69	0.70	0.70	0.66	0.59	0.58
		ECM	0.68	0.69	0.69	0.66	0.61	0.6
		ALR	0.56	0.58	0.52	0.55	0.42	0.44
		WRF	0.61	0.61	0.60	0.60	0.56	0.61
		GFS	0.58	0.60	0.58	0.55	0.47	0.43
	CFS	0.63	0.64	0.64	0.57	0.49	0.52	

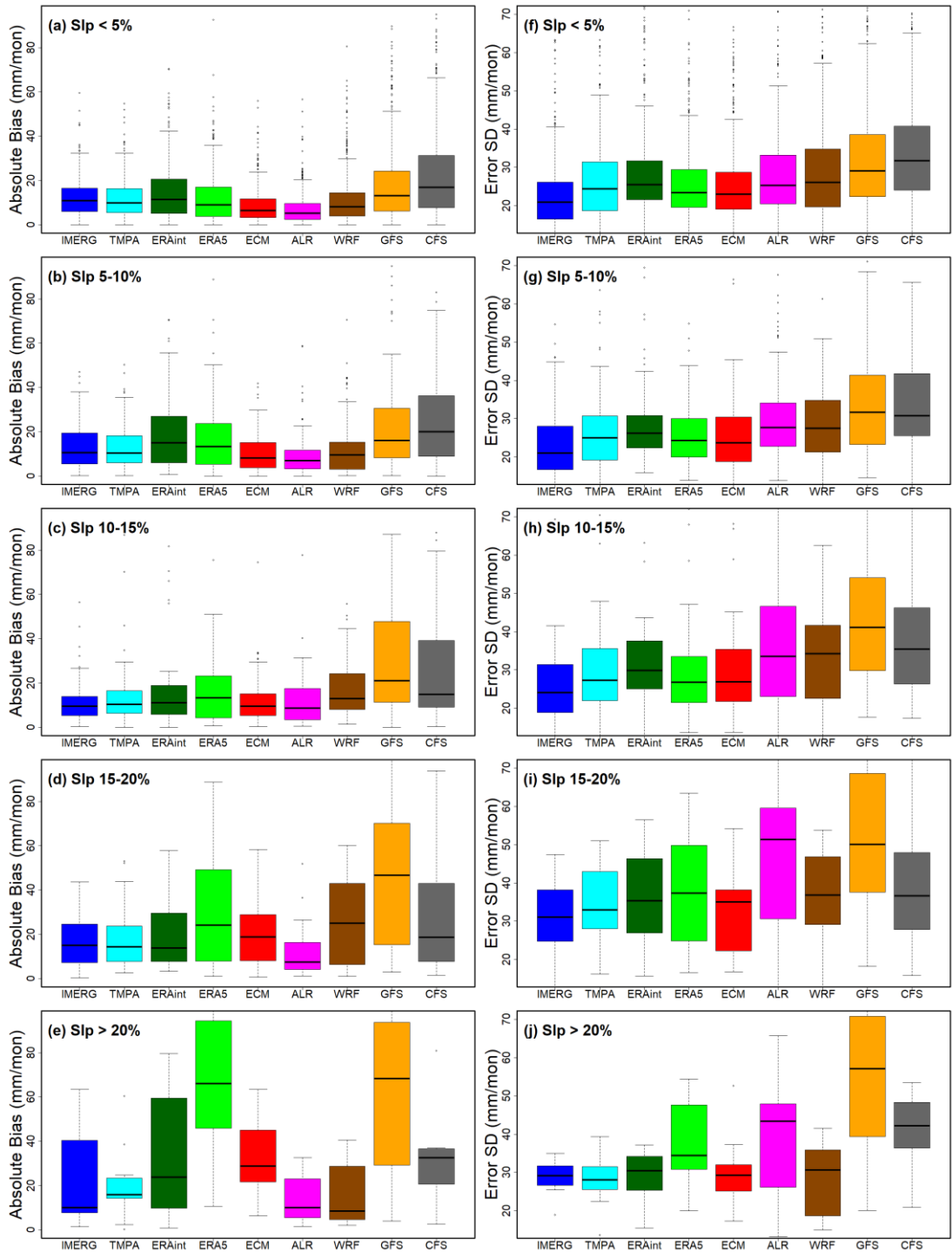


Figure 3.13. Boxplots for monthly absolute Bias (from (a) to (e)) and monthly ErrSD (from (f) to (j)) for slope classes

Considering the variation in terrain slopes (Figure 3.13), although both the absolute Bias and ErrSD tend to increase over the slope range of 0-20%, the change in these two statistics is not linear for all the products.

3.1.2.7. Correlation Histograms

To investigate the frequency of correlations over entire study area, histograms of the monthly CC of the products with the observed data were prepared. Histograms for CC of research-grade products (Figure 3.14a) suggest that higher CC values (say > 0.8) occur more frequently in case of IMERG as compared to TMPA, which in turn, results in the higher average CC of IMERG.

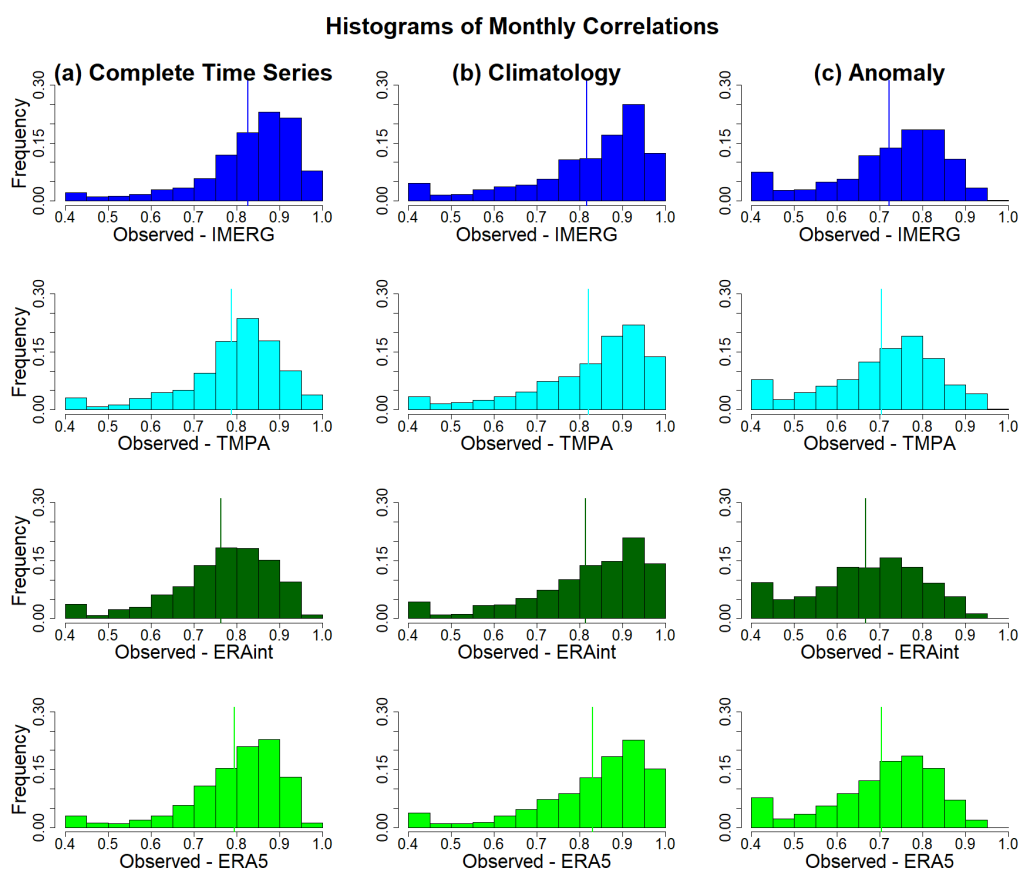


Figure 3.14. Histograms of monthly CC between the observed data and research-grade products; (a) Complete Time Series, (b) Climatology, and (c) Anomaly. The color-coded vertical lines show mean monthly CC for the respective dataset with the observed data

A similar situation exists between ERAint and ERA5, where ERAint shows relatively lower frequency bars against higher values of monthly CC as compared to those shown by ERA5. Among the components of the monthly complete time series, climatology components (Figure 3.14b) of the products are more correlated compared to anomaly components (Figure 3.14c), thus showing higher frequency bars against higher CC values.

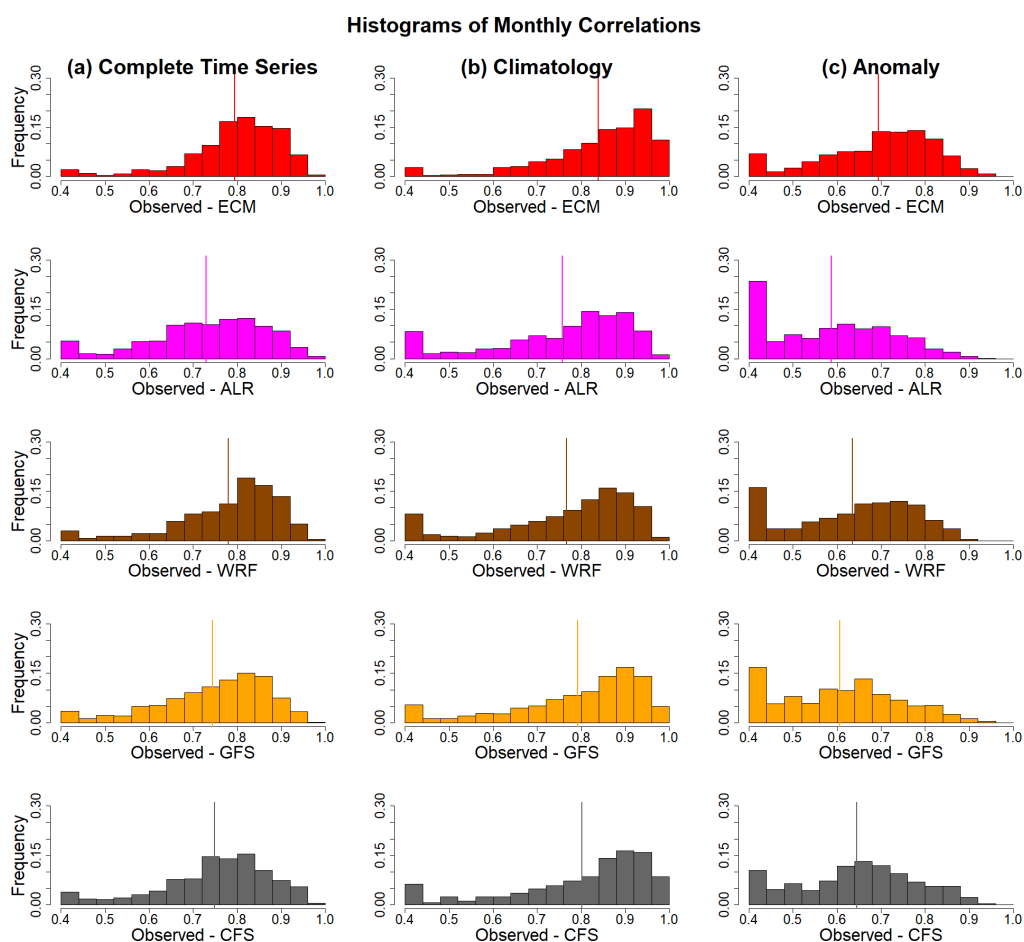


Figure 3.15. Histograms of monthly CC between the observed data and research-grade products; (a) Complete Time Series, (b) Climatology, and (c) Anomaly. The color-coded vertical lines show mean monthly CC for the respective dataset with the observed data.

Among the real-time forecast datasets (Figure 3.15), ECM and WRF equally show the lowest frequency bars against lower CC values (say < 0.6). Overall, ECM shows the most frequent occurrence of higher CC values (slightly better than WRF). Considering

complete (Figure 3.15a), climatology (Figure 3.15b), and anomaly (Figure 3.15c) time series, ALR shows the highest frequency bars against the lowest CC values (say < 0.4), thus depicting its worst performance related to monthly CC with the observed data. CFS shows slightly better CC as compared to GFS.

3.1.3. Annual Time Scale

Table 3.19. Annual spatial mean precipitation and its SD

Dataset	Annual Mean (mm/year)	Annual SD (mm/year)
OBS	590.6	232.2
IMERG	691.2	192.5
TMPA	658.1	160.0
ERAint	690.5	177.7
ERA5	737.1	291.4
ECM	669.2	253.5
ALR	558.9	271.3
WRF	693.5	289.0
GFS	699.1	405.2
CFS	814.6	382.6

For the observed data and the products, the annual mean precipitation in space and its SD are shown in Table 3.19. The wet Bias in the products have been already discussed over both the daily and monthly time scales. Here, the purpose of presenting Table 3.19 is to show the precipitation variability in the space displayed by each dataset. TMPA shows the least spatial variability (SD value of 160 mm/year) in annual precipitation, while GFS shows it to be 405.2 mm/year against the observed annual precipitation SD of 232.2 mm/year. Although ECM shows a wet Bias of 78.6 mm/year, its variability of annual spatial precipitation (SD of 253.5 mm/year) is the closest (among all the products) to the observed SD.

The spatial distribution of observed precipitation and the nine products is shown in Figure 3.16, where the station-based precipitation data are converted from point to spatial maps using inverse distance weighting interpolation (using data from 3 closest neighboring stations). Although IMERG displays the most smooth transitions, the spatial distribution of observed annual average precipitation (Figure 3.16a) is visually

best captured by IMERG (Figure 3.16b), ECM (Figure 3.16f), and ALR (Figure 3.16g) as compared to all the other products. For example, the northeastern part of the Black Sea coastal region has very high observed annual precipitation of (~2500 mm/year) while southern parts of this wet region receive much lower precipitation (~500 mm/year), making a very sharp transition (Figure 3.16a). Location-wise, this sharp transition is well captured via all the products except for ERAint (Figure 3.16d), WRF (Figure 3.16h), and CFS (Figure 3.16j).

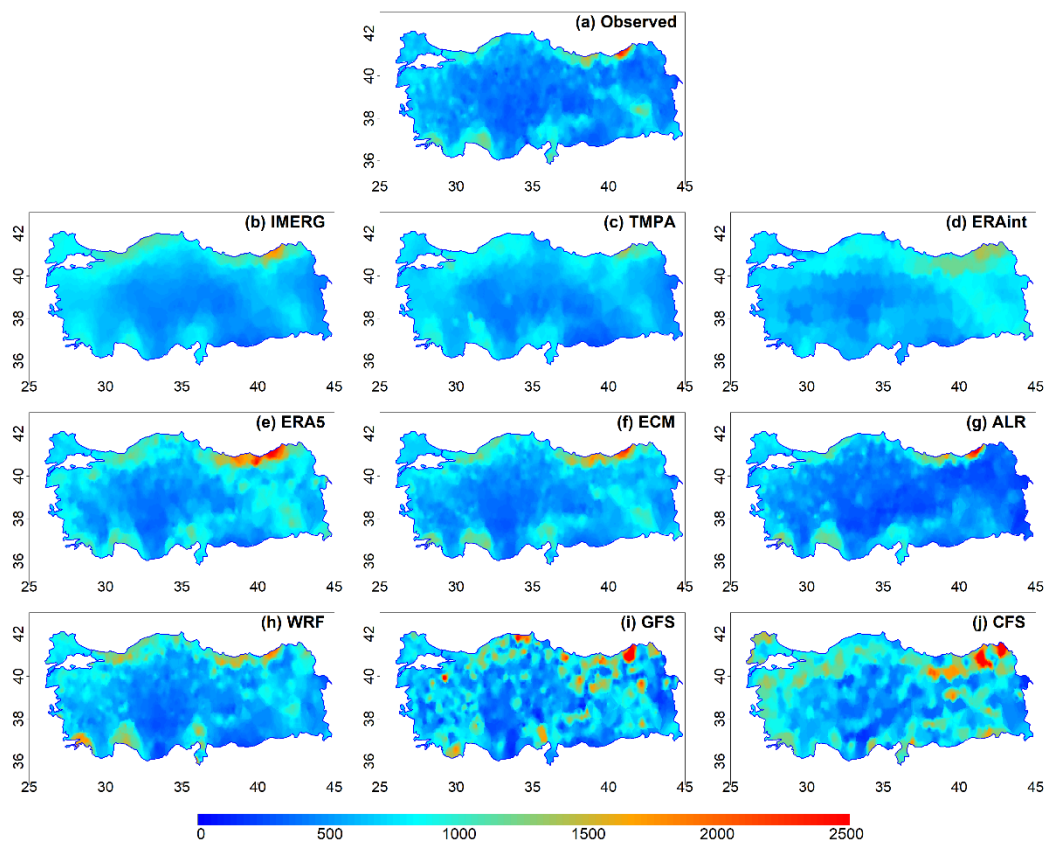


Figure 3.16. Spatial distribution maps for annual average precipitation (mm/year)

ERA-Interim have very low visual sensitivity to high magnitude precipitation or to this sharp transition (Figure 3.16d); perhaps it captures the spatial variability in this area the worst, while its predecessor ERA5 has a much better representation of the transition even though it overestimates the high precipitation amounts (Figure 3.16e). Similarly, the wet strip (~ 800-1000 mm/year) starting from the south-east corner of

the country towards the central parts is better captured by IMERG, ECM, and ERA5. The spatial precipitation variability over the south-western part is well represented by all the products except ERAint, GFS, and CFS. The transitions from the relatively wetter (around 800 mm/year) to drier (below 500 mm/year) regions towards the central parts are accurately captured by all products except GFS and CFS.

On average, the highest observed annual precipitation amounts in the study area are associated with the lowest elevations (Figure 3.17a). This might be because of the orography effect on the precipitation amounts falling over coastlines (i.e., the lowest elevation) where the moist air masses pour major amount of precipitation over the windward side of those mountains. This is potentially true for the case of the eastern Black Sea region (northeast of Turkey). The central parts of Turkey, having an average elevation around 500 m to 1500 m (Figure 2.2b), mostly contain dryer stations and receive lower amounts of precipitation (Figures 3.16a and 3.17a). It is interesting that the observed precipitation is still less over the regions with higher elevations (mostly attributed towards mountainous regions) whereas all the products (except ALR) show a considerable uptrend in precipitation over highly elevated regions (Figure 3.17a). This might be because a gauge station installed over the leeward side of a mountain would report less precipitation despite being at high elevation.

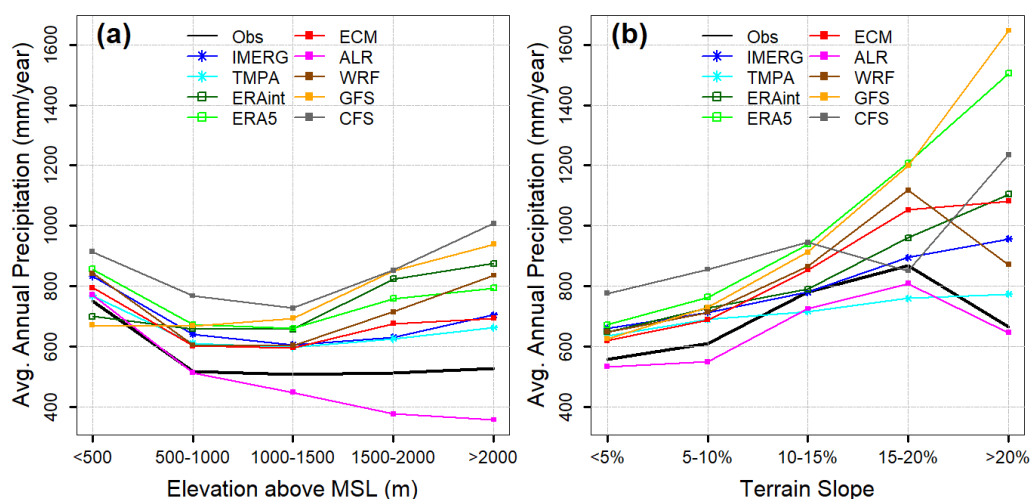


Figure 3.17. Annual average precipitation against varying (a) elevations, and (b) slopes

With increasing slope (which denotes increasing complexity of topography) till 20%, all ten datasets (including the reference dataset and the products) show increasing trends in annual average precipitation (Figure 3.17b). Here, we may associate the stations with a higher % slope (mountainous regions) to wet regions. However, over the regions with slopes greater than 20%, only WRF and ALR follow the decreasing trend of the observed precipitation. ALR performs the best in matching the observed annual precipitation trends, with a small underestimation, over all the slope classes.

3.2. Evaluation of Merged Forecasts

After merging the real-time forecast products (ECM, ALR, WRF, GFS, and CFS) by the two merging methods (i.e., simple merging and merging after rescaling the products), the individual and merged precipitation products were evaluated using the ground-based observed data as an independent reference data. The evaluation analyses included categorical performance indices and intensity-frequency analysis over a 1-daily time scale, while evaluation metrics (including Mean, SD, ErrSD, and CC) were determined over 1-3 daily time scales. The evaluation procedure was applied to the three variables: TP, CP, and LSP. The evaluation results are presented and discussed below.

3.2.1. Daily Evaluation Statistics

For brevity, only the boxplots depicting three statistics (i.e., CC, Bias, and ErrSD) over the entire study area (i.e., 755 stations) for individual and merged forecasts are included here. Among the individual forecasts, ECM shows the highest 1-daily CC with the observed data (Figures 3.18a to 3.18c) for all three variables (i.e., TP, CP, and LSP). However, the simple merge (SimpMRG) of these forecasts is better correlated to the observed data than all the individual products, especially in the cases of TP (Figure 3.18a) and CP (Figure 3.18b); which shows a considerable improvement in CC of the individual products when they are simply merged by taking their ensemble mean. On the other hand, as ECM has the highest CC among the individual

products, producing a merge of all the forecasts after rescaling them on ECM space (i.e., MRG_ECM_reg) results in a product having the highest CC; which shows the benefit of choosing a better reference product to produce a merge after regression-based rescaling. The CC values of the individual products, like CFS and ALR, considerably improve (studies like Afshar et al. (2019) have also reported the improvement in CC of soil moisture products due to merging) when they are merged by either method of merging.

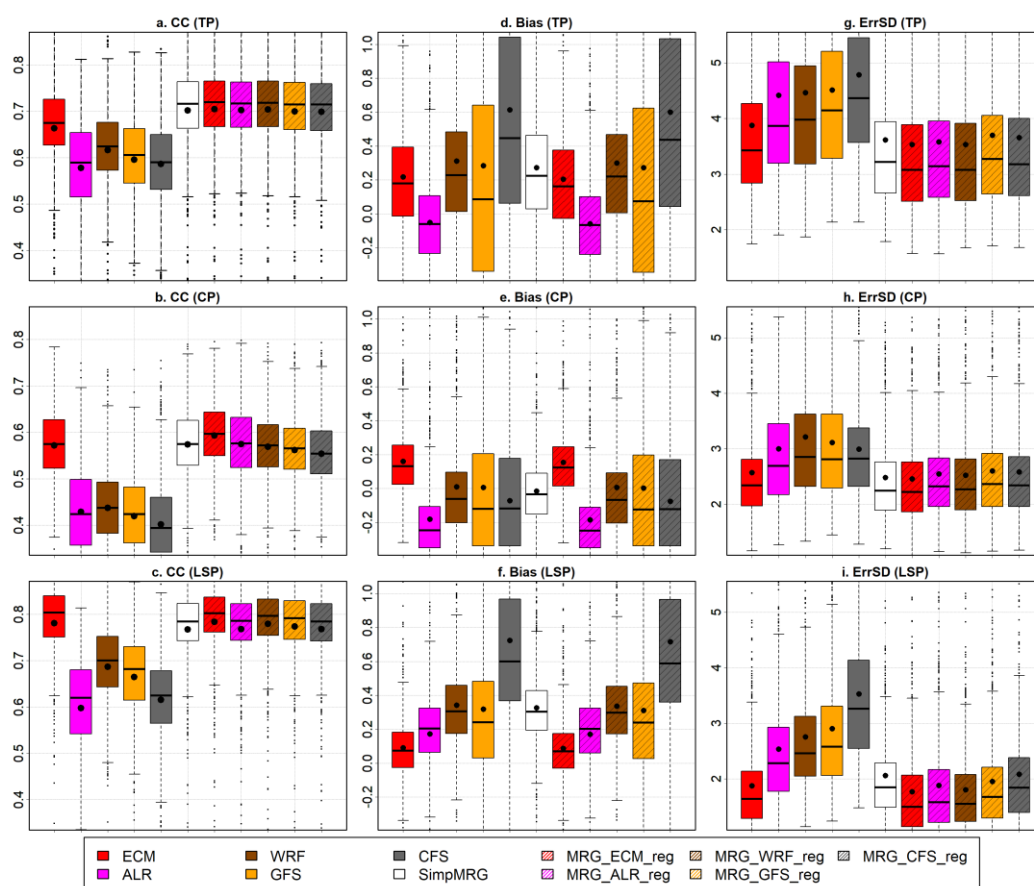


Figure 3.18. For individual and merged forecasts, boxplots for 1-daily CC (from (a) to (c)), Bias (from (d) to (f)), and ErrSD (from (g) to (i)) for TP, CP and LSP. The bold black dots show the mean of the particular statistics

Considering the biases of daily products (Figures 3.18d to 3.18f), the SimpMRG improves the Bias of only the products having already higher individual Bias (e.g., CFS), although the improvement in Bias of those particular products is not as

pronounced as it was the case with CC. Moreover, SimpMRG shows higher Bias than individual forecasts with lower Bias (e.g., ALR); this is because we are merging low-bias products with very high-bias products with the same weight. For a given product (say ALR), the Bias in the individual product and MRG_ALR_reg product is almost the same because in the linear regression-based rescaling, means of all the rescaled products are replaced with the mean of the reference product (here it is ALR).

The daily ErrSD of ECM is the lowest among the individual products for TP (Figure 3.18g), CP (Figure 3.18h), and LSP (Figure 3.18i). Like the improvement in CC, the improvement in 1-daily ErrSD due to merging is substantial. Both merging methods (1. Simple merging or taking the ensemble mean of the products, and 2. Simple merging the products after rescaling them by linear regression) improve the ErrSD of individual products. Merging improves the ErrSD of the individual forecasts not only for TP but for CP and LSP as well, which might have a vital implication in the operational fields like flood management.

When the error statistics of TP for individual and merged forecasts are investigated over wetness classes, the results show that the 1-daily ErrSD values (Table 3.20) of the individual products are improved over all the wetness classes. The combined average ErrSD over dry, moderately dry, moderately wet, and wet regions decrease from 3.4, 4.4, 5.4, and 7.3 mm/day for the individual products to 2.8, 3.6, 4.4, and 6.3 mm/day for the merged products. For the same arrangement, daily CC improves from 0.57, 0.62, 0.66, and 0.64 for the individual products to 0.67, 0.71, 0.76, and 0.74 for the merged products (Table 3.21).

Both the merging methods improve the daily ErrSD (Table 3.22) and CC (Table 3.23) over each elevation region. For example, the average ErrSD over the five elevation classes decrease from 5.7, 3.8, 3.7, 4.1, and 4.5 mm/day for the combined individual products to 4.8, 3.0, 3.0, 3.2, and 3.5 mm/day for the combined merged products (Table 3.22). Moreover, for the same arrangement, daily CC improves from 0.63, 0.62,

0.60, 0.56, and 0.50 for the combined individual products to 0.72, 0.71, 0.69, 0.66, and 0.59 for the combined merged products (Table 3.23).

Table 3.20. *Bias and ErrSD for 1-daily individual and merged forecasts over the entire study area and different wetness classes*

Wetness		Entire	Dry	Mod-Dry	Mod-Wet	Wet
No. of Stations		755	279	303	123	50
BIAS (mm/day)	ECM	0.22	0.27	0.19	0.20	0.16
	ALR	-0.05	-0.06	-0.07	-0.01	0.03
	WRF	0.31	0.27	0.33	0.29	0.50
	GFS	0.28	0.36	0.39	0.26	-0.76
	CFS	0.61	0.70	0.82	0.39	-0.59
	SimpMRG	0.27	0.31	0.33	0.22	-0.15
	MRG_ECM_reg	0.20	0.26	0.17	0.18	0.14
	MRG_ALR_reg	-0.06	-0.07	-0.08	-0.02	0.03
	MRG_WRF_reg	0.30	0.25	0.32	0.28	0.49
	MRG_GFS_reg	0.27	0.35	0.38	0.25	-0.76
	MRG_CFS_reg	0.60	0.68	0.81	0.38	-0.60
ErrSD (mm/day)	ECM	3.88	3.04	3.86	4.75	6.52
	ALR	4.42	3.33	4.42	5.51	7.80
	WRF	4.47	3.38	4.49	5.52	7.84
	GFS	4.51	3.57	4.52	5.54	7.18
	CFS	4.78	3.91	4.88	5.51	7.30
	SimpMRG	3.61	2.84	3.63	4.32	6.06
	MRG_ECM_reg	3.53	2.67	3.55	4.37	6.20
	MRG_ALR_reg	3.58	2.72	3.60	4.41	6.26
	MRG_WRF_reg	3.53	2.68	3.56	4.34	6.13
	MRG_GFS_reg	3.70	2.82	3.67	4.54	6.70
	MRG_CFS_reg	3.66	2.81	3.63	4.46	6.57

Table 3.21. *CC for 1-daily individual and merged forecasts over the entire study area and different wetness classes*

Wetness		Entire	Dry	Mod-Dry	Mod-Wet	Wet
No. of Stations		755	279	303	123	50
CC with the Observed Data	ECM	0.66	0.63	0.67	0.71	0.70
	ALR	0.58	0.55	0.59	0.63	0.59
	WRF	0.62	0.59	0.62	0.66	0.66
	GFS	0.60	0.55	0.61	0.66	0.62
	CFS	0.59	0.54	0.60	0.66	0.62
	SimpMRG	0.70	0.66	0.71	0.76	0.74
	MRG_ECM_reg	0.70	0.67	0.71	0.76	0.74
	MRG_ALR_reg	0.70	0.67	0.71	0.76	0.73
	MRG_WRF_reg	0.70	0.67	0.71	0.76	0.74
	MRG_GFS_reg	0.70	0.66	0.70	0.76	0.73
	MRG_CFS_reg	0.70	0.66	0.70	0.76	0.73

Table 3.22. Bias and ErrSD for 1-daily individual and merged forecasts over the entire study area and different elevation classes

Elevation (m)		Entire	Elev <500	Elev 500-1000	Elev 1000-1500	Elev 1500-2000	Elev > 2000
No. of Stations		755	237	219	209	77	13
BIAS (mm/day)	ECM	0.22	0.15	0.21	0.22	0.42	0.42
	ALR	-0.05	0.12	0.00	-0.15	-0.37	-0.50
	WRF	0.31	0.31	0.24	0.28	0.51	0.77
	GFS	0.28	-0.21	0.38	0.48	0.87	1.06
	CFS	0.61	0.47	0.66	0.58	0.89	1.27
	SimpMRG	0.27	0.17	0.30	0.28	0.46	0.59
	MRG_ECM_reg	0.20	0.14	0.20	0.21	0.39	0.39
	MRG_ALR_reg	-0.06	0.12	-0.01	-0.16	-0.38	-0.52
	MRG_WRF_reg	0.30	0.30	0.23	0.27	0.49	0.74
	MRG_GFS_reg	0.27	-0.22	0.37	0.47	0.85	1.03
MRG_CFS_reg	0.60	0.46	0.65	0.56	0.87	1.24	
ErrSD (mm/day)	ECM	3.88	5.16	3.26	3.22	3.52	3.77
	ALR	4.42	5.87	3.76	3.70	3.85	4.11
	WRF	4.47	5.98	3.73	3.65	4.10	4.60
	GFS	4.51	5.44	3.99	4.00	4.48	4.91
	CFS	4.78	6.03	4.25	4.04	4.45	4.85
	SimpMRG	3.61	4.76	3.07	3.00	3.28	3.62
	MRG_ECM_reg	3.53	4.79	2.95	2.91	3.05	3.35
	MRG_ALR_reg	3.58	4.77	2.98	3.00	3.24	3.55
	MRG_WRF_reg	3.53	4.80	2.95	2.88	3.08	3.39
	MRG_GFS_reg	3.70	4.99	3.08	3.04	3.30	3.56
MRG_CFS_reg	3.66	4.92	3.05	3.01	3.27	3.58	

Table 3.23. CC for 1-daily individual and merged forecasts over the entire study area and different elevation classes

Elevation (m)		Entire	Elev <500	Elev 500-1000	Elev 1000-1500	Elev 1500-2000	Elev > 2000
No. of Stations		755	237	219	209	77	13
CC with the Observed Data	ECM	0.66	0.68	0.68	0.66	0.62	0.56
	ALR	0.58	0.62	0.60	0.55	0.50	0.45
	WRF	0.62	0.62	0.63	0.62	0.59	0.54
	GFS	0.60	0.62	0.60	0.58	0.56	0.49
	CFS	0.59	0.63	0.59	0.57	0.52	0.46
	SimpMRG	0.70	0.72	0.71	0.69	0.66	0.59
	MRG_ECM_reg	0.70	0.72	0.72	0.69	0.66	0.60
	MRG_ALR_reg	0.70	0.72	0.71	0.69	0.66	0.60
	MRG_WRF_reg	0.70	0.72	0.72	0.70	0.66	0.60
	MRG_GFS_reg	0.70	0.72	0.71	0.69	0.65	0.59
MRG_CFS_reg	0.70	0.72	0.71	0.69	0.65	0.58	

The similar trends of improvements in daily ErrSD and CC over wetness and elevation classes are witnessed over different slope classes as well. Summarizing Table 3.24, which shows the Bias and ErrSD of individual and merged forecasts, the ErrSD improves from 4.4, 4.3, 5.1, 5.3, and 4.9 mm/day to 3.6, 3.5, 4.1, 4.2, and 3.4 mm/day

(over the five slope classes, respectively) due to merging. Although the daily ErrSD of the merged products also increases with increasing terrain complexity, they show improvement in ErrSD compared to the individual products over each slope class. Similarly, merging improves the daily CC (Table 3.25) from 0.60, 0.62, 0.61, 0.63, and 0.59 to 0.70, 0.71, 0.71, 0.73, and 0.70 (over the five slope classes, respectively).

Table 3.24. *Bias and ErrSD for 1-daily individual and merged forecasts over the entire study area and different slope classes*

Slope (%)		Entire	Slope < 5%	Slope 5-10%	Slope 10-15%	Slope 15-20%	Slope > 20%
No. of Stations		755	499	170	56	19	11
BIAS (mm/day)	ECM	0.22	0.18	0.21	0.28	0.53	1.06
	ALR	-0.05	-0.03	-0.12	-0.02	-0.10	-0.13
	WRF	0.31	0.29	0.31	0.34	0.78	0.50
	GFS	0.28	0.18	0.32	0.41	0.91	2.61
	CFS	0.61	0.61	0.67	0.53	-0.02	1.48
	SimpMRG	0.27	0.25	0.28	0.30	0.39	1.08
	MRG_ECM_reg	0.20	0.17	0.20	0.27	0.51	1.03
	MRG_ALR_reg	-0.06	-0.03	-0.13	-0.03	-0.11	-0.14
	MRG_WRF_reg	0.30	0.28	0.30	0.32	0.76	0.47
	MRG_GFS_reg	0.27	0.17	0.30	0.40	0.89	2.57
MRG_CFS_reg	0.60	0.60	0.65	0.51	-0.04	1.44	
ErrSD (mm/day)	ECM	3.88	3.87	3.70	4.36	4.41	3.86
	ALR	4.42	4.34	4.27	5.13	5.52	4.64
	WRF	4.47	4.42	4.29	5.10	5.37	4.62
	GFS	4.51	4.36	4.37	5.50	5.92	6.03
	CFS	4.78	4.74	4.64	5.36	5.29	5.43
	SimpMRG	3.61	3.59	3.45	4.12	4.11	3.69
	MRG_ECM_reg	3.53	3.52	3.38	4.04	4.04	3.15
	MRG_ALR_reg	3.58	3.55	3.46	4.09	4.20	3.39
	MRG_WRF_reg	3.53	3.52	3.38	4.03	3.98	3.18
	MRG_GFS_reg	3.70	3.66	3.55	4.33	4.22	3.58
MRG_CFS_reg	3.66	3.63	3.48	4.23	4.42	3.45	

Table 3.25. *CC for 1-daily individual and merged forecasts over the entire study area and different slope classes*

Slope (%)		Entire	Slope < 5%	Slope 5-10%	Slope 10-15%	Slope 15-20%	Slope > 20%
No. of Stations		755	499	170	56	19	11
CC with the Observed Data	ECM	0.66	0.65	0.68	0.68	0.71	0.67
	ALR	0.58	0.58	0.58	0.58	0.56	0.47
	WRF	0.62	0.61	0.63	0.63	0.67	0.63
	GFS	0.60	0.59	0.61	0.59	0.61	0.58
	CFS	0.59	0.58	0.59	0.59	0.59	0.58
	SimpMRG	0.70	0.70	0.71	0.71	0.73	0.70
	MRG_ECM_reg	0.70	0.70	0.72	0.71	0.74	0.71
	MRG_ALR_reg	0.70	0.70	0.71	0.71	0.73	0.69
	MRG_WRF_reg	0.70	0.70	0.72	0.71	0.74	0.71
	MRG_GFS_reg	0.70	0.69	0.71	0.71	0.73	0.70
MRG_CFS_reg	0.70	0.69	0.71	0.71	0.73	0.70	

3.2.2. Intensity-Frequency Analysis

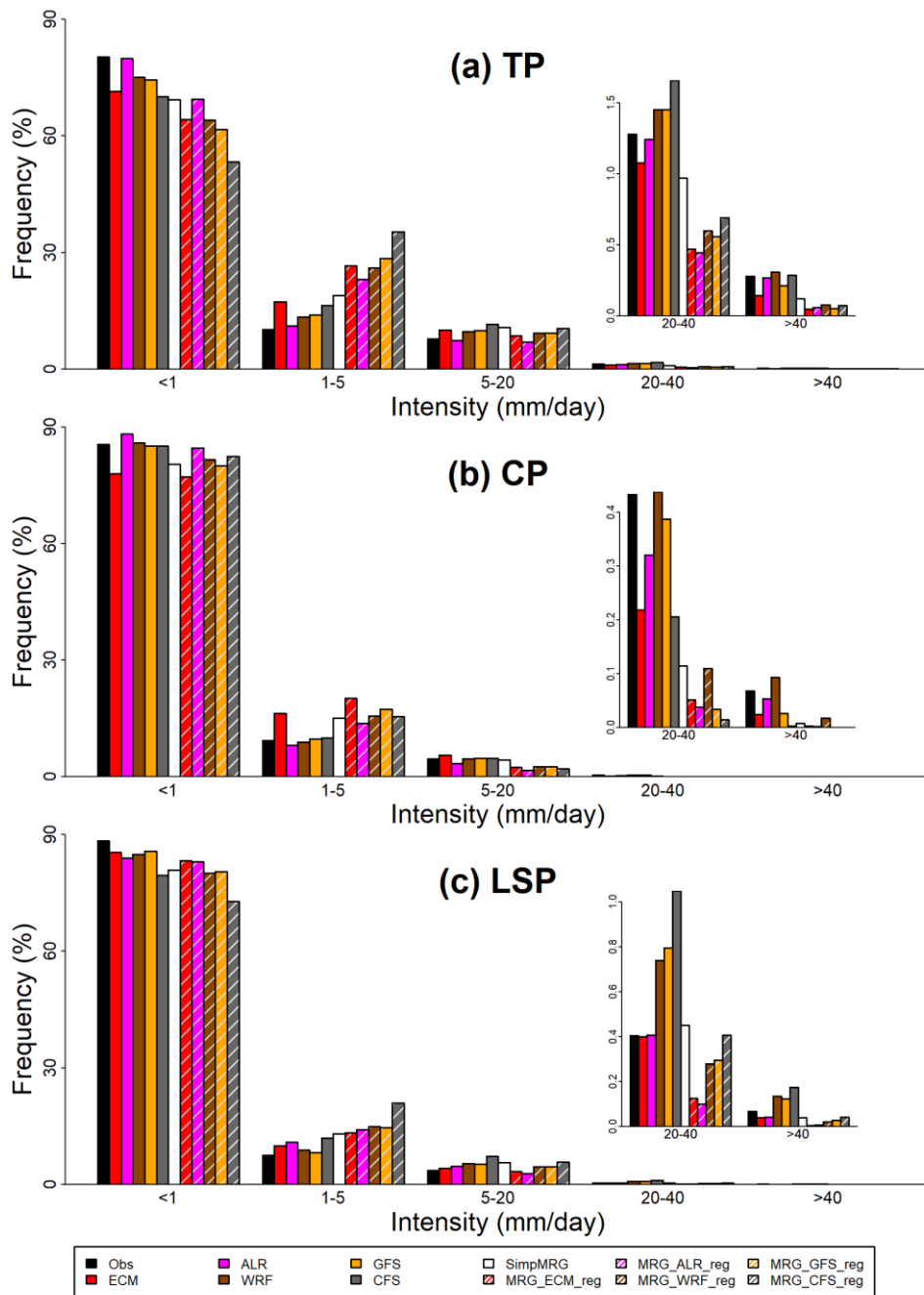


Figure 3.19. Intensity-frequency analysis for 1-daily (a) TP, (b) CP, and (c) LSP.

As mentioned earlier, model-based products show dry days (with precipitation $< 1\text{mm/day}$) as well as the extreme precipitation days (with precipitation $> 40\text{mm/day}$) occurring less frequently than the observed data. Here we are assessing the impact of merging on this intensity-frequency relation. For total precipitation (TP), overall, merging causes even further over- or under-estimation of the observed frequency of specific intensity days (Figure 3.19a), where under-estimation occurs for days with ‘no precipitation’ while over-estimation occurs for light to extreme precipitation days. However, the individual and merged products better match the frequency of days with precipitation 5-20 mm/day.

Here, an important thing to note is that, for most of the daily intensity intervals for TP (Figure 3.19a), CP (Figure 3.19b), and LSP (Figure 3.19c), SimpMRG performs better than all the other merged products (i.e., MRG_ECM_reg, MRG_ALR_reg, MRG_WRF_reg, MRG_GFS_reg, and MRG_CFS_reg) which are produced after rescaling of the individual products. For TP, SimpMRG, among all the merged forecasts, better matches the observed frequency against all the daily intensity intervals (Figure 3.19a). Compared to their performance in matching the observed frequency of dry days for TP, the merged products show improvement in cases of both CP (Figure 3.19b) and LSP (Figure 3.19c). The under-estimation of the frequency of days with light to moderate precipitation intensities is also improved in CP and LSP.

3.2.3. Categorical Performance Indices

Specifying a threshold of detection (i.e., precipitation $\geq 1\text{mm/day}$), the categorical performance indices (CPI) were investigated for the individual and merged forecasts. Merging generally further improves the POD of individual products for TP (Figure 3.20a) and LSP (Figure 3.20c); it also improves POD of all the individual products (except ECM) for the case of CP (Figure 3.20b). However, it further increases the FAR of the products, which already had higher FAR values, especially for TP (Figure 3.20d) and LSP (Figure 3.20f). Overall, merging seems to improve the CSI of individual products for TP (Figure 3.20g), CP (Figure 3.20h), and LSP (Figure 3.20i).

Compared to all the merged products produced after rescaling, SimpMRG shows an overall better CSI, especially for TP. Whereas, for CP and LSP, MRG_ECM_reg shows the highest CSI, as the CSI of individual ECM is already high.

The choice of reference product for regression-based rescaling and merging has a noticeable impact on the performance of merge in CPI. However, a simple merge (i.e., ensemble mean) of the forecasts results in overall improvement regarding, especially the CSI, which goes in favor of simple merging here.

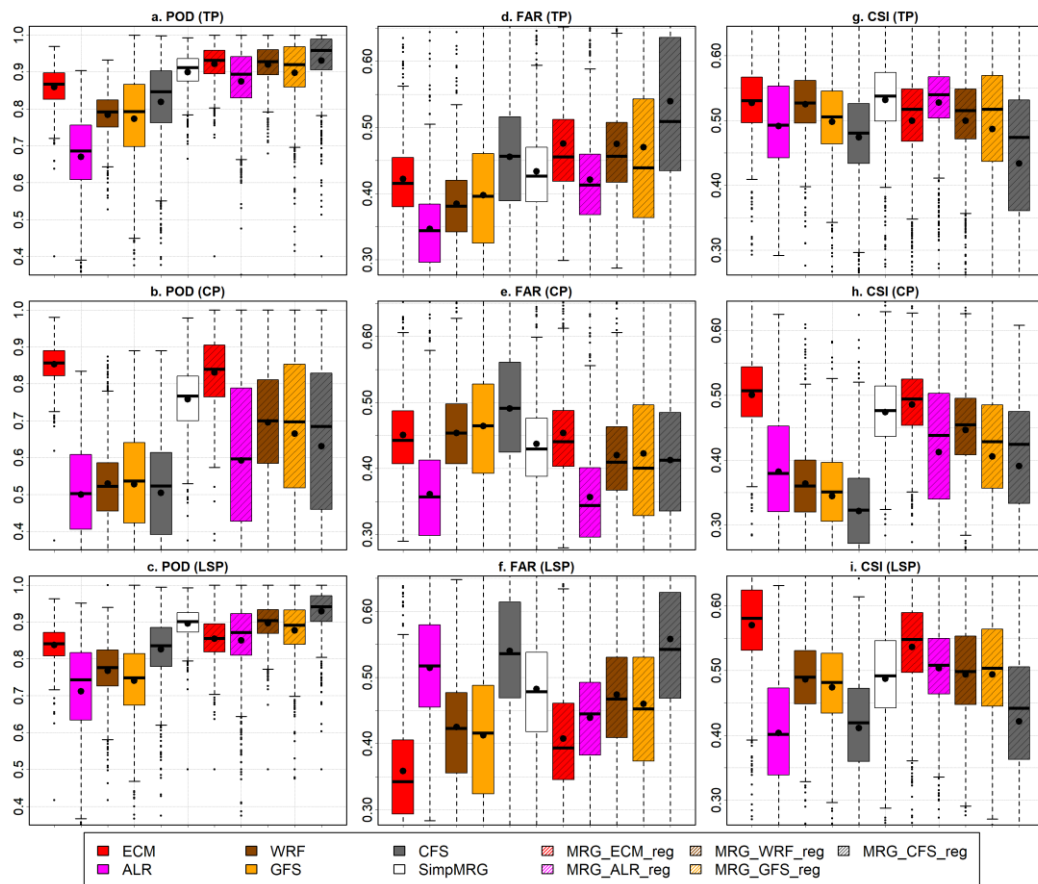


Figure 3.20. 1-daily Categorical Performance Indices. POD for TP, CP, and LSP ((a) to (c)); FAR for TP, CP, and LSP ((d) to (f)); CSI for TP, CP, and LSP ((g) to (i)). The bold black dots represent mean values for the particular CPI

3.2.4. Improvement in ErrSD and CC Due to Merging

Here, we investigate the percent improvement in two of the most critical statistics (i.e., ErrSD and CC) of the individual products when they are merged by the two methods. The individual ECM has less margin of improvement in ErrSD in the sense that it already has lower ErrSD. Therefore, SimpMRG and the other merges add the least improvement in ErrSD of ECM over 1-3 daily time scales for TP (Table 3.26), CP (Table 3.27) and LSP (Table 3.28). Still, this is a very encouraging fact that merging can further improve the ErrSD of ECM. Considering TP (Table 3.26) and LSP (Table 3.28), the average 1-3 daily benefit (improvement in ErrSD) due to merging increases

Table 3.26. *Percent improvement, due to merging, in ErrSD for Total Precipitation of the individual products*

Percent Improvement in ErrSD for TP due to Merging							
	Data	ECM	ALR	WRF	GFS	CFS	Average
1-Daily	SimMRG	8.0	23.1	24.3	28.2	36.0	23.9
	MRG_ECM_reg	11.6	27.1	28.6	33.6	41.7	28.5
	MRG_ALR_reg	9.8	24.9	26.5	31.4	39.4	26.4
	MRG_WRF_reg	11.6	27.2	28.5	33.6	41.7	28.5
	MRG_GFS_reg	6.6	21.6	22.8	26.2	35.4	22.5
	MRG_CFS_reg	7.8	22.9	24.2	29.0	35.3	23.8
2-Daily	SimMRG	8.4	24.4	29.5	30.7	37.0	26.0
	MRG_ECM_reg	13.0	29.6	35.3	37.8	44.5	32.0
	MRG_ALR_reg	11.1	27.1	32.9	35.3	41.9	29.7
	MRG_WRF_reg	12.7	29.2	34.6	37.4	44.0	31.6
	MRG_GFS_reg	6.8	22.6	27.8	28.2	36.5	24.4
	MRG_CFS_reg	8.2	24.1	29.5	31.9	35.8	25.9
3-Daily	SimMRG	9.1	24.9	33.4	32.3	36.5	27.2
	MRG_ECM_reg	14.3	30.6	40.0	40.1	44.7	33.9
	MRG_ALR_reg	12.1	27.9	37.3	37.4	41.9	31.3
	MRG_WRF_reg	13.6	29.9	38.8	39.3	43.8	33.1
	MRG_GFS_reg	7.5	23.1	31.8	29.6	36.2	25.6
	MRG_CFS_reg	9.1	24.8	33.7	33.9	35.3	27.4
Average Improvement		10.1	25.8	31.1	33.1	39.3	

with the order of individual forecasts: ECM > ALR > WRF > GFS > CFS. Whereas, this order changes to ECM > ALR > CFS > GFS > WRF for CP (Table 3.27). Considering TP, although SimpMRG considerably improves (on average, 23.9%), the ErrSD of the individual products, MRG_ECM_reg and MRG_WRF_reg add more

Table 3.27. Percent improvement, due to merging, in ErrSD for Convective Precipitation of the individual products

Percent Improvement in ErrSD for CP due to Merging							
	Data	ECM	ALR	WRF	GFS	CFS	Average
1-Daily	SimMRG	4.3	21.2	29.1	28.3	22.8	21.1
	MRG_ECM_reg	5.7	23.0	31.2	31.0	24.7	23.1
	MRG_ALR_reg	1.3	18.0	25.9	25.5	19.4	18.0
	MRG_WRF_reg	2.9	19.7	27.4	27.5	21.4	19.8
	MRG_GFS_reg	-0.1	16.2	23.8	22.9	17.8	16.1
	MRG_CFS_reg	0.5	16.9	24.8	24.6	18.6	17.1
2-Daily	SimMRG	3.1	21.0	33.1	31.8	25.7	22.9
	MRG_ECM_reg	5.2	23.6	36.2	35.9	28.6	25.9
	MRG_ALR_reg	-0.1	17.5	29.6	28.9	21.9	19.6
	MRG_WRF_reg	1.9	19.7	31.3	31.7	24.6	21.8
	MRG_GFS_reg	-2.4	14.7	26.2	24.3	19.3	16.4
	MRG_CFS_reg	-0.7	16.5	28.6	28.2	21.3	18.8
3-Daily	SimMRG	2.7	21.0	35.7	33.0	26.8	23.8
	MRG_ECM_reg	5.1	24.0	39.5	38.2	30.4	27.4
	MRG_ALR_reg	-0.7	17.3	32.0	30.2	22.9	20.3
	MRG_WRF_reg	1.6	20.0	34.0	33.5	26.0	23.0
	MRG_GFS_reg	-3.3	14.1	28.0	24.5	19.8	16.6
	MRG_CFS_reg	-0.9	16.8	31.5	30.0	22.6	20.0
Average Improvement		1.5	19.0	30.4	29.4	23.0	

improvement. However, for CP and LSP, the improvement in ErrSD of individual products brought by MRG_ECM_reg stands alone as the best among all. Overall, the improvement added by merging to the 1-3 daily ErrSD of the individual products is larger in the case of LSP (Table 3.28) than CP (3.27).

For TP, on average, SimpMRG adds a 17.1% improvement in 1-daily CC of the individual products (Table 3.29), while MRG_ECM_reg adds the highest improvement (17.6%) in CC of the individual products. For TP (Table 3.29) and LSP (3.31), ALR receives the greatest improvement in 1-3 daily CC due to merging, as the individual ALR shows the lowest correlation with the observed data, thus having more margin for improvement. Overall, the improvement added by merging to the 1-3 daily CC of the individual products is larger in the case of CP (Table 3.30) than LSP (3.31).

Table 3.28. Percent improvement, due to merging, in ErrSD for Large-scale Precipitation of the individual products

Percent Improvement in ErrSD for LSP due to Merging							
	Data	ECM	ALR	WRF	GFS	CFS	Average
1-Daily	SimMRG	-9.5	24.7	37.2	43.5	77.3	34.6
	MRG_ECM_reg	9.6	51.0	68.0	79.1	123.1	66.2
	MRG_ALR_reg	4.3	42.8	59.5	70.4	112.7	57.9
	MRG_WRF_reg	5.6	45.5	59.9	71.4	113.8	59.2
	MRG_GFS_reg	-0.7	37.2	51.7	55.4	101.4	49.0
2-Daily	MRG_CFS_reg	-7.4	27.6	41.6	49.9	78.1	38.0
	SimMRG	-11.0	26.7	43.7	42.9	75.0	35.5
	MRG_ECM_reg	10.7	57.9	81.2	84.2	128.3	72.5
	MRG_ALR_reg	4.9	48.3	71.0	74.2	116.5	63.0
	MRG_WRF_reg	4.6	49.1	68.4	72.3	114.0	61.7
3-Daily	MRG_GFS_reg	-1.4	41.0	60.7	55.7	102.2	51.6
	MRG_CFS_reg	-9.3	29.2	48.0	49.2	73.9	38.2
	SimMRG	-10.4	27.0	48.8	43.7	73.6	36.5
	MRG_ECM_reg	12.6	59.8	89.6	87.2	129.5	75.7
	MRG_ALR_reg	6.5	49.9	78.4	76.7	117.4	65.8
Average Improvement	MRG_WRF_reg	5.5	49.6	74.4	73.6	113.0	63.2
	MRG_GFS_reg	0.3	42.9	68.3	58.3	103.4	54.6
	MRG_CFS_reg	-8.3	29.9	53.8	50.7	72.5	39.7
Average Improvement		0.4	41.1	61.3	63.2	101.4	

Table 3.29. Percent improvement, due to merging, in CC for Total Precipitation of the individual products

Percent Improvement in CC for TP due to Merging							
	Data	ECM	ALR	WRF	GFS	CFS	Average
1-Daily	SimMRG	6.3	24.0	14.5	19.8	20.7	17.1
	MRG_ECM_reg	6.8	24.6	15.0	20.3	21.3	17.6
	MRG_ALR_reg	6.5	23.9	14.6	20.0	20.9	17.2
	MRG_WRF_reg	6.7	24.5	14.8	20.3	21.2	17.5
	MRG_GFS_reg	5.9	23.6	14.1	19.3	20.3	16.6
2-Daily	MRG_CFS_reg	5.9	23.5	14.0	19.3	20.1	16.6
	SimMRG	5.7	23.6	15.1	18.8	16.5	15.9
	MRG_ECM_reg	6.2	24.2	15.6	19.2	17.0	16.4
	MRG_ALR_reg	5.8	23.4	15.2	18.8	16.6	16.0
	MRG_WRF_reg	6.0	24.0	15.4	19.1	16.9	16.3
3-Daily	MRG_GFS_reg	5.5	23.4	14.9	18.3	16.2	15.7
	MRG_CFS_reg	5.6	23.5	15.1	18.6	16.3	15.8
	SimMRG	2.7	21.9	17.8	18.8	14.3	15.1
	MRG_ECM_reg	2.2	21.7	18.6	19.3	14.8	15.3
	MRG_ALR_reg	1.8	20.9	18.0	18.8	14.3	14.8
Average Improvement	MRG_WRF_reg	2.0	21.5	18.2	19.1	14.6	15.1
	MRG_GFS_reg	1.2	20.7	17.9	18.4	14.0	14.4
	MRG_CFS_reg	0.6	20.3	18.7	18.9	14.3	14.6
Average Improvement		4.6	23.0	16.0	19.2	17.2	

Table 3.30. Percent improvement, due to merging, in CC for Convective Precipitation of the individual products

Percent Improvement in CC for CP due to Merging							
	Data	ECM	ALR	WRF	GFS	CFS	Average
1-Daily	SimMRG	-0.3	39.7	34.5	34.4	49.5	31.6
	MRG_ECM_reg	3.3	44.6	39.5	39.1	55.1	36.3
	MRG_ALR_reg	-0.3	38.7	34.6	34.8	49.7	31.5
	MRG_WRF_reg	-1.2	38.7	32.7	33.2	48.3	30.3
	MRG_GFS_reg	-2.3	37.2	31.9	30.9	46.2	28.8
	MRG_CFS_reg	-4.2	35.5	30.2	29.4	42.5	26.7
2-Daily	SimMRG	-0.3	34.3	33.2	33.8	41.1	28.4
	MRG_ECM_reg	2.9	39.2	38.0	38.8	46.2	33.0
	MRG_ALR_reg	0.3	34.7	34.3	35.2	42.4	29.4
	MRG_WRF_reg	-0.9	33.6	31.9	33.2	40.4	27.6
	MRG_GFS_reg	-1.4	33.3	31.9	31.2	38.8	26.8
	MRG_CFS_reg	-1.8	32.2	31.0	30.9	36.4	25.7
3-Daily	SimMRG	-1.1	32.7	33.8	34.2	37.3	27.4
	MRG_ECM_reg	2.3	37.7	39.5	39.5	42.7	32.3
	MRG_ALR_reg	-0.2	33.5	35.4	35.9	39.1	28.7
	MRG_WRF_reg	-1.5	32.0	32.8	33.9	37.0	26.8
	MRG_GFS_reg	-1.9	31.9	33.6	31.9	35.3	26.2
	MRG_CFS_reg	-2.6	31.0	32.9	31.9	33.4	25.3
Average Improvement		-0.6	35.6	34.0	34.0	42.3	

Table 3.31. Percent improvement, due to merging, in CC for Large-scale Precipitation of the individual products

Percent Improvement in CC for LSP due to Merging							
	Data	ECM	ALR	WRF	GFS	CFS	Average
1-Daily	SimMRG	-1.3	33.4	12.1	17.0	26.3	17.5
	MRG_ECM_reg	0.7	36.4	14.8	19.6	28.9	20.1
	MRG_ALR_reg	-1.3	32.6	12.3	17.2	26.4	17.4
	MRG_WRF_reg	0.1	35.6	14.0	18.9	28.1	19.3
	MRG_GFS_reg	-0.6	34.5	13.2	17.9	27.2	18.4
	MRG_CFS_reg	-1.4	33.5	12.4	17.1	26.0	17.5
2-Daily	SimMRG	-1.1	37.2	14.7	15.7	20.8	17.5
	MRG_ECM_reg	0.8	40.0	17.0	18.0	23.2	19.8
	MRG_ALR_reg	-1.5	35.4	14.3	15.3	20.3	16.8
	MRG_WRF_reg	0.1	39.0	16.1	17.2	22.4	19.0
	MRG_GFS_reg	-0.4	38.4	15.7	16.5	21.8	18.4
	MRG_CFS_reg	-0.7	37.7	15.2	16.2	21.2	17.9
3-Daily	SimMRG	-1.1	41.9	17.1	15.6	18.8	18.5
	MRG_ECM_reg	0.8	44.7	19.4	17.7	21.1	20.7
	MRG_ALR_reg	-1.9	38.8	16.2	14.6	17.8	17.1
	MRG_WRF_reg	0.0	43.5	18.3	16.8	20.2	19.8
	MRG_GFS_reg	-0.4	43.0	18.0	16.3	19.7	19.3
	MRG_CFS_reg	-0.6	42.6	17.7	16.1	19.3	19.0
Average Improvement		-0.5	38.2	15.5	16.9	22.8	

From the results presented till now, MRG_ECM_reg might be considered as a merged product showing the least ErrSD and the highest CC values for 1-3 daily time scales for all the three variables (i.e., TP, CP, and LSP). Thus, Figure 3.31 shows a summary of the comparison between the improvement in ErrSD and CC for TP, CP, and LSP of the individual products brought by the two merges: SimpMRG and MRG_ECM_reg. The larger improvement in accuracy of the individual products brought by MRG_ECM_reg indicates the importance of choice of the reference product while rescaling the products before merging them (Afshar et al., 2019).

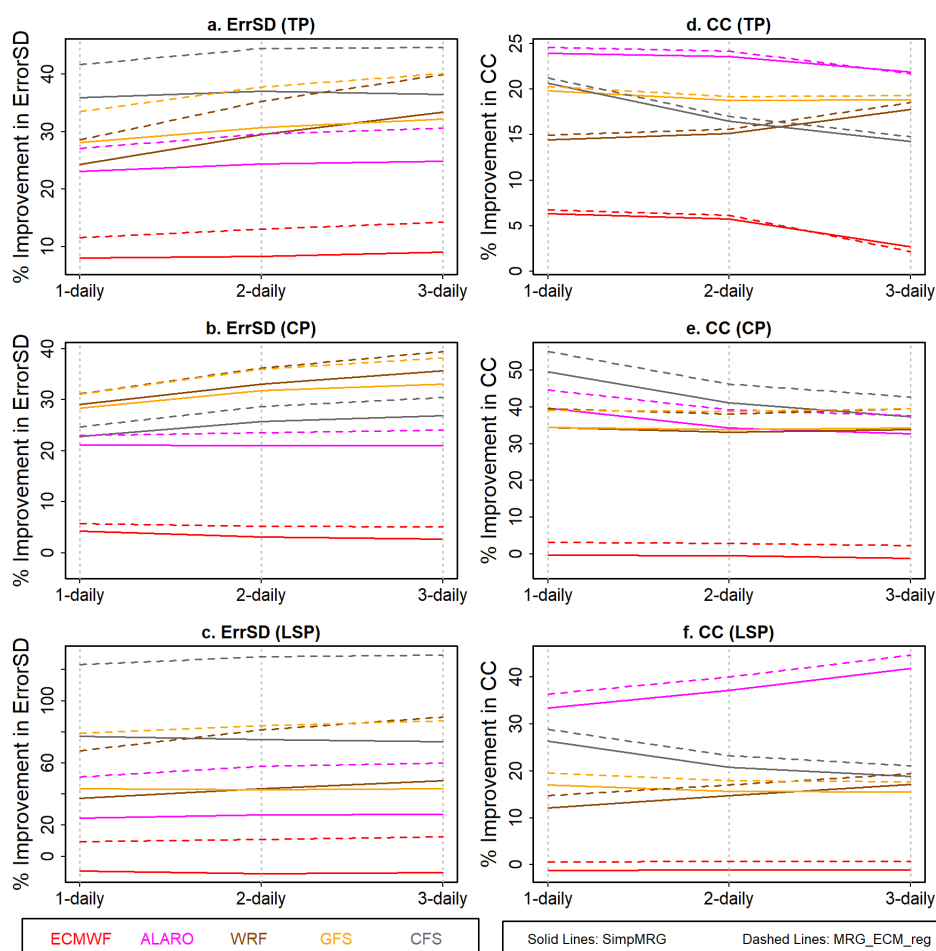


Figure 3.21. Comparison of improvement, due to two merging methods, in ErrSD for TP (a), CP (b), and LSP (c) and CC for TP (d), CP (e), and LSP (f)

3.3. Evaluation of Merged Research-Grade Products

After merging the research-grade products (IMERG, TMPA, ERAint, and ERA5) by the two merging methods (i.e., simple merging and merging after rescaling the products), the individual and merged precipitation products were evaluated using the ground-based observed data as truth. The accuracy assessment included categorical performance indices and intensity-frequency analysis over daily time scale, while evaluation metrics (including Mean, SD, ErrSD, and CC) were determined over daily and monthly time scales. The evaluation results are presented and discussed below.

3.3.1. Daily and Monthly Evaluation Statistics

Considering the entire study area (i.e., all 755 stations), the individual ERA5 has the highest daily CC (Figure 3.22a) among the products. However, when these daily datasets are accumulated to a monthly time scale, IMERG shows the highest monthly CC (Figure 3.22b) with the observed data. MRG_ERA5_reg shows the highest daily CC among the merged products, while taking an ensemble mean (SimpMRG) also improves the daily CC of all the individual products by a considerable amount. For example, although TMPA has the lowest daily CC, a simple merge of it with the other three products improves the daily CC from 0.47 to 0.70. The advantageous thing about merging is that it improves the daily CC of even the products (e.g., ERA5), which have already high daily CC values. Both merging methods improve the monthly CC of TMPA, ERAint, and ERA5. As the Bias is more of a magnitude-dependent variable, comparing the biases on daily (Figure 3.22c) or monthly (Figure 3.22d) time scales is the same. So, considering monthly Bias in the individual and merged products, SimpMRG improves the Bias of ERA5 individual product, which had high Bias (Figure 3.22d). However, the selection of the reference product for merging after regression-based rescaling is more important in the case of Bias. Daily (Figure 3.22e) and monthly (Figure 3.22f) ErrSD of the individual products are considerably improved due to SimpMRG. IMERG, having the lowest monthly ErrSD, when used as a reference product for rescaling, the resulting merged product MRG_IMERG_reg

shows the lowest monthly ErrSD among all the individual and merged products (Figure 3.22f). For the sake of brevity, Figure 3.22 includes only the overall (the entire study area) CC, Bias, and ErrSD over daily and monthly time scales, while the detailed results on monthly scale are presented in following tables (Tables 3.33 to 3.38) over wetness, elevation, and slope classes. Please refer to Appendix A for detailed results over daily time scale where Appendix Tables 0.1 to 0.6 show the daily metrics for the individual and merged products investigated in detail over wetness, elevation, and slope classes.

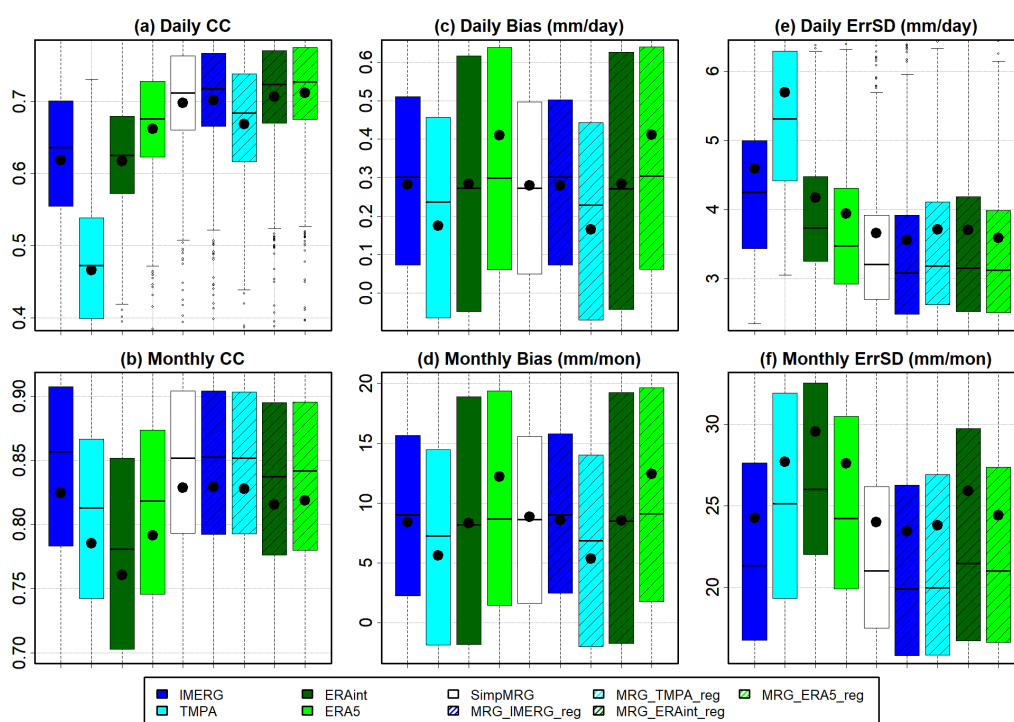


Figure 3.22. For individual and merged research-grade products, boxplots for daily (a) and monthly (b) CC, daily (c) and monthly (d) Bias, and daily (e) and monthly (f) ErrSD. The bold black dots show the mean of the particular statistics

Considering the monthly error variations over wetness classes, merging improves the monthly ErrSD (Table 3.32) of individual products over the entire study area as well as over all the wetness classes. The average monthly ErrSD over the four wetness classes decrease from 22.4, 26.4, 31.8, and 48.8 mm/month for the combined

individual products to 17.8, 23.5, 30.9, and 48.9 for the combined merged products. For the same arrangement, daily CC improves from 0.78, 0.80, 0.81, and 0.74 for the combined individual products to 0.81, 0.84, 0.85, and 0.79 for the combined merged products (Table 3.33).

Table 3.32. *Monthly Bias and ErrSD for individual and merged research-grade products over the entire study area and different wetness classes*

Wetness		Entire	Dry	Mod-Dry	Mod-Wet	Wet
No. of Stations		755	279	303	123	50
BIAS (mm/mon)	GPM	8.4	13.1	10.5	1.1	-13.0
	TMPA	5.6	12.6	8.6	-5.2	-24.6
	ERAint	8.3	19.9	9.6	-5.3	-30.4
	ERA5	12.2	15.1	11.6	9.3	7.1
	SimpMRG	8.8	15.5	10.2	0.2	-15.2
	MRG_IMERG_reg	8.6	13.2	10.7	1.6	-12.7
	MRG_TMPA_reg	5.4	12.3	8.3	-5.4	-24.9
	MRG_ERAint_reg	8.5	20.1	9.8	-5.0	-30.2
ErrSD (mm/mon)	MRG_ERA5_reg	12.4	15.3	11.8	9.7	7.4
	GPM	24.3	19.5	24.1	27.9	42.9
	TMPA	27.7	21.8	27.4	33.4	48.4
	ERAint	29.5	25.5	27.7	33.4	54.0
	ERA5	27.6	22.7	26.6	32.3	49.8
	SimpMRG	24.0	19.7	23.0	27.9	44.6
	MRG_IMERG_reg	23.4	17.0	22.9	30.0	46.5
	MRG_TMPA_reg	23.8	17.1	23.2	31.0	47.8
MRG_ERAint_reg	25.9	17.8	24.8	34.6	56.8	
MRG_ERA5_reg	24.4	17.7	23.9	31.0	49.0	

Table 3.33. *Monthly CC for individual and merged research-grade products over the entire study area and different wetness classes*

Wetness		Entire	Dry	Mod-Dry	Mod-Wet	Wet
No. of Stations		755	279	303	123	50
CC with the Observed Data	GPM	0.82	0.81	0.84	0.84	0.78
	TMPA	0.79	0.79	0.79	0.78	0.72
	ERAint	0.76	0.74	0.77	0.79	0.71
	ERA5	0.79	0.77	0.80	0.82	0.73
	SimpMRG	0.83	0.81	0.84	0.85	0.79
	MRG_IMERG_reg	0.83	0.82	0.84	0.85	0.79
	MRG_TMPA_reg	0.83	0.82	0.84	0.85	0.79
	MRG_ERAint_reg	0.82	0.80	0.83	0.84	0.78
MRG_ERA5_reg	0.82	0.80	0.83	0.85	0.78	

Both the merging methods improve the monthly ErrSD (Table 3.34) and CC (Table 3.35) over each elevation region. For example, the average monthly ErrSD over the five elevation classes decrease from 33.1, 23.2, 24.0, 28.6, and 35.3 mm/month for the combined individual products to 31.2, 19.7, 20.8, 24.6, and 30.7 mm/month for the combined merged products (Table 3.34). Moreover, for the same arrangement, the monthly CC values improve from 0.80, 0.81, 0.79, 0.74, and 0.67 for the combined individual products to 0.84, 0.84, 0.82, 0.78, and 0.71 for the combined merged products (Table 3.35).

Table 3.34. *Monthly Bias and ErrSD for individual and merged research-grade products over the entire study area and different elevation classes.*

Elevation (m)		Entire	Elev <500	Elev 500-1000	Elev 1000-1500	Elev 1500-2000	Elev > 2000
No. of Stations		755	237	219	209	77	13
BIAS (mm/mon)	GPM	8.4	7.6	9.3	7.8	8.9	14.3
	TMPA	5.6	2.1	6.8	7.0	8.5	10.9
	ERAint	8.3	-3.6	10.7	12.0	25.0	28.5
	ERA5	12.2	9.5	12.0	12.3	19.5	21.8
	SimpMRG	8.8	3.9	9.9	10.0	16.0	19.2
	MRG_IMERG_reg	8.6	8.1	9.5	7.8	8.9	14.3
	MRG_TMPA_reg	5.3	1.9	6.5	6.7	8.2	10.5
	MRG_ERAint_reg	8.5	-3.3	10.9	12.1	25.1	28.5
ErrSD (mm/mon)	MRG_ERA5_reg	12.4	9.8	12.2	12.4	19.6	21.8
	GPM	24.3	29.8	19.8	21.3	26.0	35.5
	TMPA	27.7	34.0	24.3	24.2	26.9	32.2
	ERAint	29.5	34.9	25.1	26.4	32.4	39.7
	ERA5	27.6	33.6	23.6	24.1	28.9	33.6
	SimpMRG	24.0	29.4	19.9	21.3	25.1	31.3
	MRG_IMERG_reg	23.4	29.6	18.9	20.2	24.7	30.5
	MRG_TMPA_reg	23.8	30.3	19.5	20.4	24.4	30.1
MRG_ERAint_reg	25.9	35.3	20.3	21.3	24.4	30.7	
MRG_ERA5_reg	24.4	31.6	19.9	20.7	24.3	30.8	

Table 3.35. *Monthly CC for individual and merged research-grade products over the entire study area and different elevation classes*

Elevation (m)		Entire	Elev <500	Elev 500-1000	Elev 1000-1500	Elev 1500-2000	Elev > 2000
No. of Stations		755	237	219	209	77	13
CC with the Observed Data	GPM	0.82	0.84	0.85	0.82	0.75	0.68
	TMPA	0.79	0.79	0.80	0.79	0.75	0.70
	ERAint	0.76	0.77	0.78	0.76	0.71	0.61
	ERA5	0.79	0.80	0.81	0.79	0.75	0.68
	SimpMRG	0.83	0.84	0.85	0.82	0.78	0.71
	MRG_IMERG_reg	0.83	0.84	0.85	0.82	0.78	0.71
	MRG_TMPA_reg	0.83	0.84	0.85	0.82	0.78	0.72
	MRG_ERAint_reg	0.82	0.83	0.83	0.81	0.77	0.69
MRG_ERA5_reg	0.82	0.83	0.83	0.81	0.77	0.70	

The similar trends of improvements in monthly ErrSD and CC over wetness and elevation classes are observed over different slope classes as well (Table 3.36). For example, the monthly ErrSD improves from 26.5, 26.6, 32.5, 37.0, and 31.3 mm/month to 23.6, 23.7, 30.2, 32.6, and 24.0 mm/month (over the five slope classes, respectively) due to merging. Although the monthly ErrSD of the merged products also increases with increasing terrain complexity, they show improvement in ErrSD compared to the individual products over each slope class. Similarly, merging improves the monthly CC (Table 3.37) from 0.79, 0.81, 0.78, 0.72, and 0.71 to 0.83, 0.83, 0.82, 0.78, and 0.77 (over the five slope classes, respectively).

Table 3.36. Monthly Bias and ErrSD for individual and merged research-grade products over the entire study area and different slope classes

Slope (%)		Entire	Slope < 5%	Slope 5-10%	Slope 10-15%	Slope 15-20%	Slope > 20%
No. of Stations		755	499	170	56	19	11
BIAS (mm/mon)	GPM	8.4	9.0	8.4	1.5	3.4	23.0
	TMPA	5.6	6.9	6.4	-3.7	-7.9	7.8
	ERAint	8.3	7.9	9.6	2.4	8.8	35.4
	ERA5	12.2	9.9	12.6	14.8	29.5	68.8
	SimpMRG	8.8	8.6	9.4	4.0	8.8	34.1
	MRG_IMERG_reg	8.6	9.3	8.6	1.6	3.4	22.8
	MRG_TMPA_reg	5.3	6.6	6.0	-4.1	-8.3	7.2
	MRG_ERAint_reg	8.5	8.2	9.7	2.5	8.9	35.2
ErrSD (mm/mon)	MRG_ERA5_reg	12.4	10.2	12.8	14.9	29.5	68.5
	GPM	24.3	23.4	23.9	29.1	33.4	27.5
	TMPA	27.7	27.2	26.9	31.8	36.7	28.0
	ERAint	29.5	28.8	28.8	35.7	38.3	29.4
	ERA5	27.6	26.6	26.6	33.2	39.4	40.4
	SimpMRG	24.0	23.4	23.4	28.8	31.6	24.8
	MRG_IMERG_reg	23.4	22.6	22.9	29.5	32.3	23.6
	MRG_TMPA_reg	23.8	23.0	23.3	29.8	33.2	24.2
MRG_ERAint_reg	25.9	25.2	25.2	32.4	33.5	23.7	
MRG_ERA5_reg	24.4	23.6	23.8	30.7	32.4	23.6	

Table 3.37. Monthly CC for individual and merged research-grade products over the entire study area and different slope classes

Slope (%)		Entire	Slope < 5%	Slope 5-10%	Slope 10-15%	Slope 15-20%	Slope > 20%
No. of Stations		755	499	170	56	19	11
CC with the Observed Data	GPM	0.82	0.83	0.82	0.82	0.76	0.75
	TMPA	0.79	0.79	0.79	0.77	0.70	0.70
	ERAint	0.76	0.76	0.77	0.74	0.70	0.72
	ERA5	0.79	0.79	0.80	0.79	0.73	0.68
	SimpMRG	0.83	0.83	0.83	0.82	0.79	0.78
	MRG_IMERG_reg	0.83	0.83	0.83	0.83	0.79	0.78
	MRG_TMPA_reg	0.83	0.83	0.83	0.82	0.78	0.78
	MRG_ERAint_reg	0.82	0.82	0.82	0.81	0.77	0.77
MRG_ERA5_reg	0.82	0.82	0.82	0.81	0.77	0.76	

3.3.2. Intensity-Frequency analysis

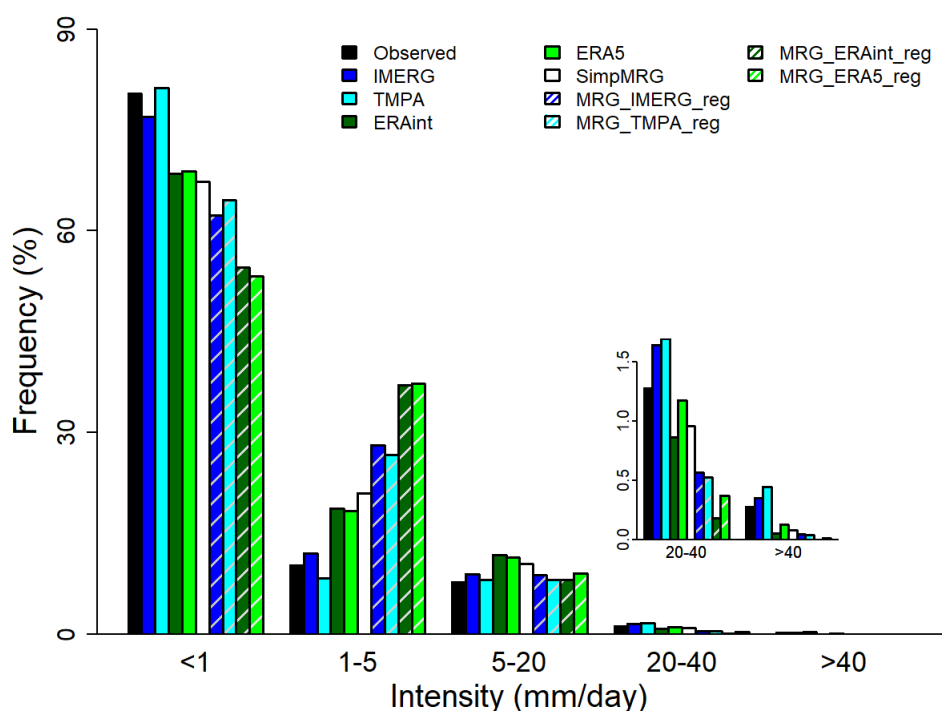


Figure 3.23. Daily intensity-frequency analysis of individual and merged research-grade products

Merging causes further under- and over-estimation of the observed frequency of dry days (with precipitation < 1 mm/day) and light precipitation intensity days (with precipitation of 1-5 mm/day), respectively (Figure 3.23). However, SimpMRG performs better than all the other merges produced after rescaling of the individual products over all the daily intensity intervals. Merging slightly improves the ability of individual products to match the frequency of observed days with moderate precipitation intensities (i.e., 5-20 mm/day). In matching the observed frequency of heavy to extreme precipitation days (i.e., 20-40 to >40 mm/day), SimpMRG slightly edges ahead of the other merged products.

3.3.3. Categorical Performance Indices

Merging, generally, improves the POD of individual products (Figure 3.24a). A simple merge of the individual products shows an improvement in the POD of even ERA5 which already had the highest POD among the individual products. However, merging further increases the FAR of the products (Figure 3.24b), although the improvement in POD is more than the decline in FAR. SimpMRG shows an overall better CSI than the individual and merged products (Figure 3.24c). The choice of reference product for regression-based rescaling and merging has a substantial effect on the performance of merge in CPI. However, a simple merge (i.e., ensemble mean) of the forecasts results in an overall improvement regarding, especially, the CSI, which goes in favor of the simple merging of the research-grade products.

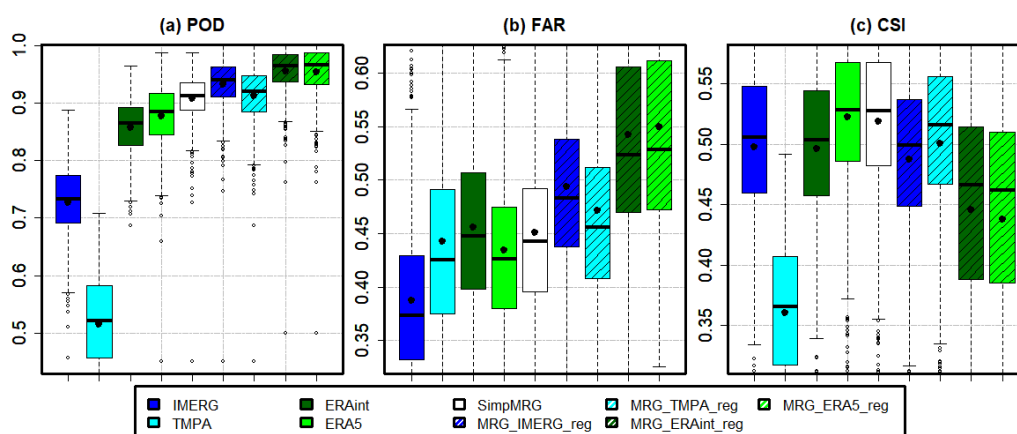


Figure 3.24. Daily Categorical Performance Indices for individual and merged research-grade products. (a) POD, (b) FAR, and (c) CSI. The bold black dots represent mean values for the particular CPI

3.3.4. Improvement in ErrSD and CC Due to Merging

The improvement added by merging in the daily ErrSD is more significant in cases of the individual satellite-based products, whereas monthly ErrSD has more margin for improvement in cases of the individual model-based reanalysis products (Table 3.39). On average, merging adds more improvement in the ErrSD of individual products on the daily time scale. On both the daily and monthly time scales, MRG_IMERG_reg adds the greatest average improvement in ErrSD of the individual products. IMERG

receives the least improvement, due to merging, in the monthly ErrSD (Table 3.38), as it already has the lowest ErrSD among the individual products.

Table 3.38. *Percent improvement, due to merging, in ErrSD of the individual research-grade products*

Percent Improvement in ErrSD due to Merging						
	Data	IMERG	TMPA	ERAint	ERA5	Average
Daily	SimMRG	28.0	61.7	16.1	8.7	28.6
	MRG_IMERG_reg	34.1	69.7	21.7	13.8	34.8
	MRG_TMPA_reg	28.1	61.7	16.2	8.8	28.7
	MRG_ERAint_reg	30.4	65.0	18.0	10.5	31.0
	MRG_ERA5_reg	33.3	68.6	20.7	12.9	33.9
Monthly	SimMRG	1.6	17.5	26.0	16.7	15.5
	MRG_IMERG_reg	7.6	23.8	34.7	24.7	22.7
	MRG_TMPA_reg	6.6	21.7	33.5	23.5	21.3
	MRG_ERAint_reg	0.1	15.0	23.7	14.6	13.4
	MRG_ERA5_reg	3.5	19.2	28.4	18.5	17.4

Table 3.39. *Percent improvement, due to merging, in CC of the individual research-grade products*

Percent Improvement in CC due to Merging						
	Data	IMERG	TMPA	ERAint	ERA5	Average
Daily	SimMRG	14.8	55.2	13.5	5.6	22.3
	MRG_IMERG_reg	15.4	56.1	14.2	6.3	23.0
	MRG_TMPA_reg	9.4	47.1	8.6	1.1	16.6
	MRG_ERAint_reg	17.0	58.1	14.9	7.0	24.3
	MRG_ERA5_reg	17.7	59.1	15.6	7.7	25.0
Monthly	SimMRG	2.9	6.5	10.4	5.6	6.4
	MRG_IMERG_reg	2.9	6.7	10.6	5.8	6.5
	MRG_TMPA_reg	2.7	6.3	10.3	5.6	6.2
	MRG_ERAint_reg	1.3	4.9	8.2	3.6	4.5
	MRG_ERA5_reg	1.7	5.3	8.8	4.0	5.0

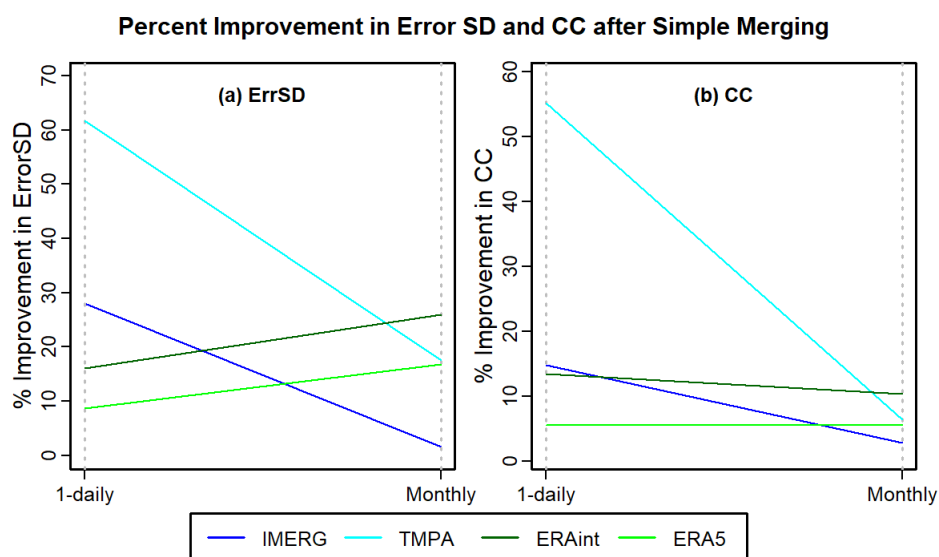


Figure 3.25. The improvement, added by SimpMRG, in the daily and monthly statistics of the individual research-grade products. (a) ErrSD and (b) CC.

MRG_ERA5_reg adds the most substantial average improvement in the daily CC of the individual products (Table 3.39), while SimpMRG and MRG_IMERG_reg cause the most significant improvements in the CC on the monthly time scale.

Summarizing, Figure 3.25 shows the percent improvement which SimpMRG brings, in daily and monthly ErrSd and CC of the individual products.

3.4. Discussion

Here, nine products with variety of spatial resolutions (i.e., 0.045° to 0.75°) are simultaneously evaluated and inter-compared for their statistical performance against the in-situ observed precipitation data. The difference in spatial resolution is considered as an influential driver for the accuracy of a given dataset, and downscaling/upscaling the spatial resolutions of various datasets to a common resolution is considered as an arguable solution. However, this study did not convert the datasets with different resolutions to a common resolution. Rather it extracts the

products data from the grids closest to the ground-based station locations (i.e., point-to-grid). This results in addition of no uncertainty introduced by interpolation. The author did upscaling IMERG (0.1°), TMPA (0.25°), ERA5 (0.25°), and ERAint (0.75°) to a set of coarser resolutions (ranging between 0.15° to 1.5°), and then investigated the impact of change in grid-scale resolution on the accuracy of the individual products by adopting the point-to-grid evaluation technique. The conclusion was that there was no significant change in the accuracy of the products. Therefore, for this study, the point-to-grid evaluation methodology has been applied on the products with their native spatial resolutions.

Simultaneous evaluation of all the products against the in-situ observed precipitation data indicates that, among the real-time forecasts, ECM has the highest CC as well as the smallest ErrSD, which finds its applications in real-time operational purposes like energy production, agriculture, and flood forecasting and management. IMERG could be referred as the most suitable product (among the research products) for non-real-time researches and applications like drought management, as it has the highest monthly CC and the smallest ErrSD.

This study included a simultaneous evaluation and inter-comparison of precipitation products based on model-based forecasts against those based on model-based reanalysis with the intention to investigate the utility of real-time accessible forecasts vs. post-real-time accessible reanalysis. However, it did not consider cross merging these products (i.e., no forecast has been merged with reanalysis). There are two main reasons for not merging forecasts with reanalysis-based products: (1) The differences in their processing algorithms and (2) The difference in accessibility which in turn decides their specific applications. While producing a forecast, the model estimates a wide variety of physical parameters such as precipitation, turbulent fluxes, radiation fields, cloud properties, soil moisture, etc. The accuracy of these model-generated estimates naturally depends on the quality of the model physics as well as that of the analysis data that are always done by operational data assimilation system which could be performed to provide an initial condition for a subsequent forecasting. There are

frequent improvements or changes in the forecasting model physics as well as in the data assimilation processes. On the other hand, reanalysis data are produced the same way with a frozen model - so there is no change in time, the resolution is not varying with time, and mainly the resolution is lower than the resolution of the analysis data produced at the time when the re-analysis data are produced. Reanalysis data are regenerated by using data assimilation models and adding more observations from several non-real-time dataset.

As mentioned in Section 2.5.1. that the observed 1-daily TP data obtained from MGM did not contain any information about the proportions of CP and LSP within TP for a specific day, this study had to rely on the skills of the ECMWF forecast model in segregating CP and LSP proportions. Hence, the proportions of CP and LSP for the observed data were dependent on ECM. This might have played a role in comparatively better performance of ECM and MRG_ECM_reg regarding CP and LSP. However, both ECM and MRG_ECM_reg showed values of ErrSD and CC for TP competitive to even those for ERA5 and IMERG. This implies that splitting the proportions of CP and LSP based on ECM did not have a significance influence on the independence of the truth data (i.e., ground-based observation data).

The choice of the reference product in producing merged products after regression-based rescaling largely affects the error variability of the merged product. For example, among the merged forecasts, MRG_ALR_reg yields the smallest bias because ALR has the smallest Bias among all the individual forecasts. Similarly, MRG_ECM_reg has the smallest ErrSD and the highest CC compared with the other merged forecasts because its reference product (ECM) has the smallest ErrSD and the highest CC among the individual forecasts.

CHAPTER 4

SUMMARY AND CONCLUSIONS

4.1. Summary

This study evaluates and merges a total of nine precipitation products (two satellite-based products: GPM IMERGv05 and TMPA 3B42V7; two model-based reanalysis products: ERA-Interim and ERA5; and five real-time forecasts: ECMWF HRES, ALARO, WRF, GFS, and CFS) by using ground-based observed precipitation data as a reference. Evaluation analyses were conducted over stations of the entire study area as well as over different classes of stations based on their wetness, elevation, and terrain slope. Evaluation procedure included determination of evaluation metrics (i.e., Mean, Standard Deviation (SD), Bias, Error Standard Deviation (ErrSD), and Correlation Coefficient (CC)) over daily and monthly time scales, as well as, the investigation of time-series variability and spatial error variability on the monthly time scale. In addition to this, intensity-frequency analysis and analysis related to categorical performance indices were conducted over a daily time scale. The spatial distribution of annual precipitation was also investigated under the evaluation analysis.

After the initial evaluation of the individual products, they were divided into two groups (i.e., real-time forecasts and research-grade products), and the products of each group were merged using two methods: a simple merging method and the method of simple merging after regression-based rescaling of the products. The individual and merged products were then evaluated, and inter-compared using the ground-based observed precipitation data. The added utility of merging the real-time forecasts was investigated over 1-3 daily time scales, while that of merging the research-grade products was investigated over daily and monthly time scales.

4.2. Conclusions

4.2.1. Conclusions from the Initial Evaluation of Individual Products

- For successor products vs. predecessor products comparison, IMERG and ERA5 show lower ErrSD, higher CC, and better CPI compared with their predecessors (TMPA and ERAint, respectively). However, TMPA and ERAint have smaller bias values compared with those of IMERG and ERA5
- All the products, except ALR, tend to overestimate the observed precipitation not only over dry to moderately dry classes but also over almost all the elevation and slope classes
- Among all nine precipitation products, ALR has the smallest bias (a dry bias of 2.6 mm/month), whereas CFS shows the most substantial wet bias (18.7 mm/month)
- Averaged over the entire study area, the climatology components of the products have lower ErrSD (on average, 19.9 mm/month) and higher monthly CC (on average, 0.80) as compared to their anomaly components (ErrSD: 25.1 mm/month, CC: 0.64)
- All three meteorological parameters, investigated in this study, have prominent role in error variation of the precipitation products. Compared to elevation, wetness has a more prominent role in the error variability of the products in the study area
- The errors of the products increase, and their CC values decrease with the increasing terrain complexity
- The performance of model-based products is more adversely affected by increasing terrain complexity than that of satellite-based products
- ECM outperforms the other real-time forecasts regarding CPI, ErrSD, and CC, thus indicating its better suitability in operational purposes.
- IMERG consistently outperforms all the other products regarding ErrSD over varying slopes, while ECM shows the second-best ErrSD values after IMERG

- Almost all the products have less bias display over the central parts of the study area where most of the dry to moderately dry areas as well as flatter areas exist

4.2.2. Conclusions from Merging of the Real-Time Forecasts

- The choice of the reference product in producing merged products after regression-based rescaling largely affects not only the error variability of the merged product, but also its categorical performance indices
- On average, merging the individual forecasts improves their 1-3 daily ErrSD and CC not only over the entire study area, but also over all the wetness, elevation, and slope classes
- SimpMRG performs better than the other merged products (which are produced by merging after rescaling) regarding the detection ability against various precipitation intensity thresholds
- Considering total precipitation, SimpMRG, MRG_ECM_reg, and MRG_WRF_reg considerably improve the 1-daily ErrSD (on average, 23.9%, 28.5%, and 28.5%, respectively) and CC (on average, 17.1%, 17.6%, and 17.5%, respectively) of the individual forecasts
- Merging the forecasts after rescaling them in the space of ECM (i.e., MRG_ECM_reg) brings the highest improvement in 1-3 daily ErrSD and CC of the individual forecasts

4.2.3. Conclusions from Merging of the Research-Grade Products

- Both the merging methods (1. Simple merging or taking the ensemble mean, and 2. Simple merging the products after rescaling them with linear regression) consistently improve the monthly CC and ErrSD of the research products
- Merging improves the daily CC of even the products (e.g., ERA5) which have already high daily CC with the observed data
- On both the daily and monthly time scales, MRG_IMERG_reg adds the most significant average improvement in ErrSD of the individual products

- Considering CPI, SimpMRG performs better than all the other merged products (produced after rescaling the individual products) against all the daily intensity intervals

4.3. Recommendations

- Real-time and non-real-time datasets could be merged just to investigate their added utility in different applications
- Hybrid merging technique could be applied by taking, at a time, two to nine products under consideration
- Merging could be done by considering only the best performing products (e.g., ALR has the smallest bias, ECM has the highest CC and the smallest ErrSD over daily time scale, IMERG has the highest CC and the smallest ErrSD over monthly time scale)
- Real-time and seasonal forecasts for different variables could be merged to investigate the utility of merging in the applications like crop yield assessment

4.4. Future Studies

The intended future studies include:

- Expanding the list of products to be merged
- Applying the evaluation and merging analyses over a sub region of Turkey with dense network of ground-based gauge stations so that grid-to-grid evaluation could be adopted
- Applying the same analyses of this study by using triple-located gauge stations data as the truth data
- A dedicated and comprehensive investigation of utility of real-time forecasts against their reanalysis data
- Applying triple-located error technique of merging on different combinations like seasonality-anomaly, signal-noise, and complete time series

REFERENCES

- Afshar, M.H., Yilmaz, M.T., Crow, W.T., 2019. Impact of Rescaling Approaches in Simple Fusion of Soil Moisture Products. *Water Resour. Res.* 55, 7804–7825. <https://doi.org/10.1029/2019WR025111>
- Amatulli, G., Domisch, S., Tuanmu, M.N., Parmentier, B., Ranipeta, A., Malczyk, J., Jetz, W., 2018. Data Descriptor: A suite of global, cross-scale topographic variables for environmental and biodiversity modeling. *Sci. Data* 5, 1–15. <https://doi.org/10.1038/sdata.2018.40>
- Awadallah, A.G., 2012. Selecting optimum locations of rainfall stations using kriging and entropy. *Int. J. Civ. Environ. Eng* 12, 36–41. <https://doi.org/10.1056/NEJMe078207>
- Beck, H.E., Pan, M., Roy, T., Weedon, G.P., Pappenberger, F., Van Dijk, A.I.J.M., Huffman, G.J., Adler, R.F., Wood, E.F., 2019. Daily evaluation of 26 precipitation datasets using Stage-IV gauge-radar data for the CONUS. *Hydrol. Earth Syst. Sci.* 23, 207–224. <https://doi.org/10.5194/hess-23-207-2019>
- Berg, P., Norin, L., Olsson, J., 2016. Creation of a high resolution precipitation data set by merging gridded gauge data and radar observations for Sweden. *J. Hydrol.* 541, 6–13. <https://doi.org/10.1016/j.jhydrol.2015.11.031>
- Berndt, C., Rabiei, E., Haberlandt, U., 2014. Geostatistical merging of rain gauge and radar data for high temporal resolutions and various station density scenarios. *J. Hydrol.* 508, 88–101. <https://doi.org/10.1016/j.jhydrol.2013.10.028>
- Bıyık, G., Unal, Y., Onol, B., 2009. Assessment of Precipitation Forecast Accuracy over Eastern Black Sea Region using WRF-ARW 11, 2009.
- Boudevillain, B., Delrieu, G., Wijbrans, A., Confoland, A., 2016. A high-resolution rainfall re-analysis based on radar–raingauge merging in the Cévennes-Vivarais region, France. *J. Hydrol.* 541, 14–23. <https://doi.org/10.1016/j.jhydrol.2016.03.058>
- Cai, Y., Jin, C., Wang, A., Guan, D., Wu, J., Yuan, F., Xu, L., 2016. Comprehensive precipitation evaluation of TRMM 3B42 with dense rain gauge networks in a mid-latitude basin, northeast, China. *Theor. Appl. Climatol.* 126, 659–671. <https://doi.org/10.1007/s00704-015-1598-4>
- Chakraborty, A., 2010. The Skill of ECMWF Medium-Range Forecasts during the Year of Tropical Convection 2008. *Mon. Weather Rev.* 138, 3787–3805. <https://doi.org/10.1175/2010MWR3217.1>
- Chiang, Y.M., Hsu, K.L., Chang, F.J., Hong, Y., Sorooshian, S., 2007. Merging

- multiple precipitation sources for flash flood forecasting. *J. Hydrol.* 340, 183–196. <https://doi.org/10.1016/j.jhydrol.2007.04.007>
- Chiaravalloti, F., Brocca, L., Procopio, A., Massari, C., Gabriele, S., 2018. Assessment of GPM and SM2RAIN-ASCAT rainfall products over complex terrain in southern Italy. *Atmos. Res.* 206, 64–74. <https://doi.org/10.1016/j.atmosres.2018.02.019>
- Davis, C.A., Brown, B., Bullock, R., 2006. Object-based verification of precipitation forecasts. Part I: Application to convective rain systems. *Mon. Weather Rev.* 134, 1785–1795. <https://doi.org/10.1175/MWR3146.1>
- Dee, D.P., Uppala, S.M., Simmons, A.J., Berrisford, P., Poli, P., Kobayashi, S., Andrae, U., Balmaseda, M.A., Balsamo, G., Bauer, P., Bechtold, P., Beljaars, A.C.M., van de Berg, L., Bidlot, J., Bormann, N., Delsol, C., Dragani, R., Fuentes, M., Geer, A.J., Haimberger, L., Healy, S.B., Hersbach, H., Hólm, E. V., Isaksen, L., Kållberg, P., Köhler, M., Matricardi, M., McNally, A.P., Monge-Sanz, B.M., Morcrette, J.J., Park, B.K., Peubey, C., de Rosnay, P., Tavolato, C., Thépaut, J.N., Vitart, F., 2011. The ERA-Interim reanalysis: Configuration and performance of the data assimilation system. *Q. J. R. Meteorol. Soc.* 137, 553–597. <https://doi.org/10.1002/qj.828>
- Demir, İ., Kiliç, G., Coşkun, M., 2018. İklim Değişikliği ve Çevre Türkiye ve bölgesi için PRECIS bölgesel iklim modeli çalışmaları Application of Regional Climate Model PRECIS over Turkey and its neighborhood İklim Değişikliği ve Çevre 11–17.
- Derin, Y., Anagnostou, E., Berne, A., Borga, M., Boudevillain, B., Buytaert, W., Chang, C.-H., Delrieu, G., Hong, Y., Hsu, Y.C., Lavado-Casimiro, W., Manz, B., Moges, S., Nikolopoulos, E.I., Sahl, D., Salerno, F., Rodríguez-Sánchez, J.-P., Vergara, H.J., Yilmaz, K.K., 2016. Multiregional Satellite Precipitation Products Evaluation over Complex Terrain. *J. Hydrometeorol.* 17, 1817–1836. <https://doi.org/10.1175/JHM-D-15-0197.1>
- Derin, Y., Yilmaz, K.K., 2014. Evaluation of Multiple Satellite-Based Precipitation Products over Complex Topography. *J. Hydrometeorol.* 15, 1498–1516. <https://doi.org/10.1175/JHM-D-13-0191.1>
- Done, J., Davis, C.A., Weisman, M., 2004. The next generation of NWP: Explicit forecasts of convection using the weather research and forecasting (WRF) model. *Atmos. Sci. Lett.* 5, 110–117. <https://doi.org/10.1002/asl.72>
- Durai, V.R., Roy Bhowmik, S.K., Mukhopadhyay, B., 2010. Performance evaluation of precipitation prediction skill of NCEP global Forecasting System (GFS) over Indian region during summer monsoon 2008. *Mausam* 61, 139–154.
- El Kenawy, A.M., Lopez-Moreno, J.I., McCabe, M.F., Vicente-Serrano, S.M., 2015. Evaluation of the TMPA-3B42 precipitation product using a high-density rain

- gauge network over complex terrain in northeastern Iberia. *Glob. Planet. Change* 133, 188–200. <https://doi.org/10.1016/j.gloplacha.2015.08.013>
- Ghajarnia, N., Liaghat, A., Daneshkar Arasteh, P., 2015. Comparison and evaluation of high resolution precipitation estimation products in Urmia Basin-Iran. *Atmos. Res.* 158–159, 50–65. <https://doi.org/10.1016/j.atmosres.2015.02.010>
- Goudenhoofdt, E., Delobbe, L., 2009. Evaluation of radar-gauge merging methods for quantitative precipitation estimates. *Hydrol. Earth Syst. Sci.* 13, 195–203. <https://doi.org/10.5194/hess-13-195-2009>
- Guo, H., Chen, S., Bao, A., Behrangi, A., Hong, Y., Ndayisaba, F., Hu, J., Stepanian, P.M., 2016. Early assessment of Integrated Multi-satellite Retrievals for Global Precipitation Measurement over China. *Atmos. Res.* 176–177, 121–133. <https://doi.org/10.1016/j.atmosres.2016.02.020>
- Hamill, T.M., Hagedorn, R., Whitaker, J.S., 2008. Probabilistic forecast calibration using ECMWF and GFS ensemble reforecasts. Part II: Precipitation. *Mon. Weather Rev.* 136, 2620–2632. <https://doi.org/10.1175/2007MWR2411.1>
- He, Z., Yang, L., Tian, F., Ni, G., Hou, A., Lu, H., 2017. Intercomparisons of Rainfall Estimates from TRMM and GPM Multisatellite Products over the Upper Mekong River Basin. *J. Hydrometeorol.* 18, 413–430. <https://doi.org/10.1175/JHM-D-16-0198.1>
- Heidinger, H., Yarlequé, C., Posadas, A., Quiroz, R., 2012. TRMM rainfall correction over the Andean Plateau using wavelet multi-resolution analysis. *Int. J. Remote Sens.* 33, 4583–4602. <https://doi.org/10.1080/01431161.2011.652315>
- Hénin, R., Liberato, M.L.R., Ramos, A.M., Gouveia, C.M., 2018. Assessing the use of satellite-based estimates and high-resolution precipitation datasets for the study of extreme precipitation events over the Iberian Peninsula. *Water (Switzerland)* 10. <https://doi.org/10.3390/w10111688>
- Herbach, H., Dee, D.P., 2016. ECMWF Newsletter Spring 2016. *ECMWF Newsl.* 7.
- Herold, N., Alexander, L. V., Donat, M.G., Contractor, S., Becker, A., 2016. How much does it rain over land? *Geophys. Res. Lett.* 43, 341–348. <https://doi.org/10.1002/2015GL066615>
- Hirpa, F.A., Gebremichael, M., Hopson, T., 2010. Evaluation of high-resolution satellite precipitation products over very complex terrain in Ethiopia. *J. Appl. Meteorol. Climatol.* 49, 1044–1051. <https://doi.org/10.1175/2009JAMC2298.1>
- Hou, A.Y., Kakar, R.K., Neeck, S., Azarbarzin, A.A., Kummerow, C.D., Kojima, M., Oki, R., Nakamura, K., Iguchi, T., 2014. The global precipitation measurement mission. *Bull. Am. Meteorol. Soc.* 95, 701–722. <https://doi.org/10.1175/BAMS-D-13-00164.1>

- Huffman, G.J., Bolvin, D.T., 2018. TRMM and Other Data Precipitation Data Set Documentation "Recent" News 46.
- Huffman, G.J., Bolvin, D.T., Nelkin, E.J., 2015. Day 1 IMERG Final Run: Release Notes 1–9. https://doi.org/http://pmm.nasa.gov/sites/default/files/document_files/IMERG_FinalRun_Day1_release_notes.pdf
- Huffman, G.J., Bolvin, D.T., Nelkin, E.J., Wolff, D.B., Adler, R.F., Gu, G., Hong, Y., Bowman, K.P., Stocker, E.F., 2007. The TRMM Multisatellite Precipitation Analysis (TMPA): Quasi-Global, Multiyear, Combined-Sensor Precipitation Estimates at Fine Scales. *J. Hydrometeorol.* 8, 38–55. <https://doi.org/10.1175/JHM560.1>
- Hughes, D.A., 2006. Comparison of satellite rainfall data with observations from gauging station networks. *J. Hydrol.* 327, 399–410. <https://doi.org/10.1016/j.jhydrol.2005.11.041>
- Islam, T., Rico-Ramirez, M.A., Han, D., Srivastava, P.K., Ishak, A.M., 2012. Performance evaluation of the TRMM precipitation estimation using ground-based radars from the GPM validation network. *J. Atmos. Solar-Terrestrial Phys.* 77, 194–208. <https://doi.org/10.1016/j.jastp.2012.01.001>
- Kidd, C., Huffman, G., 2011. Global precipitation measurement. *Meteorol. Appl.* 18, 334–353. <https://doi.org/10.1002/met.284>
- Kucera, P.A., Ebert, E.E., Turk, F.J., Levizzani, V., Kirschbaum, D., Tapiador, F.J., Loew, A., Borsche, M., 2013. Precipitation from space: Advancing earth system science. *Bull. Am. Meteorol. Soc.* 94, 365–375. <https://doi.org/10.1175/BAMS-D-11-00171.1>
- Li, C., Tang, G., Hong, Y., 2018. Cross-evaluation of ground-based, multi-satellite and reanalysis precipitation products: Applicability of the Triple Collocation method across Mainland China. *J. Hydrol.* 562, 71–83. <https://doi.org/10.1016/j.jhydrol.2018.04.039>
- Li, M., Shao, Q., 2010. An improved statistical approach to merge satellite rainfall estimates and raingauge data. *J. Hydrol.* 385, 51–64. <https://doi.org/10.1016/j.jhydrol.2010.01.023>
- Luo, L., Wood, E.F., Pan, M., 2007. Bayesian merging of multiple climate model forecasts for seasonal hydrological predictions. *J. Geophys. Res. Atmos.* 112, 1–13. <https://doi.org/10.1029/2006JD007655>
- Ma, Y., Zhang, Y., Yang, D., Farhan, S. Bin, 2015. Precipitation bias variability versus various gauges under different climatic conditions over the Third Pole Environment (TPE) region. *Int. J. Climatol.* 35, 1201–1211. <https://doi.org/10.1002/joc.4045>

- Manzato, A., Cicogna, A., Pucillo, A., 2016. 6-hour maximum rain in Friuli Venezia Giulia: Climatology and ECMWF-based forecasts. *Atmos. Res.* 169, 465–484. <https://doi.org/10.1016/j.atmosres.2015.07.013>
- Mayor, Y.G., Tereshchenko, I., Fonseca-Hernández, M., Pantoja, D.A., Montes, J.M., 2017. Evaluation of error in IMERG precipitation estimates under different topographic conditions and temporal scales over Mexico. *Remote Sens.* 9, 1–18. <https://doi.org/10.3390/rs9050503>
- Michaelides, S., Levizzani, V., Anagnostou, E., Bauer, P., Kasparis, T., Lane, J.E., 2009. Precipitation: Measurement, remote sensing, climatology and modeling. *Atmos. Res.* 94, 512–533. <https://doi.org/10.1016/j.atmosres.2009.08.017>
- Milewski, A., Elkadiri, R., Durham, M., 2015. Assessment and comparison of TMPA satellite precipitation products in varying climatic and topographic regimes in Morocco. *Remote Sens.* 7, 5697–5717. <https://doi.org/10.3390/rs70505697>
- Murali Krishna, U. V., Das, S.K., Deshpande, S.M., Doiphode, S.L., Pandithurai, G., 2017. The assessment of Global Precipitation Measurement estimates over the Indian subcontinent. *Earth Sp. Sci.* 4, 540–553. <https://doi.org/10.1002/2017EA000285>
- Pappenberger, F., Buizza, R., 2009. The Skill of ECMWF Precipitation and Temperature Predictions in the Danube Basin as Forcings of Hydrological Models. *Weather Forecast.* 24, 749–766. <https://doi.org/10.1175/2008WAF2222120.1>
- Prakash, S., Mitra, A.K., AghaKouchak, A., Liu, Z., Norouzi, H., Pai, D.S., 2018. A preliminary assessment of GPM-based multi-satellite precipitation estimates over a monsoon dominated region. *J. Hydrol.* 556, 865–876. <https://doi.org/10.1016/j.jhydrol.2016.01.029>
- Prakash, S., Mitra, A.K., Pai, D.S., AghaKouchak, A., 2016. From TRMM to GPM: How well can heavy rainfall be detected from space? *Adv. Water Resour.* 88, 1–7. <https://doi.org/10.1016/j.advwatres.2015.11.008>
- Rozante, J.R., Moreira, D.S., de Goncalves, L.G.G., Vila, D.A., 2010. Combining TRMM and surface observations of precipitation: Technique and validation over South America. *Weather Forecast.* 25, 885–894. <https://doi.org/10.1175/2010WAF2222325.1>
- Sahlu, D., Moges, S.A., Nikolopoulos, E.I., Anagnostou, E.N., Hailu, D., 2017. Evaluation of High-Resolution Multisatellite and Reanalysis Rainfall Products over East Africa. *Adv. Meteorol.* 2017. <https://doi.org/10.1155/2017/4957960>
- Scheel, M.L.M., Rohrer, M., Huggel, C., Santos Villar, D., Silvestre, E., Huffman, G.J., 2011. Evaluation of TRMM Multi-satellite Precipitation Analysis (TMPA) performance in the Central Andes region and its dependency on spatial and

- temporal resolution. *Hydrol. Earth Syst. Sci.* 15, 2649–2663. <https://doi.org/10.5194/hess-15-2649-2011>
- Sensoy, S., 2004. The Mountains Influence On Turkey Climate Climate of Turkey 25–29.
- Sharifi, E., Steinacker, R., Saghafian, B., 2016. Assessment of GPM-IMERG and other precipitation products against gauge data under different topographic and climatic conditions in Iran: Preliminary results. *Remote Sens.* 8. <https://doi.org/10.3390/rs8020135>
- Sooraj, K.P., Annamalai, H., Kumar, A., Wang, H., 2012. A comprehensive assessment of CFS seasonal forecasts over the tropics. *Weather Forecast.* 27, 3–27. <https://doi.org/10.1175/WAF-D-11-00014.1>
- Tan, M.L., Duan, Z., 2017. Assessment of GPM and TRMM precipitation products over Singapore. *Remote Sens.* 9, 1–16. <https://doi.org/10.3390/rs9070720>
- Tang, G., Ma, Y., Long, D., Zhong, L., Hong, Y., 2016. Evaluation of GPM Day-1 IMERG and TMPA Version-7 legacy products over Mainland China at multiple spatiotemporal scales. *J. Hydrol.* 533, 152–167. <https://doi.org/10.1016/j.jhydrol.2015.12.008>
- Thiemig, V., Rojas, R., Zambrano-Bigiarini, M., Levizzani, V., De Roo, A., 2012. Validation of Satellite-Based Precipitation Products over Sparsely Gauged African River Basins. *J. Hydrometeorol.* 13, 1760–1783. <https://doi.org/10.1175/JHM-D-12-032.1>
- Tong, K., Su, F., Yang, D., Zhang, L., Hao, Z., 2014. Tibetan Plateau precipitation as depicted by gauge observations, reanalyses and satellite retrievals. *Int. J. Climatol.* 34, 265–285. <https://doi.org/10.1002/joc.3682>
- Toros, H., Kahraman, A., Tilev-Tanriover, S., Geertsema, G., Cats, G., 2018. İstanbul’da 8-9 Eylül 2009’da Meydana Gelen Aşırı Yağışın HARMONIE, HIRLAM ve WRF-ARW ile Simülasyonu. *Eur. J. Sci. Technol.* 1–12. <https://doi.org/10.31590/ejosat.417535>
- Verdin, A., Rajagopalan, B., Kleiber, W., Funk, C., 2015. A Bayesian kriging approach for blending satellite and ground precipitation observations. *Water Resour. Res.* 51, 908–921. <https://doi.org/10.1002/2014WR015963>
- Wang, W., Chen, M., Kumar, A., 2010. An assessment of the CFS real-time seasonal forecasts. *Weather Forecast.* 25, 950–969. <https://doi.org/10.1175/2010WAF2222345.1>
- Wang, Z., Zhong, R., Lai, C., Chen, J., 2017. Evaluation of the GPM IMERG satellite-based precipitation products and the hydrological utility. *Atmos. Res.* 196, 151–163. <https://doi.org/10.1016/j.atmosres.2017.06.020>

- Woldemeskel, F.M., Sivakumar, B., Sharma, A., 2013. Merging gauge and satellite rainfall with specification of associated uncertainty across Australia. *J. Hydrol.* 499, 167–176. <https://doi.org/10.1016/j.jhydrol.2013.06.039>
- Wolff, J.K., Harrold, M., Fowler, T., Gotway, J.H., Nance, L., Brown, B.G., 2014. Beyond the basics: Evaluating model-based precipitation forecasts using traditional, spatial, and object-based methods. *Weather Forecast.* 29, 1451–1472. <https://doi.org/10.1175/WAF-D-13-00135.1>
- Wu, H., Adler, R.F., Hong, Y., Tian, Y., Policelli, F., 2012. Evaluation of Global Flood Detection Using Satellite-Based Rainfall and a Hydrologic Model. *J. Hydrometeorol.* 13, 1268–1284. <https://doi.org/10.1175/jhm-d-11-087.1>
- Xie, P., Arkin, P.A., 1996. Analyses of global monthly precipitation using gauge observations, Satellite Estimates, and Numerical Model Predictions. *Journal-of-Climate.*
- Xie, P., Xiong, A.Y., 2011. A conceptual model for constructing high-resolution gauge-satellite merged precipitation analyses. *J. Geophys. Res. Atmos.* 116, 1–14. <https://doi.org/10.1029/2011JD016118>
- Xu, R., Tian, F., Yang, L., Hu, H., Lu, H., Hou, A., 2017. Ground validation of GPM IMERG and trmm 3B42V7 rainfall products over Southern Tibetan plateau based on a high-density rain gauge network. *J. Geophys. Res.* 122, 910–924. <https://doi.org/10.1002/2016JD025418>
- Ye, J., He, Y., Pappenberger, F., Cloke, H.L., Manful, D.Y., Li, Z., 2014. Evaluation of ECMWF medium-range ensemble forecasts of precipitation for river basins. *Q. J. R. Meteorol. Soc.* 140, 1615–1628. <https://doi.org/10.1002/qj.2243>
- Yilmaz, M.T., Crow, W.T., 2013. The optimality of potential rescaling approaches in land data assimilation. *J. Hydrometeorol.* 14, 650–660. <https://doi.org/10.1175/JHM-D-12-052.1>
- Yilmaz, M.T., Houser, P., Shrestha, R., Anantharaj, V.G., 2010. Optimally merging precipitation to minimize land surface modeling errors. *J. Appl. Meteorol. Climatol.* 49, 415–423. <https://doi.org/10.1175/2009JAMC2305.1>
- Yong, B., Chen, B., Gourley, J.J., Ren, L., Hong, Y., Chen, X., Wang, W., Chen, S., Gong, L., 2014. Intercomparison of the Version-6 and Version-7 TMPA precipitation products over high and low latitudes basins with independent gauge networks: Is the newer version better in both real-time and post-real-time analysis for water resources and hydrologic extremes? *J. Hydrol.* 508, 77–87. <https://doi.org/10.1016/j.jhydrol.2013.10.050>
- Yuan, F., Zhang, L., Wah Win, K.W., Ren, L., Zhao, C., Zhu, Y., Jiang, S., Liu, Y., 2017. Assessment of GPM and TRMM multi-satellite precipitation products in streamflow simulations in a data sparse mountainous watershed in Myanmar.

Remote Sens. 9. <https://doi.org/10.3390/rs9030302>

- Yucel, I., 2015. Assessment of a flash flood event using different precipitation datasets. *Nat. Hazards* 79, 1889–1911. <https://doi.org/10.1007/s11069-015-1938-9>
- Yucel, I., Kuligowski, R.J., Gochis, D.J., 2011. Evaluating the hydro-estimator satellite rainfall algorithm over a mountainous region. *Int. J. Remote Sens.* 32, 7315–7342. <https://doi.org/10.1080/01431161.2010.523028>
- Yucel, I., Onen, A., 2014. Evaluating a mesoscale atmosphere model and a satellite-based algorithm in estimating extreme rainfall events in northwestern Turkey. *Nat. Hazards Earth Syst. Sci.* 14, 611–624. <https://doi.org/10.5194/nhess-14-611-2014>
- Zambrano-Bigiarini, M., Nauditt, A., Birkel, C., Verbist, K., Ribbe, L., 2017. Temporal and spatial evaluation of satellite-based rainfall estimates across the complex topographical and climatic gradients of Chile. *Hydrol. Earth Syst. Sci.* 21, 1295–1320. <https://doi.org/10.5194/hess-21-1295-2017>
- Zhang, S., Wang, D., Qin, Z., Zheng, Y., Guo, J., 2018. Assessment of the GPM and TRMM Precipitation Products Using the Rain Gauge Network over the Tibetan Plateau. *J. Meteorol. Res.* 32, 324–336. <https://doi.org/10.1007/s13351-018-7067-0>

APPENDICES

A. Appendix: Resulting Statistics Tables from Merging the Research-Grade Products

Table 0.1. *Bias and ErrSD for daily individual and merged research-grade products over wetness classes*

Wetness		Entire	Dry	Mod-Dry	Mod-Wet	Wet
No. of Stations		755	279	303	123	50
BIAS (mm/day)	GPM	0.28	0.42	0.35	0.07	-0.38
	TMPA	0.17	0.39	0.27	-0.16	-0.78
	ERAint	0.28	0.65	0.32	-0.14	-0.95
	ERA5	0.41	0.49	0.39	0.34	0.29
	SimpMRG	0.28	0.48	0.32	0.02	-0.48
	MRG_IMERG_reg	0.28	0.42	0.35	0.07	-0.38
	MRG_TMPA_reg	0.17	0.38	0.26	-0.17	-0.79
	MRG_ERAint_reg	0.28	0.65	0.32	-0.13	-0.95
ErrSD (mm/day)	MRG_ERA5_reg	0.41	0.49	0.39	0.34	0.29
	GPM	4.59	3.69	4.60	5.38	7.65
	TMPA	5.69	4.66	5.65	6.69	9.24
	ERAint	4.17	3.41	4.08	4.94	7.12
	ERA5	3.94	3.13	3.89	4.73	6.76
	SimpMRG	3.66	2.89	3.58	4.39	6.60
	MRG_IMERG_reg	3.56	2.65	3.50	4.48	6.71
	MRG_TMPA_reg	3.71	2.78	3.62	4.69	7.02
MRG_ERAint_reg	3.70	2.66	3.62	4.80	7.32	
MRG_ERA5_reg	3.58	2.66	3.55	4.51	6.71	

Table 0.2. *CC for daily individual and merged research-grade products over wetness classes*

Wetness		Entire	Dry	Mod-Dry	Mod-Wet	Wet
No. of Stations		755	279	303	123	50
CC with the Observed Data	GPM	0.62	0.59	0.64	0.66	0.57
	TMPA	0.47	0.44	0.49	0.49	0.40
	ERAint	0.62	0.58	0.62	0.66	0.64
	ERA5	0.66	0.63	0.67	0.72	0.68
	SimpMRG	0.70	0.67	0.71	0.74	0.68
	MRG_IMERG_reg	0.70	0.67	0.71	0.74	0.68
	MRG_TMPA_reg	0.67	0.64	0.69	0.71	0.63
	MRG_ERAint_reg	0.71	0.68	0.72	0.76	0.71
MRG_ERA5_reg	0.71	0.68	0.72	0.76	0.71	

Table 0.3. *Bias and ErrSD for daily individual and merged research-grade products over elevation classes*

Elevation (m)		Entire	Elev <500	Elev 500-1000	Elev 1000-1500	Elev 1500-2000	Elev > 2000
No. of Stations		755	237	219	209	77	13
BIAS (mm/day)	GPM	0.28	0.26	0.32	0.25	0.30	0.45
	TMPA	0.17	0.05	0.22	0.22	0.27	0.33
	ERAint	0.28	-0.11	0.37	0.40	0.83	0.92
	ERA5	0.41	0.32	0.41	0.41	0.65	0.70
	SimpMRG	0.28	0.11	0.32	0.31	0.52	0.60
	MRG_IMERG_reg	0.28	0.26	0.31	0.25	0.29	0.45
	MRG_TMPA_reg	0.17	0.05	0.21	0.21	0.26	0.31
	MRG_ERAint_reg	0.28	-0.11	0.37	0.40	0.83	0.92
ErrSD (mm/day)	MRG_ERA5_reg	0.41	0.32	0.41	0.41	0.65	0.70
	GPM	4.59	5.88	3.96	3.93	4.21	4.67
	TMPA	5.69	7.11	5.03	4.95	5.29	5.58
	ERAint	4.17	5.36	3.57	3.52	3.96	4.34
	ERA5	3.94	5.16	3.36	3.29	3.60	3.84
	SimpMRG	3.66	4.80	3.07	3.07	3.37	3.71
	MRG_IMERG_reg	3.56	4.75	2.94	2.98	3.23	3.47
	MRG_TMPA_reg	3.71	4.93	3.08	3.11	3.36	3.59
MRG_ERAint_reg	3.70	5.15	3.01	3.01	3.16	3.42	
MRG_ERA5_reg	3.58	4.85	2.97	2.96	3.14	3.40	

Table 0.4. *CC for daily individual and merged research-grade products over elevation classes*

Elevation (m)		Entire	Elev <500	Elev 500-1000	Elev 1000-1500	Elev 1500-2000	Elev > 2000
No. of Stations		755	237	219	209	77	13
CC with the Observed Data	GPM	0.62	0.66	0.64	0.59	0.52	0.45
	TMPA	0.47	0.51	0.49	0.43	0.38	0.34
	ERAint	0.62	0.63	0.63	0.61	0.57	0.49
	ERA5	0.66	0.68	0.68	0.65	0.61	0.55
	SimpMRG	0.70	0.72	0.72	0.68	0.63	0.56
	MRG_IMERG_reg	0.70	0.72	0.72	0.69	0.63	0.56
	MRG_TMPA_reg	0.67	0.70	0.69	0.65	0.59	0.53
	MRG_ERAint_reg	0.71	0.73	0.72	0.69	0.65	0.58
MRG_ERA5_reg	0.71	0.73	0.73	0.70	0.65	0.58	

Table 0.5. *Bias and ErrSD for daily individual and merged research-grade products over slope classes*

Slope (%)		Entire	Slope < 5%	Slope 5-10%	Slope 10-15%	Slope 15-20%	Slope > 20%
No. of Stations		755	499	170	56	19	11
BIAS (mm/day)	GPM	0.28	0.30	0.29	0.08	0.11	0.72
	TMPA	0.17	0.21	0.20	-0.11	-0.28	0.21
	ERAint	0.28	0.27	0.33	0.11	0.29	1.13
	ERA5	0.41	0.33	0.43	0.52	0.97	2.23
	SimpMRG	0.28	0.27	0.30	0.14	0.26	1.06
	MRG_IMERG_reg	0.28	0.30	0.28	0.08	0.10	0.71
	MRG_TMPA_reg	0.17	0.21	0.19	-0.12	-0.30	0.19
	MRG_ERA5_reg	0.41	0.33	0.43	0.52	0.96	2.22
ErrSD (mm/day)	GPM	4.59	4.50	4.49	5.21	5.74	4.94
	TMPA	5.69	5.58	5.61	6.38	7.06	6.11
	ERAint	4.17	4.13	4.03	4.73	4.80	4.05
	ERA5	3.94	3.88	3.77	4.55	4.70	4.65
	SimpMRG	3.66	3.61	3.51	4.24	4.47	3.69
	MRG_IMERG_reg	3.56	3.49	3.43	4.20	4.48	3.55
	MRG_TMPA_reg	3.71	3.63	3.58	4.38	4.75	3.82
	MRG_ERA5_reg	3.70	3.66	3.55	4.34	4.42	3.38
	MRG_ERA5_reg	3.58	3.55	3.45	4.18	4.26	3.32

Table 0.6. *CC for daily individual and merged research-grade products over slope classes*

Slope (%)		Entire	Slope < 5%	Slope 5-10%	Slope 10-15%	Slope 15-20%	Slope > 20%
No. of Stations		755	499	170	56	19	11
CC with the Observed Data	GPM	0.62	0.63	0.62	0.59	0.52	0.49
	TMPA	0.47	0.48	0.46	0.43	0.36	0.30
	ERAint	0.62	0.61	0.63	0.62	0.64	0.62
	ERA5	0.66	0.66	0.68	0.67	0.69	0.63
	SimpMRG	0.70	0.70	0.71	0.69	0.68	0.65
	MRG_IMERG_reg	0.70	0.70	0.71	0.69	0.67	0.63
	MRG_TMPA_reg	0.67	0.67	0.67	0.65	0.60	0.55
	MRG_ERA5_reg	0.71	0.70	0.72	0.70	0.71	0.68
	MRG_ERA5_reg	0.71	0.71	0.72	0.71	0.71	0.68

CURRICULUM VITAE

PERSONAL INFORMATION

Surname, Name : Amjad, Muhammad
Nationality : Pakistani
Date and Place of Birth : 1 June 1987, Multan, Pakistan
Phone : +905070945649, +923126307917
E-mail : amjadiqm@gmail.com

EDUCATION

Degree	Institution	Year of Graduation
B.Sc. Agricultural Engineering	BZU, Multan, Pakistan	2010
M.Sc. Water Resources Mgt.	UET, Lahore, Pakistan	2013
PhD in Civil Engineering	METU, Ankara, Turkey	2020

FOREIGN LANGUAGES

English

PUBLICATIONS

Peer Reviewed Publication:

1. Meric Yilmaz, M. Tugrul Yilmaz, *Muhammad Amjad*, Burak Bulut (2017). Uydu Kaynaklı Yağmur Verilerinin Hata Oranlarının Deniz Kıyılarına Olan Uzaklığına Bağlı Analizi. Teknik Dergi, 484, 7993-8005, (in Turkish), <https://doi.org/10.18400/tekderg.306970>.

Peer Reviewed Conference Papers:

1. M.H. Afshar, *M. Amjad*, B. Bulut, E. Duzenli, K.P. Yousefi, M.T. Yilmaz (2019). Validation of TMPA and ECMWF Precipitation Estimates Using Gauge Based Observations over West Azarbayjan province of Iran. The 1st International and 4th National Congress on Iranian Irrigation and Drainage, Urmia, Iran.

2. **M. Amjad**, E. Düzenli, M.H. Afşar, B. Bulut, A.U.G. Şenocak, K.K. Yılmaz, M.T. Yılmaz, İ. Yücel (2019). TMPA VE ECMWF yağış verilerinin yer gözlem verileriyle doğrulanması. 10. Ulusal Hidroloji Kongresi.

3. M. Tuğrul Yılmaz, **Muhammad Amjad**, İsmail Yücel, Burak Bulut (2017). TRMM VE GPM UZAKTAN ALGILAMA VE ECMWF NUMERİK MODEL KAYNAKLI YAĞIŞ VERİLERİNİN DOĞRULANMASI. UZALMET III. Meteorolojik Uzaktan Algılama Sempozyumu (16-19 Ekim 2017, Antalya).

4. M. T. Yılmaz, **M. Amjad**, M. Selamoğlu (2015). Tropical Rainfall Measuring Mission Uydu Kaynaklı Yağmur Verilerinin Yer Gözlemleri ile Karşılaştırılması. II. Meteorolojik Uzaktan Algılama Sempozyumu, Antalya, 3-5 Kasım 2015.

Conference Presentations:

1. **Muhammad Amjad**, B. Bulut, E. Düzenli, A.U.G. Şenocak, M.T. Yılmaz, İ. Yücel, K.P. Yousefi, M.H. Afshar, K.K. Yılmaz (2020). Intercomparison Of the Accuracy Statistics of ERA5 and ERA-Interim Reanalysis Precipitation Products Over Turkey. 14th International Conference on Hydrosience and Engineering.

2. **Muhammad Amjad**, M. Tugrul Yilmaz, Ismail Yucel, and Koray K. Yilmaz (2019). The Evaluation of Remotely Sensed and Model-Based Soil Moisture Products According to Different Soil Type, Vegetation Cover and Climate Regime Using Station-Based Observations over Turkey. HS6.4 EGU2019-15438. EGU General Assembly 2019.

3. **Muhammad Amjad** et al. (2019). Uncertainty Assessment of Satellite- and Model-based Precipitation Products over Complex Terrain of Turkey. AS1.32 EGU2019-12786. EGU General Assembly 2019.

4. **Muhammad Amjad**, M. Tugrul Yilmaz, Ismail Yucel, and Koray K. Yilmaz (2018). Inter-comparison and Accuracy Assessment of Satellite and Model Precipitation Products. Geophysical Research Abstracts, Vol. 20, EGU2017-6834, EGU General Assembly 2018.

5. **Muhammad Amjad** and M. Tugrul Yilmaz (2017). Evaluation of Satellite and Model Precipitation Products Over Turkey. H51J-1403. American Geophysical Union Fall Meeting, 2017.

6. **Muhammad Amjad** and M. Tugrul Yilmaz (2016). Inter-comparison and accuracy assessment of TRMM 3B42 products over Turkey. Geophysical Research Abstracts, Vol. 18, EGU2016, 2016, EGU General Assembly 2016.

7. **M. Amjad**; M.T. Yilmaz (2015). Accuracy assessment of TRMM 3B42 V6 and V7 products using station data over various topographical regions in Turkey. American Geophysical Union Fall Meeting, 2015.

8. **Muhammad Amjad** and M. Tugrul Yilmaz (2015). Accuracy assessment of TRMM 3B42 V6 and V7 products over regions with varying hydro-climatology and

topography using station data over Turkey. Geophysical Research Abstracts (17), EGU2015-9860, EGU General Assembly 2015.

HOBBIES

Research analysis through coding, Internet surfing, Sports, Singing, Poetry, Cooking